UNIVERSIDAD DE DEUSTO

TRAIN POSITIONING SYSTEM BASED ON INERTIAL SENSORS

by
Jon Otegui Arruti

A dissertation submitted in partial fulfillment of the requirements for the degree of Doctor of Philosophy, within the PhD. Program in Engineering for the Information Society and Sustainable Development.

Supervised by Dr. Alfonso Bahillo Martínez
and Dr. Iban Lopetegi Zinkunegi

UNIVERSIDAD DE DEUSTO

TRAIN POSITIONING SYSTEM BASED ON INERTIAL SENSORS

by
Jon Otegui Arruti

A dissertation submitted in partial fulfillment of the requirements for the degree of Doctor of Philosophy, within the PhD. Program in Engineering for the Information Society and Sustainable Development.

Supervised by Dr. Alfonso Bahillo Martínez
and Dr. Iban Lopetegi Zinkunegi

The candidate	The supervisor	The supervisor

Bilbao, February 2020

Train Positioning System based on Inertial Sensors

Author: Jon Otegui Arruti
Advisor: Alfonso Bahillo Martínez
Advisor: Iban Lopetegi Zinkunegi

Text printed in Bilbao
First edition, February 2020

Begiak noraino,
nahia haraino.

Abstract

Positioning accurately and safely a train is nowadays a great challenge. Safety and cost-efficiency requirements in addition to the technical limitations of current positioning system have propitiated this research area. Consequently, several research projects have been launched regarding to the train positioning systems over the last lustrum.

The current train positioning systems are based mainly on odometry and track circuits but they present both technical and economical limitations. The combination of Global Navigation Satellite System (GNSS) and Inertial Navigation System (INS) arise as prominent solution to overcome the current system limitations. However, the lack of agreement of the main research works about GNSS integration into the train positioning system, has set it aside for short-term solutions.

This dissertation is focused on the integration of an INS as a complementary source to wheel speed sensors in order to achieve the functionality, interoperability and cost-efficiency requirements of fail-safe train positioning system. The design and development of the proposed solution has propitiated four papers that are directly related to the research objectives.

First, the main train positioning solutions published up-to-date are evaluated and main research gaps are highlighted. Following these gaps, a experimental test is carried out to evaluate GNSS and INS-based solution and its performance is compared to current train navigation solution. Once detected the potentialities of INS-based solution, it arises as propitious system to complement wheel speed sensors. However, before providing a commercial solution, a flexible and one-stop simulation framework is developed in order to design and test different train

navigation algorithms, mechanization methods, etc. in multiples scenarios (changing the features of trains, tracks, sensors and so on). Finally, a comparison of the performance of different commercial IMUs has been carried out in a experimental test in order to optimize the cost of the proposed solution.

Resumen

Hoy en día la localización precisa y segura de un tren es un reto. Este área de investigación ha venido motivado por la necesidad de un nuevo sistema de posicionamiento ferroviario que venciera las limitaciones del sistema actual, cumpliendo los requisitos de seguridad funcional y la eficiencia de coste. Consecuentemente, se han promovido varios proyectos de investigación, especialmente en Europa y en los últimos cinco años.

El sistema de posicionamiento ferroviario actual se basa principalmente en la odometría del equipo embarcado y en los equipos de vía (balizas, circuitos de vía, contadores de ejes, etc.). Sin embargo, los sensores que lo componen presentan limitaciones y el coste de mantenimiento de los equipos de vía resulta elevado. En este contexto, surgen soluciones como los sistemas de posicionamiento global basados en satélites (GNSS) y los sistemas inerciales basados en acelerómetros y giróscopos (INS). Sin embargo, la diversidad de posibilidades defendidas por los operadores ferroviarios para integrar GNSS en el sistema de posicionamiento de un tren ha hecho descartar esta opción como solución a corto plazo.

Esta tesis está enfocada en la integración de sensores inerciales en un sistema de posicionamiento ferroviario como fuente complementaria a los sensores de rueda. De esta forma se pretenden alcanzar los requisitos de funcionalidad, interoperabilidad y coste definidos en la tesis. El diseño y el desarrollo de la solución óptima ha resultado en cuatro artículos de investigación recogidos en este libro.

En primer lugar, se han evaluado los principales trabajos propuestos hasta la fecha sobre sistemas de posicionamiento ferroviario. Este trabajo ha mostrado los *research gaps* más relevantes en este contexto. A partir de estos, se han desarrollado el resto de los artículos. En primer lugar, se ha realizado una prueba experimental donde se ha comparado la solución obtenida de GNSS e INS contra la solución actual, basada en sensores de rueda y radar Doppler. Vistas las posibilidades ofrecidas por el sistema inercial, se ha optado por complementarlo con el sensor de rueda y dar así una solución eficiente. Sin embargo, antes de comercializarlo, se ha preparado un completo y flexible entorno de simulación donde probar diferentes algoritmos de navegación, métodos de mecanización, etc. en múltiples escenarios modificando las características del tren, la vía, los sensores, etc. Por último, se ha presentado una comparativa de diferentes IMUs ya que el rango de precios de estos sensores pueden ir desde los 3€ hasta los 30.000€.

Laburpena

Gaur egungo tren baten lokalizazio ziur eta zehatza lortzea erronka handi bat da. Ikerketa alor honen garapena egungo tren lokalizazio sistemaren beharretatik abiatu da, seguratasun eta kostu irizpideak oinarri izanik. Ondorioz, azken urteotan Europatik zuzenduriko ikerketa proiektu ugari jarri dira martxan.

Egungo tren baten lokalizazio sistema ibilgailuan jarritako eta trenbidean jarritako sistemen arteko elkarrekintzan datza. Hala ere, erabili ohi diren sentsoreek muga nabarmenak dituztela eta trenbideetako sistemen mantentze-lanen gastua handia dela ondorioztatu dute trengintza eragileek. Kontextu honetan, bi teknologia aztertu izan dira etorkizuneko ibilgailuen lokalizazioan eragina izan dezaketenak: alde batetik, sateliteetan oinarrituriko sistema globalak leudeke, GNSS deritzenak. Bestalde, azelerometro eta giroskopoetan oinarrituriko sistema inertzialak, INS deritzenak. Hala ere, lehenengoak epe laburrerako soluzio modura baztertuak izan dira, trengintza eragileen desadostasunak medio.

Tesi hau sentsore inertzialetan oinarritu da, zeinak egungo sistemaren informazio iturri osagarri modura proposatu diren. Horrela, funtzionaltasun, eraginkortasun eta kostu irizpideak betetzea helburu du tesi honek eta bere garapenean, liburu honetan jaso diren lau ikerketa artikulu idatzi dira, horietatik hiru onartuak izanik.

Lehenik, aurretik aurkezturiko lanen ebaluazioa egin da irizpide desberdinak kontuan hartuta. Lan honetan *research gap* garrantzitsuenak detektatu dira trenen lokalizazioaren textuinguruan. Bertatik abiatuta gainontzeko artikuluak garatu dira. Lehenik eta behin, GNSS eta INS

sistemak bateratuz lorturiko soluzioa, egungo sistemaren soluzioarekin alderatu da (takometro eta Doppler radarretan oinarritua), trenbide bateko neurketak erabiliz. Sentsore inertzialen aukerak ondorioztatuta, hauek takometroekin erabiltzea proposatu da. Sistema honen erantzuna neurtzeko, simulazio ingurune bat garatu da non nabigazio algoritmoak, mekanizazio metodoak, eta abar probatu daitezken (edozein tren, sentsore, trenbide eta abiadura kontuan hartuta). Azkenik, IMU desberdinen alderaketa bat eskeini da, sentsore hauen prezioa 3€-tik 30.000€-raino izan baitaiteke.

Acknowledgements

There are many people without whom this work would not have been possible. First, I would like to thank my co-advisors, Alfonso Bahillo Martínez and Iban Lopetegi Zinkunegi. This work has only reached its completion through their unceasing support, guidance and hard-work.

A special thanks to Luis Enrique Díez, for his technical insights, and for helping me introducing and reviewing the research articles.

I would like to thank other members of the Mobility team and of the CAF I+D company. Particularly, I would like to thank Pedro, Luis Manuel, Josune, Xabi, Jorge, Izaskun, Xabi, Nerea, Naiara, Aitor, Javi, Oihane, Ioritz, Ibai, Julen, Ane, Rene, Fernando, Oscar, Ion. It is a great experience working with all of you.

I would also like to express my gratitude to the various anonymous reviewers who have provided valuable inputs for the articles that comprise this dissertation, and which have truly bolstered its quality.

I am also very thankful to my family, who has accompanied me through this journey. Particularly, to Juan María, my father, and to María Jesús, my mother, who have trust on me from the beginning of my days. Specially to Asier, my brother, who has supported me throughout all of these years.

I would like to thank my friends, Mikel Irastorza, Marta Iturriza, Iñigo Martínez and Joseba Sagardia for all these years (and for the years to come) sharing laughter, engineering and life.

A special thanks to Fermín Mourenza and Cristina Olarra for accepting nothing less than excellence from me each day.

And last, but not least, I would like to say a heartfelt thank you to Irati for encouraging me to follow my dreams, becoming part of one of them.

Many thanks, also, to the rest of my family, friends and to those whose names, for brevity, I do not explicitly include here.

Eskerrik asko,

Jon Otegui Arruti

February 2020

Contents

List of Figures **xiii**

List of Tables **xv**

Acronyms **xvii**

1 Introduction **1**

1.1 Thesis Statement 7

1.2 Main research objectives 8

1.3 Research methodology 9

1.4 Publications 10

1.4.1 Paper I 10

1.4.2 Paper II 11

1.4.3 Paper III 12

1.4.4 Paper IV 12

1.5 Outline 14

2 Train Navigation Background **15**

3 Candidate Sensors Analysis **29**

4 Simulation Framework **45**

5 Comparative of IMU **63**

6 Conclusions and Future Work **79**

6.1 Conclusions 79

6.2 Future work 81

Bibliography **83**

List of Figures

1.1 Relationship between the research objectives and publications. . . 10

3.1 Comparative of velocity solution between GNSS+INS and current system. 30

4.1 The proposed simulation framework for testing train navigation algorithms. 47

List of Tables

2.1 Test track analysis of the state-of-the-art proposals 16
2.2 Sensors characteristics analysis of the state-of-the-art proposals. . 17
2.3 Research results analysis 17

4.1 A comparison of the simulation frameworks. 46

5.1 IMU's characteristics 64
5.2 Euler angles statistical analysis 64

Acronyms

ATO Automated Train Operation

ATP Automatic Train Protection

EKF Extended Kalman Filter

ERTMS European Rail Traffic Management System

ETCS European Train Control System

GNSS Global Navigation Satellites System

GT Ground Truth

IMU Inertial Measurement Unit

INS Inertial Navigation System

ITS Intelligent Transport Systems

KF Kalman Filter

MEMS Micro-Electromechanical Systems

OEM Original Equipment Manufacturer

OSM Open-Street Maps

PF Particle Filter

RLG Ring Laser Gyros

ACRONYMS

RMS Root Mean Square

SIL Safety Integrity Level

UKF Unscented Kalman Filter

VB Virtual Balise

Research is to see what everybody else has seen, and to think what nobody else has thought.

Albert Szent-Györgyi

CHAPTER

1

Introduction

Intelligent transport systems (ITS) have at their core technological systems that work together to improve transportation performance [1]. ITS are built mainly on three technology pillars named as information, communication and positioning technologies, where this last one seems to be the least familiar amongst transport stakeholders [2]. However, it is today well known that ITS strongly rely on location information which can be considered the key technology pillar for several applications such as fleet dispatching, passenger information or maintenance and track infrastructure reduction [3]. Consequently, research effort is focused on the development of positioning systems for automobiles, trains and aerial vehicles.

Focused on the train positioning system, it plays a key role in the so called Automated Train Operation (ATO) where the responsibility for managing operations are transferred from the driver to the train control system. The train control system requires seamless positioning information to guarantee the availability of the ATO and it demands exigent requirements regarding to the functionality, interoperability, safety, energy and cost issues. In order to provide the positioning information fulfilling the asked requirements, current train positioning systems must be improved.

1. INTRODUCTION

The current train positioning systems are based mainly on on-board sensors and track equipment. The track equipment is a composition of devices (e.g. track circuits, axle counters, beacon or balises, etc.) installed at infrastructure level. In general, the railway track is divided into co-called cantons and at the beginning of each canton, a beacon is placed. When a train passes over it, the traffic management system detects that a train is in that canton (usually the length of the train is measured with axle counters). If another train is located right after this canton, the driver is notified and if there is no response after several seconds, the train is stopped automatically by its Automatic Train Protection (ATP) system [4]. Once the train is inside a canton, the on-board sensors provide the velocity and the covered distance (i.e. odometry) from the last beacon. The main on-board sensors used up to date are wheel speed sensors (a.k.a. velocity encoders, tachometers and phonic wheels) and Doppler radars [5].

The current positioning system deals with several limitations that can be gathered according to safety, energy, functionality, interoperability and economical issues:

- Functionality: According to the on-board sensors used in current train positioning, the wheel speed sensor loses accuracy when instantaneous wheel radius differs from nominal value (e.g. due to wear and conicity of the wheels) and the angular rate is incoherent to train longitudinal velocity (e.g. due to slip or skid phenomena). The Doppler radar also present limitations due to the loss of discrimination in the emitting and reflected signal in very smooth surfaces (such as snow, glass, etc.) [6]. These sensors only are able to provide velocity and covered distance, which makes the positioning information to be limited (neither orientation nor absolute position is given).

- Interoperability: The track equipment used for positioning is related to the train control system which can be particular for each railway. Several train control systems with different functionalities and technologies are used in Europe, so there has always been a problem of interoperability and migration of new systems (even on national level). The development of the European Rail Traffic Management System (ERTMS) has been promoted to harmonize railway rules and regulations making future architectures of train positioning systems to fulfill ERTMS requirements. The current regulations have defined

a minimum operational requirement stating that the train position shall meet 5m + 5% accuracy since last read beacon [7]. The ERMTS has promoted the positioning systems to be on-board in order to reduce the dependency of track equipment and standardizing the balises used in tracks.

- Safety: The train positioning system can be used for non-safety or safety related applications. Not safety related purposes are those where errors can result in disadvantages such as delays, wrong information to passengers and economic losses, but cannot cost human life or damage equipment (e.g. time-table asset). Nevertheless, safety related purposes are those whose failures can cause accidents, either alone or in combination with other errors (e.g. doors opening when a train arrives at a station). Thus, the requirements for the components are very high to ensure safe working in all possible conditions such as different speed of trains, different weather conditions, etc. The safety purposes can be further distinguished in terms of whether the erroneous non-detection or the erroneous detection at the wrong time can cause danger. Consequently, train positioning systems demand the highest safety integrity level (SIL-4) where the tolerable hazard rate must be below 10^{-9} hazard/h [8].

- Energy: Recent research works on energy recovery and optimal traction have demonstrated that the target operating point is located near the maximum torque of the engine [9],[10],[11]. This operation point is located as well, in severe slipping scenario where the wheel speed sensor will tend to overestimate the train velocity. Consequently, the wheel speed sensor must be complemented if accuracy reached is expected to fulfill ERTMS requirements. In this context, the multi-sensor architectures can be proposed to enhance the wheel speed sensor measurements.

- Cost: In case of economical drawbacks of the current positioning system, the purchase cost of Doppler radars and maintenance cost of track circuits have motivated the proposals of new candidate sensors. The development of micro-electromechanical systems (MEMS) has propitiated the utilization of inertial sensors for different positioning purposes (e.g. for pedestrian,

land-vehicular and unmanned aerial vehicles) [12]. The railway environment due to the track constrains, smooth curves and altitude changes makes them propitious to use in combination of some of the current sensors [13].

Over the last decade, important efforts have been made with regard to overcome the main limitations cited previously. As a sign of interest, the railway sector has always been present in different European research programs such as FP7 and Horizon 2020. According to Horizon 2020, all the investigation activities related to the railway are collected in Shift2Rail (S2R), the first European rail initiate that seeks research and innovation market-driven solutions to be integrated into innovative rail products [14]. Most of the projects encompassed into S2R deal with the integration of new candidate sensors evaluating them in experimental tests (e.g. ERSAT-EAV, RHINOS, STARS, etc.). Further information about these research projects can be found in [3] and [4].

The majority of the proposals presented up to date concludes multi-sensor data fusion architectures are required to solve each sensor individual limitations. However, there is an open discussion about the most appropriate candidate sensors to include in the multi-sensor architectures.

- Global Navigation Satellites System (GNSS): Satellite-based localization systems are new technologies that can play an important role for reducing the rail infrastructure costs because, instead of relying on equipment installed all along the tracks, trains can use satellite signals to calculate their position in an autonomous way [15]. The manufacturing cost of GNSS chipsets has now dropped sufficiently to enable high performance receivers to be manufactured at low cost (around 100€) [16]. The main advantages of satellite navigation are its global availability and the high accuracy measurement (m-level standalone and cm-level with correction techniques) that is not prone to drift [17]. However, there are also several disadvantages, such as shadowing or multipath of satellites in railway tunnels, forest aisles and urban environments resulting in none or an uncertain measurement. Consequently, seamless positioning solution is not reachable using GNSS stand-alone and it is used with complementary data such as inertial sensors [18], eddy-current sensors [17], wheel speed sensors [19], imaging information [20], etc.

- Inertial Measurement Unit (IMU): The IMU is an integrated sensor package that combines multiple accelerometers and gyrocopes to produce a three-dimensional measurement of both specific force and angular rate, with respect to an inertial reference frame. The IMU by itself does not provide any kind of navigation solution (position, velocity, attitude). It only actuates as a sensor, in opposition to the INS (Inertial Navigation System), which integrate the measurements of its internal IMU to provide a navigation solution. For instance, an Inertial Navigation System (INS) uses an IMU to form a self-contained navigation system which uses measurements provided by the IMU to track the position, velocity and orientation of an object relative to a starting point, orientation and velocity. Unlike wheel speed sensors, Doppler radars and GNSS whose errors are partly related to the terrain in which the vehicle is traveling, inertial sensors are fully self-contained [21]. Their performance, however, is limited on the measurement errors and their propagation to velocity or position estimation, where time integration make the drift arise. Recent research works have proposed calibration techniques [22],[23] and drift-reduction algorithms based on non-holonomic constrains [24], external sensors measurements [25], track constrains [26], errors characterization [27],[28] etc. in order to mitigate the drift growth, especially for ultra low-cost (below 10€) devices.

In addition to the presented candidate sensors, new information sources are also investigated. The main data source that can be used for positioning purposes is related to the digitalization of railways and they are named digital maps. The digital maps are useful for positioning purposes due to the fact that railway tracks can only consist of a sequence of the following three geometric shapes: straight, transitional arc (i.e. clothoid) and circular arc. By continuously identifying the current track geometry and incorporating this knowledge in the estimation process of the data fusion algorithm, along-track and cross-track accuracy can be increased using map-matching algorithms [29], [30]. However, the generation of compact, robust, accurate and available railway maps is an incipient field [31], [32].

The integration of the multi-sensor architectures are carried out by data fusion algorithms. Multi-sensor data fusion algorithms combine observations from a num-

ber of different sources to provide a robust and complete description of a process of interest [33]. The design and/or the development of data fusion algorithms is a research field itself, but the most used techniques for positioning applications are focused on Kalman Filters (KF) and Particle Filters (PF) [34], [35]. Although PF are able to provide more accurate estimations due to the ability to operate with non-linear and non-Gaussian states, the computational cost makes its integration on commercial solution to be challenging. Consequently, the different adaptations of the KF, such as Extended-KF (EKF) [36], [37], [38], [39] or Unscented-KF (UKF) [40], [41] seems to be closer to commercial solutions.

1.1 Thesis Statement

This dissertation provides a solution to the current train positioning system by proposing a multi-sensor architecture based on a combination of current and candidate sensors: on the one hand, wheel speed sensor has been considered due to its accuracy (it guarantees 2% velocity-error in nominal operation scenarios), lack of interference and drift over time and the large knowledge of rolling-stock manufacturers on this sensor. On the other hand, a low-cost IMU is proposed to complement wheel speed sensor in those cases where wheel radius is far away the nominal value (e.g. wheel worn or excessive conicity) and the angular rate of the wheelset is not coherent to the train longitudinal velocity (e.g. slipping or skidding stages). The GNSS is also evaluated as candidate system to compensate inertial sensors errors and to provide absolute position. In addition to odometry information, train's orientation angles, acceleration, velocity and absolute position are provided to enhance the positioning solution reached up to date.

1.2 Main research objectives

This dissertation addresses the following main objectives to achieve the statement presented in the previous section:

1. The main objective is to design an on-board system that overcomes current sensors' limitations, mainly those related to wheel speed sensors. The study and integration of candidate systems (e.g. INS, GNSS) and the interaction with current system (e.g. wheel speed sensors, Doppler radars) must be performed based on several requirements.

2. According to interoperability requirements, the proposed solution shall avoid the track infrastructure (balises, track circuits, axle counters, etc.) in order not to deal with different signalling systems and for enhancing the autonomy of a train. The proposed solution cannot present interoperability conflicts and it shall be based on ERTMS but not limited to it.

3. According to functionalities requirements, the proposed solution shall be scalable to absolute position estimation. The integration of GNSS or digital maps must be considered as candidate data sources to be integrated in future developments. Consequently, the orientation angles (roll, pitch and yaw) and vehicle's absolute position shall be provided.

4. According to cost-efficiency requirements, the proposed solution shall provide a commercial and manufacturable solution. The train positioning system could be equipped on every kind of train and integrated into an odometry card.

1.3 Research methodology

In order to achieve the main research objectives, the very first work carried out is the evaluation of the state-of-the-art solutions and the search of the main research gaps of the up to date research context. It is concluded that the utilization of INS and GNSS arise as prominent field in order to overcome the current train positioning system limitations.

An experimental test is carried out to evaluate the performance of the candidate systems (INS and GNSS) and it is compared to current system solution. The INS solution has shown major potentialities according to functionality, interoperability and cost-efficiency criteria than GNSS. Consequently, the architecture proposal is focused on INS as aiding source to the current train positioning system.

The utilization of the INS in those scenarios where the wheel speed sensor provides inaccurate solution seems to fulfill the objectives and requirements set by rolling-stock manufacturers. However, an exhaustive evaluation of the proposed solution must be performed before the integration of it in a commercial train. In order to optimize the design, development and test of the proposed train positioning system, a flexible simulation framework has been developed.

Regarding the cost efficiency objectives, a comparison of different IMUs in a experimental test has been carried out. The use of calibration techniques has allowed to reduce the initial proposal reducing the IMU cost 1000 times.

1.4 Publications

This thesis is a collection of four publications. In this section, the publications are listed and briefly introduced. In addition, the relationship between papers and the link to the research objectives can be shown in Figure 1.1.

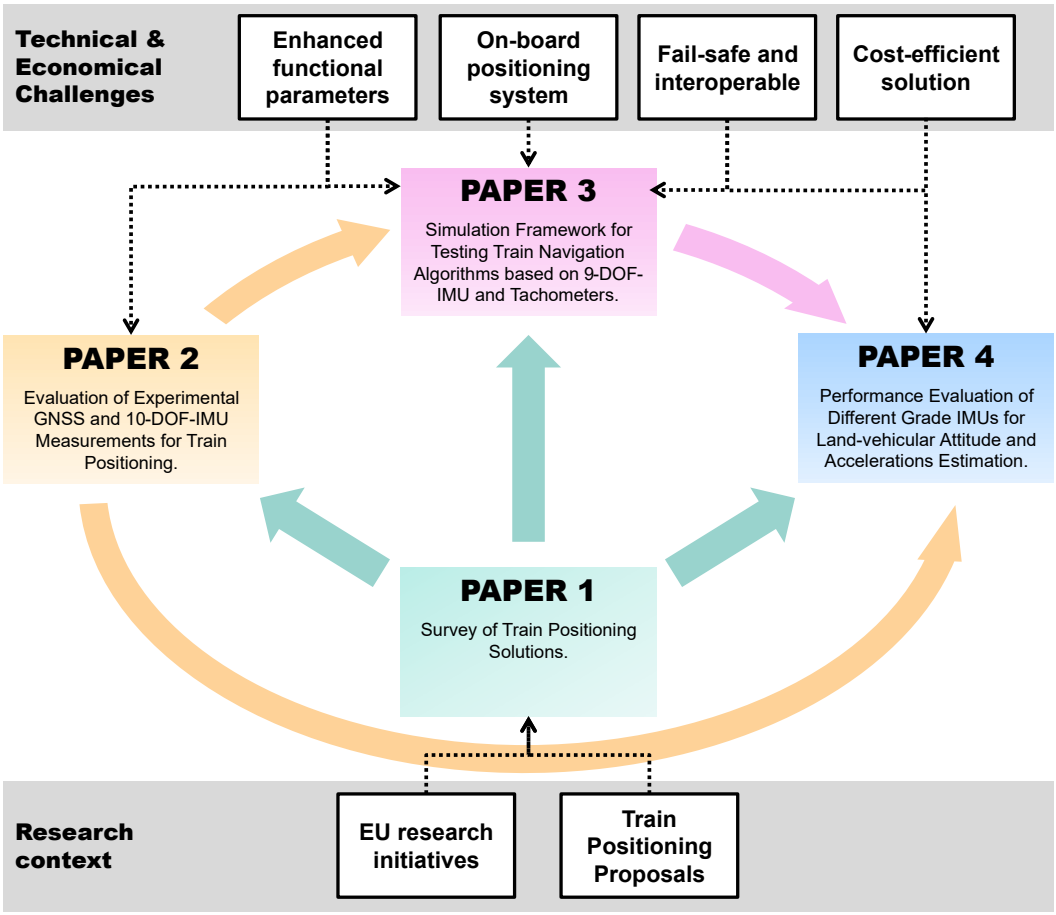

Figure 1.1: Relationship between the research objectives and publications.

1.4.1 Paper I

Paper I is titled *A Survey of Train Positioning Solutions* and it has been published in a JCR-Q1 journal (*IEEE Sensors Journal*). It presents an exhaustive evaluation of the state-of-the-art train positioning solutions under different criteria. It also highlights the main research gaps for future research.

J. Otegui, A. Bahillo, I. Lopetegi, and L. E. Díez, "A Survey of Train Positioning Solutions" IEEE Sensors Journal, vol. 17, no. 20, pp. 6788–6797, Aug. 2017.

IEEE Sensors Journal JCR IF (2017): 2.617
Q1 in Instruments & Instrumentation

9 citations in Web Of Science, 17 in Scopus and 19 in Google Scholar.
25 most downloaded Sensors Journal papers
in the month of December, 2017, January and February, 2018.

1.4.2 **Paper II**

Paper II is titled *Evaluation of Experimental GNSS and 10-DOF MEMS IMU Measurements for Train Positioning* and it has been published in a JCR-Q1 journal (*IEEE Transactions on Instrumentation and Measurement*). It presents an exhaustive experimental test description on which a GNSS and INS solution performance is compared to the current train navigation system.

J. Otegui, A. Bahillo, I. Lopetegi, and L. E. Díez, "Evaluation of Experimental GNSS and 10-DOF MEMS IMU Measurements for Train Positioning," IEEE Transactions on Instrumentation and Measurement, vol. 68, no. 1, pp. 269–279, Jan. 2019.

IEEE Transactions on Instrumentation and Measurement JCR IF (2018): 3.067
Q1 in Instruments & Instrumentation

1 citations in Web Of Science, 3 in Scopus and 2 in Google Scholar.

This work was selected to be presented in the flagship instrumentation and measurement conference, IEEE International Instrumentation and Measurement Technology Conference (I2MTC), during the poster session.

J. Otegui, A. Bahillo, I. Lopetegi, and L. E. Díez, "Evaluation of Experimental GNSS and 10-DOF MEMS IMU Measurements for Train Positioning," IEEE International Instrumentation and Measurement Technology Conference (I2MTC), Auckland, New Zealand, May 2019.

1.4.3 **Paper III**

Paper III is titled *Simulation Framework for Testing Train Navigation Algorithms based on 9-DOF-IMU and Tachometers* and it has been accepted for publishing in a JCR-Q1 journal (*IEEE Transactions on Instrumentation and Measurement*). It presents a flexible and one-stop simulation framework that enhances the functionalities of the up-to-date simulation frameworks to evaluate train navigation algorithms.

J. Otegui, A. Bahillo, I. Lopetegi, and L. E. Díez, "Simulation Framework for Testing Train Navigation Algorithms based on 9-DOF-IMU and Tachometers," IEEE Transactions on Instrumentation and Measurement, Accepted for publication.

IEEE Transactions on Instrumentation and Measurement JCR IF (2018): 3.067
Q1 in Instruments & Instrumentation

1.4.4 **Paper IV**

Paper IV is titled *Performance Evaluation of Different Grade IMUs for Land-Vehicular Attitude and Accelerations Estimation* and it is under review in a JCR-Q1 journal (*IEEE Access*). It presents a comparison of different grade IMUs, on which a calibration technique is proposed to mitigate the errors of a low-end IMU.

J. Otegui, A. Bahillo, I. Lopetegi, and L. E. Díez, "Performance Evaluation of Different Grade IMUs for Land-Vehicular Attitude and Accelerations Estimation" IEEE Access, Article under review.

IEEE Access JCR IF (2018): 4.098
Q1 in Information Systems & Computer Science

1.5 Outline

This thesis is divided into 6 chapters. Apart from introduction and conclusions, each of those chapters summarizes the publication that is dedicated to that same aspect. Each publication is self-contained. Therefore, each of them includes its own state-of-the-art section, proposes its research questions, and describes the particular strategy that it applies, which is tailored to the main research questions.

After this introduction (Chapter 1), chapter 2 presents and evaluates the main train positioning solutions published up-to-date. Chapter 3 focuses on a experimental test to evaluate GNSS and INS-based solution and its performance is compared to current train navigation solution. Chapter 4 presents a flexible and one-stop simulation framework to design and test different train navigation algorithms, mechanization methods, etc. in multiples scenarios (changing the features of trains, tracks, sensors and so on). Chapter 5 focuses on the cost optimization of the IMU, evaluating different grade solutions for land-vehicular positioning purpose. Chapter 6 summarizes the conclusions of this thesis.

The papers that comprise this thesis are appended at the end of each chapter.

If you want to have good ideas, you must have many ideas.

Linus Pauling

CHAPTER

2

Train Navigation Background

Over the last lustrum, several research projects have been launched regarding to the train positioning systems clustered into FP7 and Horizon 2020 European research and innovation programs. Most of them are related to satellite-based positioning systems and their integration into the rolling stock context. However, the safety and cost-efficiency requirements in addition to the technical limitations of current positioning system have propitiated this research area. Consequently, high amount of proposals can be found about this topic.

Although GNSS and INS arise as prominent systems to incorporate into the train positioning systems, there are no common criteria to define an architecture or to evaluate the performance of the solution achieved. In this context, this paper evaluates the 11^{th} most relevant works up to date according to test track, sensors characteristics, data fusion algorithm and the results evaluation techniques.

- Test and evaluation methodology: The track used to evaluate the positioning solution has utmost interest because it determines the features that are considered during the system evaluation. Consequently, test environment (simulated or experimental), challenging scenarios consideration (tunnels, urban

canyons, etc.), operation mode and maximum speed allowed in track, positioning mode (one- or three-dimensional), test duration and ground truth generation techniques are analysed for each work.

- Sensors characteristics: The sensors are classified into the candidate systems (GNSS and INS) and currently in use train sensors (tachometers, balise readers and Doppler radars). The evaluation is focused on candidate sensors where sensor type, model, frequency and cost among others are compared between different proposals.

- Data fusion algorithm: the estimation of navigation variables is evaluated according to the framework, data fusion algorithm, implementation mode, the number of state variables, orientation calculation and representation method, GNSS parameters and coupling method between GNSS and INS.

- Results evaluation: the performance of the proposals are compared each other regarding the analysis mode, the application, the error metrics and its values.

The main contribution of this paper is the search for research gaps in train positioning and the establishment of future standpoints. The four main research gaps concluded from this work are developed in the rest of papers of this dissertation.

Table 2.1: Test track analysis of the state-of-the-art proposals

Proposal	Test environment	Challenging features test/simulation				Train characteristics		Positioning mode	Test duration [h]	Ground Truth technique
		Slip/Slide	Tunnel	Forest	Urban	Operation mode	Maximum speed [km/h]			
(1)	Sim	Yes	Yes	No	No	VHS	400	3D	0.42	Simulated data
(2)	Exp	No	No	No	No	N/A	N/A	2D	N/A	DGPS solution
(3)	Exp	No	No	No	No	VLS	30	2D	3.00	RailML Database
(4)	Sim	Yes	No	No	No	HS	200	1D	0.16	Simulated Data
(5)	Exp	No	No	No	No	VLS	30	3D	N/A	N/A
(6)	Exp	No	Yes	No	No	HS	250	2D	N/A	N/A
(7)	Exp	No	No	Yes	No	N/A	N/A	2D	1.00	N/A
(8)	Sim	No	No	No	No	HS	200	2D	0.16	Simulated data
(9)	Exp	No	No	No	Yes	LS	70	1D	1.50	IMU + Tachometer
(10)	Exp	No	No	No	No	N/A	N/A	1D	0.03	Topography data
(11)	Exp	No	No	No	No	CS	120	1D	4.00	OSM Database

Acronyms: Experimental data (Exp) and Simulated data (Sim).
Very High Speed (VHS), High Speed (HS), Conventional Speed (CS), Low Speed (LS) and Very Low Speed (VLS).

Table 2.2: Sensors characteristics analysis of the state-of-the-art proposals.

Proposal	Candidate sensors characteristics										Currently in use train sensors
	GNSS				IMU						
	Type	Model	Frequency	Cost	Type	Tech	Model	DOF	Frequency	Cost	
(1)	High-end	N/A	1Hz	N/A	N/A	N/A	N/A	6	100Hz	N/A	Tachometer (20Hz) Balises Reader (300m)
(2)	High-end	N/A	1Hz	N/A	N/A	N/A	N/A	9	1Hz	N/A	Balises Reader (500m)
(3)	High-end	Septentrio Aste-Rx3	N/A	7100€	-	-	-	-	-	-	-
(4)	-	-	-	-	Customer Grade	MEMS	ECM S.p.A	6	N/A	N/A	Tachometer (N/A) Balises Reader (1000m)
(5)	High-end	Trimble Ashtech GG24	10Hz	1000€	Tactical Grade	MEMS	Watson BA604	6	125Hz	N/A	Tachometer (20Hz)
(6)	High-end	iNAT RQT4003	N/A	N/A	Navigation Grade	RLG	iNAT RQT4003	6	N/A	N/A	Tachometer (N/A)
(7)	N/A	N/A	2Hz	N/A	-	-	-	-	-	-	Doppler Radar (N/A) Balises Reader (N/A)
(8)	High-end	Trimble Ashtech MB100	N/A	900€	-	-	-	-	-	-	Tachometer (N/A)
(9)	-	-	-	-	Customer Grade	MEMS	MEGGITT SX43030	6	N/A	2800€	-
(10)	High-end	Septentrio Polar-Rx3	1Hz	N/A	Navigation Grade	MEMS	xSens MTi	6	10Hz	1500€	-
(11)	Low-end	u-blox LEA6T	1Hz	31.5€	Navigation Grade	MEMS	xSens MTx	6	200Hz	N/A	-

Table 2.3: Research results analysis

Proposal	Analysis mode	Application		Position and speed variables analyzed (Error metrics)	Values
		Type	Requirements		
(1)	Off-line	Non-Safety	No	Mean RMS Error	1.04m
(2)	Off-line	Non-Safety	No	Maximum RMS Error	1.5m
(3)	Off-line	Non-Safety	No	Track selectivity	94.2%
(4)	Off-line	Non-Safety	ETCS	Instantaneous Error in covered distance Instantaneous Error in speed	N/A
(5)	Off-line	Non-Safety	No	N/A	N/A
(6)	On-line	Non-Safety	No	Maximum Total Cumulative Error	27.29m
(7)	Off-line	Safety	EN50126 (RAMS and SIL)	-	-
(8)	Off-line	Non-Safety	No	Mean RMS Error Variance RMS Error	0.135m 0.136m
(9)	Off-line	Non-Safety	No	Cumulative Error in covered distance	6.4km
(10)	Off-line	Non-Safety	No	Mean RMS Error Maximum RMS Error	0.73m 1.46m
(11)	Off-line	Non-Safety	No	Track selectivity	99.7%

1. There are few works (only 27.27% of the evaluated works) that are able to test the proposed system in a flexible simulation framework, where different phenomena (e.g. wheel slip/skid, tunnels presence, vehicle vibrations, etc.) are simulated in order to analyse the system response (Table 2.1).

2. The experimental works used for evaluating proposed systems deals with lack of details on the test description (Table 2.2). The instrumentation used (train and track of the test, measuring architecture, etc.), as well as some of the characteristics of the proposed sensors (model, frequency and cost) are not given.

3. The solutions proposed in the analysed works are very ambiguous in economic cost (some proposals are around a thousand euros whereas other ones are below a hundred euros). A comparison of the performance of different candidate sensors has to be performed in order to know the main limitation of the lower cost proposals.

4. There are multiple techniques to asset the Ground Truth (GT) and to evaluate the solution metrics as shown in Table 2.3. The lack of standardized metrics makes difficult to provide an objective analysis of the solution accuracy and precision. Thus, GT establishment technique should be investigated and the quality of the method evaluated. The definition of the reference values of position has utmost relevance when evaluating the positioning solution and there is non-uniform criterion to define it (e.g. planimetry data or high-end sensors proposal are the most often used).

A Survey of Train Positioning Solutions

Jon Otegui, Alfonso Bahillo, Iban Lopetegi, and Luis Enrique Díez

***Abstract*— Positioning accurately and safely a train is nowadays a great challenge. That includes currently available railway sensors and new candidate sensors for data fusion. Global Navigation Satellite System and Inertial Measurement Unit sensors arise as prominent technologies to incorporate in railways. Although satellite-based train localization tests can be found in the scientific literature, there are no common criteria to evaluate the performance of the positioning achieved. In this paper, a series of criteria is defined and justified in order to be able to evaluate the most recent and relevant works related to train positioning. The results of this comparative analysis are gathered in tables, where the criteria defined are applied to the works compiled. According to the results obtained, a research gap in safety related applications is found. It is concluded that the economic viability of given solutions should be explored, so as to design an on-board train-integrated positioning system.**

***Index Terms*— Inertial sensors, satellite positioning, train navigation, data fusion, ground truth.**

I. Introduction

ALTHOUGH it may seem strange, nowadays, no train is positioned safely in an absolute reference frame. This means that railway operators cannot know the position of a train in precise longitude and latitude coordinates. This does not mean the railway management system is unsafe, because there are other techniques used [1]. The most usual system is one based on a beacon. The railway track is divided into so-called cantons. At the beginning of each canton, a beacon (or balise in railway jargon) is placed. When a train passes over it, the traffic management system detects that a train is in that canton (usually the length of the train is measured with axle counters). If another train is located right after this canton, the driver is notified and if there is no response after a while, the train is stopped automatically by its Automatic Train Protection (ATP) system. It is within this signaling system that odometry plays a key role in determining where the train is.

Odometry can be defined as the use of data from motion sensors in order to estimate changes in position over time. In recent years, the number of sensors available for odometry has increased significantly. These new available positioning sensors have found a gap in railway applications, and they can supplement the limitations of conventional sensors, as shown in Table I [2]–[5].

With the new paradigm of sensors available for positioning, their classification is required. Most authors have divided them into on-board sensors (tachometers, inertial sensors, satellite-based positioning systems, etc.) and infrastructure equipment (balises, track circuits, etc.) [1], [6]–[8]. In some cases, a more refined classification is made, based on the fundamentals of the sensor's technology [5]. A general sensor classification is shown in Table I, taking into account other authors works [5], [9].

Typical railway sensors include Doppler radar, the wheel sensor (also called a tachometer [2], [10], [11] or odometer [3], [5], [12], and the Balise transponder. Global Navigation Satellite System (GNSS) and Inertial Measurement Unit (IMU) are the main prominent fields for research. Eddy current sensors are a rather new kind of sensor, which recent research has demonstrated to be applicable as speed sensors [3], [6], [13]. In order to integrate sensors, data fusion is required [7], [13].

The design of train positioning architectures focused on train-integrated positioning systems itself presents many challenges. The first one is to overcome the inherent maintenance cost of infrastructure equipment [6], [14]–[16]. Track equipment is exposed to different weather conditions (temperature changes, ballast blows, rain, snow, etc.) as well as sporadic acts of vandalism, because it is installed in an open sky environment [17], [18]. Consequently, the repair and replacement of these devices contributes to increase their maintenance cost. The second one is also related to track equipment but under the interoperability point of view. Due to the historical deployment of railways, different railway management and signalling systems can be encountered over the world [1], [19]. This heterogeneity makes complicated the interoperability between countries. To overcome this limitation, Europe is deploying the European Rail Traffic Management System (ERTMS) to harmonize railway rules and regulations [19]. Future architectures of any kind of development related to interoperability shall fulfill ERTMS requirements. The third challenge is to validate the designed architecture as safety-critical, based on railway performance requirements [14].

This paper aims at presenting train positioning solutions and evaluating them based on common parameters and criteria (e.g. the sensors and algorithms used, the tests made for validation, the results obtained and analysed, etc.). The main contribution of this paper is the search for research gaps in train positioning and the establishment of future standpoints.

Manuscript received July 10, 2017; revised August 15, 2017; accepted August 17, 2017. Date of publication August 30, 2017; date of current version September 25, 2017. This work was supported by the Spanish Ministry of Economy and Competitiveness through the ESPHIA project under Grant TIN2014-56042-JIN. The associate editor coordinating the review of this paper and approving it for publication was Dr. Ying Zhang. *(Corresponding author: Jon Otegui.)*

J. Otegui is with DeustoTech-Fundación Deusto, Deusto Foundation, Av. Universidades, 48007 Bilbao, Spain (e-mail: jon.otegui@deusto.es).

A. Bahillo and L. E. Díez are with the Faculty of Engineering, University of Deusto, Av. Universidades, 48007 Bilbao, Spain (e-mail: alfonso.bahillo@deusto.es; luis.enrique.diez@deusto.es).

I. Lopetegi is with the Construcciones y Auxiliar de Ferrocarriles Investigación y Desarrollo, CAF I+D, 20200 Beasain, Spain (e-mail: ilopetegi@caf.es).

Digital Object Identifier 10.1109/JSEN.2017.2747137

TABLE I
TRAIN POSITIONING SENSOR CHARACTERISTICS

		Usual sampling frequency	Absolute positioning	Relative positioning (Dead--reckoning)	Position provided	Velocity provided	Long-term solution (large baselines)	Short-term solution (short baselines)	Instantaneous solution	Signal--denied problem	Slip and slide phenomena	Environment impact
On-board equipment	Doppler radar	N/A	No	Yes	No	Yes	No	No	Yes	No	No	Yes
	Eddy current sensor	N/A	No	Yes	No	Yes	No	No	Yes	No	No	No
	Wheel sensor	20Hz	No	Yes	No	Yes	No	No	Yes	No	Yes	Yes
	IMU	100Hz	No	Yes	No	No	No	Yes	Yes	No	No	No
	GNSS	1Hz	Yes	No	Yes	Yes	Yes	Yes	Yes	Yes	No	Yes
Track equipment	Balise transponder	N/A	No	Yes	No	No	No	Yes	Yes	No	No	Yes

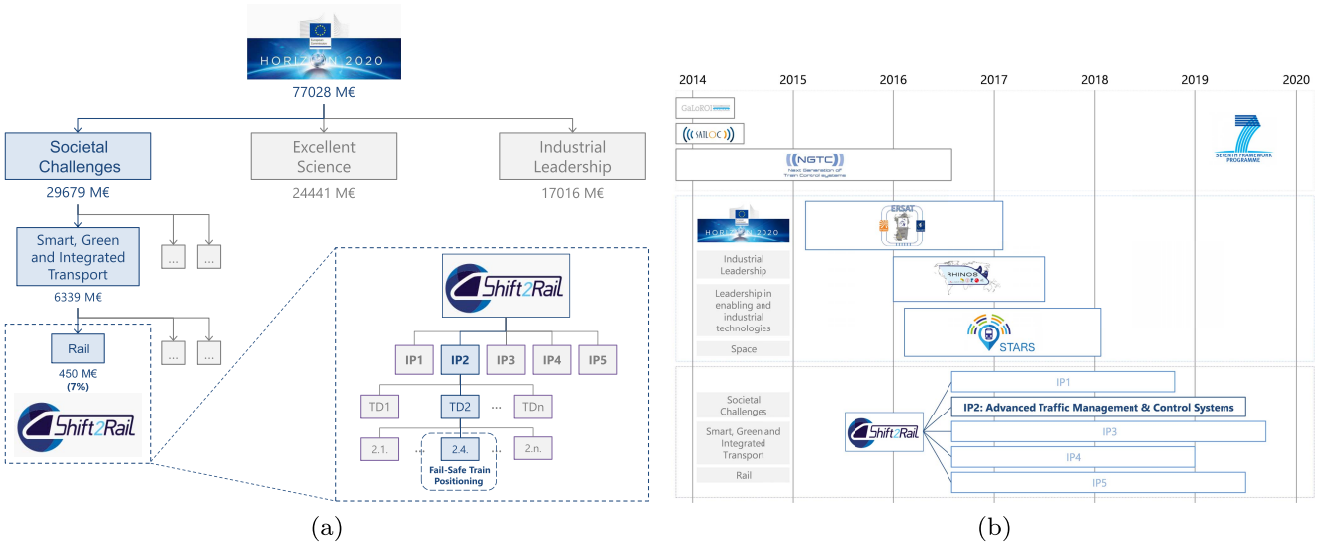

Fig. 1. European projects on train positioning: (a) Horizon 2020 and S2R breakdown. (b) Chronological train positioning context inside S2R and previous projects (GaLoROI, SATLOC, NGTC, ERSAT, RHINOS and STARS) feed.

Once the problem statement is introduced, in Section II the state of the art is presented. In Section III relevant works are evaluated by criteria defined and justified by the authors of the present paper. Finally, this paper's conclusions and future lines of research are described.

II. STATE OF THE ART

Over the last decade, important efforts have been made with regard to satellite-based positioning systems in order to adapt them to civilian applications (e.g. pedestrian and vehicle navigation). The development of Galileo (Europe) and BeiDou (China) are examples. The application of these constellations for train positioning is one of the main objectives of the European Space Agency (ESA) and the European GNSS Agency (GSA). As a sign of its interest, several projects have been funded by these institutions (INTEGRAIL [20], [21], ECORAIL [22], LOCOLOC [23], etc.).

In this section, the last three years of European research projects that have been focused on train positioning are presented. In order to have a general overview of train positioning research, the principal aims and the preceding projects are explained too. Later on, the most relevant works done in this context and the different authors' perspectives are discussed.

A. Train Positioning Research Projects

The railway sector has always been present in different European research programs developed in recent years (e.g. FP7 and Horizon 2020). Accordingly, there is a lot of information published about this topic. So, the following section aims at highlighting the most relevant conclusions, focused mainly on train positioning projects.

Horizon 2020 is the biggest European research and innovation program ever [24]. It is divided into three main areas, as shown in Figure 1a. Within it, all the investigation activities related to the railway are collected in Shift2Rail (S2R) [25].

S2R is the first European rail initiative that seeks research and innovation market-driven solutions to be integrated into innovative rail products [25], [26]. In order to tackle more specific objectives, 5 innovation programs (IP) have been designed, as shown in Figures 1a and 1b, where train navigation is tackled in the IP2 (Advanced Traffic Management and Control Systems). In the present paper, only projects based on Horizon 2020 are described, since it has been concluded that the know-how and conclusions of older research has been included in these.

ERSAT-EAV (ERTMS on Satellite Enabling Application and Validation) is the very first project launched inside S2R,

as shown in Figure 1b. The purpose is to verify the suitability of GNSS as the enabler of a cost-efficient and economically sustainable ERTMS signaling solution for railway safety applications [27]. It includes a measurement project, but it goes further, looking for a systematic solution (implemented, tested, and validated for safety applications).

RHINOS (Railway High Integrity Navigation Overlay System) is focused on applying GNSS in the railway context while ensuring architectures of high integrity. Its objective is to increase the use of GNSS to support the safety-critical train localization function for train control in emerging regional and global markets [28].

STARS (Satellite Technology for Advanced Railway Signalling) is meant to fill the gap between the needs of an ERTMS for safety critical applications and GNSS services. The key objectives are the development of a universal approach to predict the achievable GNSS performance in railway environments and the quantification of the economic benefits this technology can bring [29]. In essence, the aim is to include GNSS into ERTMS, maintaining both the safety and the interoperability of the system. The input of this project is the different work done in NGTC and ERSAT projects as well as older ones (GRAIL, LOCOPROL, LOCOLOC, etc.). The outputs should be the analysed data obtained from different railway tests.

A further survey of the research projects about the inclusion of GNSS in railway signaling systems is collected in [19].

B. Train Positioning Applications

As shown in the previous section, the applicability of GNSS to trains is of great interest. Nevertheless, its application is closely related to train safe-odometry, which necessitates the fulfillment of safety-critical requirements. These requirements are based on strong normative and this has made its introduction relatively slow [19].

GNSS presents limitations in signal-denied areas, such as tunnels, urban environments, and foliage. In such areas, no GNSS solution is available. Consequently, the safety integrity of the positioning system is jeopardized. The limitations of the availability of a GNSS signal in those areas is one of the main reasons why extra sensors are needed. Thus, researchers have focused on its integration via multisensory data fusion.

The very first article on data fusion related to train navigation presents candidate sensors for positioning and outlines a generic sensor fusion architecture [7]. The algorithms and sensors presented set the course for any later research, although some of the characteristics and technologies presented are nowadays obsolete (e.g. the selective availability in GPS signal and best accuracy reached, the nonexistence of an IMU technology based on Micro Electro Mechanical Systems (MEMS), a maximum sampling frequency of GNSS limited by 1 Hz).

Since that first publication, and in parallel with the development of technology (e.g. new GNSS constellations, the inclusion of MEMS in consumer electronics, etc.) many research articles have been published. In the following, some of the most important ones are highlighted.

Many authors have focussed on the localization of land vehicles and have extrapolated the architectures designed from this area to the railway context. Most of the literature available up to date are based on this idea [4], [12], [30]. Although trains are also land vehicles, they have special features (railway track constraints, slip and slide phenomena, smooth changes in trajectories and altitude, etc.) that necessitate a special architecture.

One of the first articles published related to this issue was a GPS and IMU fusion architecture [9]. It presents an explicit explanation of the equations needed to model the system as well as the results of field tests. It can be concluded that the same architecture nowadays will give more accurate results since the selective availability of GPS signal is now disabled. The system's overall cost will be lower too, by installing an IMU based on MEMS instead of the original one.

Other authors have tackled the train positioning problem by taking into account the dynamics of the train and the restrictions imposed by the track. The most relevant work in this sense has been done in a collaboration between the University of Florence and the University of Siena [10]. An implementation of a tachometer and a 6-DOF IMU was carried out combined with a train multibody model and the computation of multiple Kalman filters. The solution had a maximum error of about 20 m in travelled distance and 1.5 m/s in calculated speed, so it fulfills the European Train Control System (ETCS) requirements in terms of accuracy according to [31]. This work has some preceding papers, where the state of the art of railway sensors was presented and a Tachometer-IMU architecture discussed, building a railway vehicle dynamic model and developing a system with improved wheel velocity measurements [32]–[34].

A rather original standpoint is presented in [8] and [35]–[37]: instead of 3D positioning, the authors consider a train as a unidimensional vehicle constrained by a track. Thus, the algorithm only needs to solve a 1D problem. Thanks to track map information, the one-dimensional solution is then linked to a 3D map and the train can be located in absolute coordinates.

III. Review of Solutions

In this section, the most recent and relevant research done in the context of train positioning is collected and evaluated in terms of several criteria developed by the authors of the present paper. In the *Methodology* subsection, the definitions of the criteria are justified. In the *Results* subsection, the literature is evaluated based on these criteria.

A. Methodology

The evaluation methodology is divided into 4 steps, which are defined in chronological order. Firstly, the test track is analysed, that is, the environment where the presented papers are focused. Secondly, the used sensors are evaluated. As GNSS and IMU are the new sensors to be integrated into railway environments, their analysis is deeper than that of the sensors conventionally installed in trains. Thirdly, the data measured by the sensors should be treated, so the algorithms

TABLE II
TEST TRACK ANALYSIS

Authors	Test environment	Challenging features test/simulation				Train characteristics		Positioning mode	Test duration [h]	Ground Truth technique
		Slip/Slide	Tunnel	Forest	Urban	Operation mode	Maximum speed [km/h]			
[2]	Sim	Yes	Yes	No	No	VHS	400	3D	0.42	Simulated data
[4]	Exp	No	No	No	No	N/A	N/A	2D	N/A	DGPS solution
[6]	Exp	No	No	No	No	VLS	30	2D	3.00	RailML Database
[10]	Sim	Yes	No	No	No	HS	200	1D	0.16	Simulated Data
[11]	Exp	No	No	No	No	VLS	30	3D	N/A	N/A
[12]	Exp	No	Yes	No	No	HS	250	2D	N/A	N/A
[15]	Exp	No	No	Yes	No	N/A	N/A	2D	1.00	N/A
[16]	Sim	No	No	No	No	HS	200	2D	0.16	Simulated data
[30]	Exp	No	No	No	Yes	LS	70	1D	1.50	IMU + Tachometer
[36]	Exp	No	No	No	No	N/A	N/A	1D	0.03	Topography data
[37]	Exp	No	No	No	No	CS	120	1D	4.00	OSM Database

Acronyms: Experimental data (Exp) and Simulated data (Sim). Very High Speed (VHS), High Speed (HS), Conventional Speed (CS), Low Speed (LS) and Very Low Speed (VLS).

employed for that aim are evaluated. Fourthly, the outputs of the algorithms are analysed.

1) Test Track Analysis: For the test track analysis, 6 criteria have been defined and evaluated in the literature as seen in Table II. In the following paragraphs, each criterion is presented and justified.

Firstly, the test environment defines how the system is tested. In an experimental test, a set of measurements is carried out, in which a train is running on a track. This is the most realistic way to evaluate a system, but it needs a train and a track available to proceed with each test run. In some cases, this option is unfeasible (either the train is not available or there is no permission to run on the track) and a simulated test is carried out. In such a case, a track is modelled in the most similar way to a real one, taking into account the particular characteristics of a railway (radii of the curves, cants, slopes, etc.). In simulated tests, computational and programming efforts are needed in track and sensor signal construction, but more scenarios can be checked without additional cost.

The second criterion is related to the features of the test environment. The track selected for the test runs should have some restricted zones, where a GNSS signal is not available. Wheel and rail adhesion conditions should be degraded in places, as well. In simulated scenarios, these zones are rather easy to consider, but in experimental tests they depend on the track selected. That is why some tracks are more challenging for train positioning (those with large tunnels, urban canyons, foliage, or mountainous environments).

Another criterion related to the test track is the train operation mode. This can be dependent on the test track and type of train employed. Here, they are classified in terms of the maximum speed travelled in the test run (either experimental or simulated). The higher the speed, the smaller is the number of positioning nodes for a given space segment. Consequently, positioning in the same track will be done with fewer points in lines with higher speeds.

The positioning mode represents the number of variables devoted to locating the train. The unidimensional solution is a classical hypothesis in the railway context (a track constrained problem where two degrees of freedom, the cross track direction and vertical direction, are forced to be zero), where the covered distance from a known origin (relative distance) is calculated. In some papers, the relative distance is associated with a digital map that has the absolute coordinates [36], [37]. The bi-dimensional solution (longitude and latitude) is a particularization of the land vehicle localization problem (tri-dimensional) to the railway context, where the slopes are very smooth (up to 2.3 degrees in high speed lines [35]) and, hence, altitude changes can be considered negligible.

The next criterion is the duration of the test. Its justification is based on the huge amount of data that is created with larger test durations, and the associated problems that arise for the data treatment. Especially in research where track databases are used, the evaluation of the test duration is an important issue [37].

Finally, the Ground Truth (GT) technique is evaluated. GT is the reference position used to compare with the solution reached with data fusion algorithm. There exist multiple techniques for generating the GT. The easiest way is access to the railway track operator's data base. Nevertheless, this option is not always possible. An alternative is to use general purpose maps, such as Open Street Maps (OSM) or Google Maps. In these cases, the accuracy of the information provided should be evaluated [37]. Another possible method is the use of carrier phase measurements with reference station corrections in real time (RTK). This solution is proposed in the ERSAT and STARS projects [38]–[40]. However, this technique has limitations as well (GNSS signal availability, fixed base station communication, etc.) [41].

2) Analysis of the Sensors: The analysis of the characteristics of the sensors shown in Table III is focused on GNSS and IMU, which are the candidate sensors for integration into the railway environment. There are two main reasons why they were chosen for a detailed analysis. First, the know-how about these sensors and their application to the railway sector is quite limited, as is reflected in the amount of research effort that has been carried out in these areas [25], [27]–[29] [27]. Second, the market solutions available for GNSS receivers and IMU sensors are good in terms of functionality, accuracy and price. This requires an exhaustive investigation of the performance parameters required for railways.

In the case of GNSS, the first evaluation criterion is the receiver type. The GNSS receivers are classified as

TABLE III
SENSOR CHARACTERISTICS

Authors	Candidate sensors characteristics										Currently in use train sensors
	GNSS				IMU						
	Type	Model	Frequency	Cost	Type	Tech	Model	DOF	Frequency	Cost	
[2]	High-end	N/A	1Hz	N/A	N/A	N/A	N/A	6	100Hz	N/A	Tachometer (20Hz) Balises Reader (300m)
[4]	High-end	N/A	1Hz	N/A	N/A	N/A	N/A	9	1Hz	N/A	Balises Reader (500m)
[6]	High-end	Septentrio Aste-Rx3	N/A	7100€	-	-	-	-	-	-	-
[10]	-	-	-	-	Customer Grade	MEMS	ECM S.p.A	6	N/A	N/A	Tachometer (N/A) Balises Reader (1000m)
[11]	High-end	Trimble Ashtech GG24	10Hz	1000€	Tactical Grade	MEMS	Watson BA604	6	125Hz	N/A	Tachometer (20Hz)
[12]	High-end	iNAT RQT4003	N/A	N/A	Navigation Grade	RLG	iNAT RQT4003	6	N/A	N/A	Tachometer (N/A)
[15]	N/A	N/A	2Hz	N/A	-	-	-	-	-	-	Doppler Radar (N/A) Balises Reader (N/A)
[16]	High-end	Trimble Ashtech MB100	N/A	900€	-	-	-	-	-	-	Tachometer (N/A)
[30]	-	-	-	-	Customer Grade	MEMS	MEGGITT SX43030	6	N/A	2800€	-
[36]	High-end	Septentrio Polar-Rx3	1Hz	N/A	Navigation Grade	MEMS	xSens MTi	6	10Hz	1500€	-
[37]	Low-end	u-blox LEA6T	1Hz	31.5€	Navigation Grade	MEMS	xSens MTx	6	200Hz	N/A	-

high-end or low-end, depending on their functionalities (multi-constellation, multi-frequency, augmentation systems, corrections by code/carrier phase analysis, etc.) and, consequently, the performance requirements reached and price [14]. The sampling frequency in use has the utmost importance in order to evaluate the number of samples measured in a given space. The limitation of the selected sampling frequency is given by the receiver itself, that has a maximum allowable value. The manufacturer and model are used to identify the receiver.

In the case of IMU, the criteria presented are similar to those for GNSS. The IMU type, however, is classified into customer grade, navigation grade, or tactical grade, depending mainly on the bias stability [42]. However, other parameters, such as non-linearity, scale factor, or misalignment seem to be different too [43]. Furthermore, the technology employed inside the accelerometers and gyroscopes is presented. Depending on the performance wanted, different technologies are used: for tactical and navigation grades, the Ring Laser Gyroscopes (RLG) and Fiber Optic Gyroscopes (FOG) are predominant, whereas for consumer grade, MEMS seems to be the best trade-off between performance, size, and cost [42]. It is concluded that MEMS technology is the only one that is economically affordable for on-board equipment [44]. However, in future work, railway electromagnetic compatibility norms should be analysed for the case of MEMS sensors. In the very same way as GNSS receivers, the IMU manufacturer and model are used to identify the sensor. The very same criteria are used in sampling frequency and price.

A different criterion, added for the IMU, is the number of degrees of freedom (DOF). The DOF of an IMU represents the number of independent measurements that it is able to take. In a typical configuration, the IMU is formed by a tri-axial accelerometer and a tri-axial gyroscope, thus it has 6 DOF. However, in some recent land vehicle applications, a tri-axial magnetometer is added (9 DOF) so as to correct yaw drifts and attitude errors [45], [46]. In addition, a barometer can be installed (10 DOF) in some other applications in order to overcome the lack of precision of GNSS in the altitude coordinate [47].

The last sensors presented in this analysis are those currently available and installed on trains. As they are the usual sensors in the railway environment, a few criteria are used to evaluate them according to the data fusion algorithm. For instance, the frequency of the measurements: in Doppler radars and tachometers, the sampling rate is noted, whereas in balises the spacing between them is selected because their measurments depend on the train speed, location, or safety requirements.

3) Analysis of the Data Fusion Algorithm: Once the measurement system is defined by the sensors used in the test environment, a data fusion is executed. Multi-sensor data fusion relies on Bayesian theory and, more specifically, on a recursive Bayesian estimation that is used to solve the hidden Markov model (HMM) [48]. At this point, mathematical aspects and practical issues are related to each other to evaluate the data fusion techniques employed, as shown in Table IV.

The first criterion is the framework or the programming environment used to execute the data fusion algorithm. Then, the the algorithm implemented is analysed. Under recursive Bayesian estimation, the algorithms are classified into optimal filtering and non-optimal filtering [48]. Based on the literature in the railway context up to the present, the main representative algorithms of each group are the Kalman Filter (KF) and Particle Filter (PF), respectively.

The KF is a recursive linear estimator which successively calculates an estimate for a continuous valued state, which evolves over time, on the basis of periodic observations of the state [49]. Based on this definition, the general procedure behind the algorithm can be seen: the KF predicts a new state by knowing the previous state and a dynamic model of train movement. Then, it uses sensor measurements to correct the prediction made. The reason why it is classified as an optimal filter is due to its way of weighting the measured value and the

TABLE IV
DATA FUSION ALGORITHM

Authors	Framework	Algorithm	Implementation	Number of state variables	IMU to INS transformation	GNSS parameters	GNSS/IMU integration
[2]	Matlab	TS-FKF	Indirect	15	N/A	PVT solution	LC
[4]	Matlab	EKF	Indirect	13	Quaternion-based	PVT solution	LC
[6]	C++	IEKF	N/A	N/A	-	PVT solution	-
[10]	Matlab/Simulink	KF	Direct	6	Quaternion-based	-	-
[11]	Simulink	IF	Indirect	9	DCM based	PVT solution	LC
[12]	N/A	EKF	Indirect	25	N/A	Pseudorange	TC
[15]	N/A	N/A	N/A	N/A	-	PVT solution	-
[16]	Matlab	PF	N/A	6	-	PVT solution	-
[30]	Matlab	EKF	Direct	11	N/A	-	-
[36]	Matlab	PF	N/A	8	N/A	Pseudorange Doppler observable	TC
[37]	JAVA	RBPF	N/A	12	N/A	PVT solution	LC

Acronyms: Two-Staged Federated Kalman Filter (TS-FKF), Extended Kalman Filter (EKF), Iterated Extended Kalman Filter (IEKF), Kalman Filter (KF), Information Filter (IF), Particle Filter (PF), Rao-Blackwellized Particle Filter (RBPF), Loosely Coupled (LC), Tightly Coupled (TC).

predicted value, whcih is designed so that the error variance is a minimum [50].

However, the KF has some limitations in that it assumes the dynamic and measurement models are linear and normally distributed (Gaussian). In the railway context, the dynamic model of the train can be highly non-linear due to suspension stages, the wheel–rail adhesion law, etc. [51]. To overcome the restriction to linearity, the Extended Kalman Filter (EKF) can be used. In it, a linearization procedure is applied (a Taylor series expansion) to either the dynamic model or the measurement model.

In other cases, the Gaussian assumption is not fulfilled, and then the posterior probability density function should be modeled. With that aim, sub-optimal algorithms are used [48]. Some of them are variants of the KF, such as the Unscented Kalman Filter (UKF) or the Curvature Kalman Filter (CKF); others, such as the PF, present a new procedure that differs from the assumptions of the KF.

Depending on the algorithm employed, an implementation criterion is defined. The algorithms developed under the KF context can be implemented either directly or indirectly [52]. The direct implementation assumes that the measured states and the space states are equal, whereas in the indirect implementation, an error space state is defined. One of the advantages of the indirect implementation is that the errors of the states can be modelled and compesated in each iteration.

The number of navigation problem states should be at least equal to the number of unknowns in the position and velocity. In 3D positioning, the minimum number of states will be 6 (tri-dimensional position and tri-dimensional velocity). In the indirect implementation of the KF, the more state variables are used, the more error propagation parameters are modeled. But this implies using larger dimensional matrices, and consequently a higher computational burden.

The final three criteria are related to the IMU and GNSS data treatment techniques. First, a transformation is made between IMU sensor measurements (accelerations and turn rates) and the IMU sensor solution (position and velocity). This process is called mechanization, and a transformation from the body frame to the navigation frame is made. The resulting solution is called the Inertial Navigation System (INS) solution. The method of Euler angles, the direction cosine matrix (DCM), and a quaternion-based method are the most popular techniques for this process [53]. A comparison of these three methods is presented in [54].

Second, the GNSS receiver measured parameters are shown. In general, a GNSS receiver can give raw measurements of the received signal from satellites (Pseudorange, Code phase, Doppler shift) or a treated solution called the PVT (Position, Velocity and Time).

Third, the IMU and GNSS solution integration techniques are described. On the one hand, in a loosely coupled integration scheme, the filter updates the PVT solution of the GNSS receiver and the INS solution [36]. On the other hand, in a tightly coupled integration, the GNSS and IMU raw measurements are taken and fused. One of the advantages of a tightly coupled integration scheme is that the IMU accelerometers and gyroscopes can be recalibrated in real time [53]. On the contrary, some low-end GNSS receivers cannot provide raw measurements: therefore, tightly coupling is not feasible for those receivers.

4) Analysis of the Research Results: Finally, the criteria for the evaluation of the results are presented in Table V. These criteria are explained in the following paragraphs. The first criterion for the evaluation of the results is when were the results computed. The typical research analysis establishes that the data treatment is accomplished once the measurements are finished (post-processed or off-line). However, a real time data record and analysis (on-line) is of the utmost interest for train positioning because it represents a more realistic way to validate an on-board positioning system. This functionality, nevertheless, depends on the calculational power of the hardware.

Another relevant criterion is the application for which the research was intended. Depending on whether it is a safety or a non-safety application, the requirements associated to the designed system are different. The application will greatly determine the variables to be analysed in the research results.

In the case of non-safety applications, specific requirements can be analysed or a comparison of the results can be carried out in a more general way. In most cases, the research objective is focused on technological availability and technical

viability studies. Consequently, there are defined different error metrics in order to evaluate the performance of the solution.

In safety-critical applications, the governing norms are rather severe [19]. In railway applications, the reliability, availability, maintainability, and safety (RAMS) of the proposed system should be analysed according to the norm in EN 50126 [55].

Based on a RAMS analysis, the Safety Integrity Level (SIL) of the system must be determined. SIL prescribes requirements for safety-related functions so as to reduce and attain an acceptable risk [19]. The SIL related specifications are defined by qualitative measures and by a scale of Tolerable Hazard Rates (HTR) [19]. The higher the risk, the higher the SIL level and hence the requirements to be fulfilled. In the railway context, for a train protection system, the positioning is defined as SIL4 due to the dangerous situations that could arise from under- or over-estimating a train's position along the track [56].

B. Results

Using the methodology established and the criteria defined in the previous section, the most relevant literature of the last three years in the field of train positioning have been collected. The research presented here was done with different purposes and although common aspects have been highlighted, some others cannot be evaluated. The classification of the literature has been made in order of the appearance in the writing of the present paper.

The criteria that cannot be evaluated have been separated into two different types. The first refers to Not Available (N/A), which means that this criterion was used in the research but is not available in the publication. The second one is the hyphen (-), which refers to the fact that the criterion was not taken into account.

In Table II, the *Test track analysis* is collected. Most of the papers employ the experimental data obtained from systematic measurements in order to validate the research [4], [6], [11], [12], [14], [30], [36], [37]. Less than one-half of the publications (5 out of 11) use a challenging environment for the positioning sensors in their analysis. 60% of the challenging environments are real scenarios, where the train has pass through a tunnel, a forest, or an urban environment. According to the train operation mode, only 4 of these were run in high speed environments, and 2 of them are simulated environments. In positioning mode, the 2D solution is the most popular (5 out of 11) but a 1D solution accompanied by a track map is also much used (4 out of 11). The test duration seems to be quite erratic, because there is no single pattern in the literature (some are for 4 hours [37] whereas others are limited to 90 seconds [36]). Neither in the case of the GT is there a common information source. Note that some databases are not very accurate (5 meters imbalance between real and downloaded data), as has been demonstrated in [37].

In Table III, the positioning sensor characteristics are summed up. As mentioned previously, the comparison is focused on GNSS and IMU sensors. Beginning with the GNSS receivers, almost all the literature uses high-end type receivers, except for [37]. In the case of models, two papers use AsteRx/PolarRx (one is the preceding model of the other) receiver of the manufacturer Septentrio. One of the reasons why the authors have decided to use this model is related to the use of the same model in the ERSAT-EAV and STARS European research projects [38]–[40]. The sampling frequency, when it is provided, can be considered quite uniform, at 1 Hz (4 out of the 6 available) and coherent with the technology itself. The cost of the high-end type receivers in comparison with low-end type is very significant (two orders of magnitude approximately). This demonstrates that apart from their extra functionalities (multi-constellation, multi-frequency, differential GNSS, RTK, etc.) the internal signal analysis and PVT calculation algorithms, the error correction models, signal adaptation filters, etc. significantly increase the cost of the receiver.

In IMU sensors, there is a consensus on the use of MEMS technology, as was predicted in the previous section. There is only one exception, [12], where an RLG type INS is used. Although the MEMS technology is predominant, it uses different grades of sensor. Customer grade, navigation grade, and even tactical grade MEMS technology IMU sensors are presented in the analysed literature. A model made by the manufacturer XSens is used in the research reported in two different papers. The models presented (MTi and MTx) are widely used in land vehicle positioning [57], pedestrian localization [58], [59], and robotics [60]. Most of the research is based on 6-DOF measurements (7 out of 8) despite the availability of magnetometer data in some of them [11], [36], [37], but not used. The sampling frequency is not uniform at all, although mostly (3 out of 5) 100 Hz or higher is used [2], [11], [37].

As to the railway sensors, the tachometer is the most used sensor (5 out of 7) and its sampling rate is 20 Hz. In the case of balises, the spacing distance depends on the maximum allowable speed of the train. Thus, in a very high speed line, the spacing is lower (400 km/h and 300 m spacing) than in a high speed line (200 km/h and 1000 m spacing).

In Table IV the characteristics of the data fusion algorithm are highlighted. The predominant framework or programming environment is Matlab (6 out of 9). This is justified because of the nature of Bayesian estimation, which relies on multiple matrix operations, and this environment is appropriate for that [61]. As to the type of algorithm, all of them are based on recursive Bayesian estimation although the procedure employed for the data fusion can be quite different: most of them are variations of KF (7 out of 10) but some are related to PF (3 out of 10). The indirect implementation is more popular (4 out of 6) than the direct one because of the advantages presented before. The number of state variables is not uniform. All of them take position and velocity as state variables, but from this point on, the number of states associated to the errors modelled (indirect implementation) can be very different. There is not too much information presented about the transformation of the IMU measurements to the INS solution (3 available data out of 8 papers using IMU). In GNSS parameters, most of the papers employ the PVT solution (7 out of 9), which makes the loosely coupled integration scheme a common architecture.

TABLE V
RESEARCH RESULTS ANALYSIS

Authors	Analysis mode	Application		Position and speed variables analyzed (Error metrics)	Values
		Type	Requirements		
[2]	Off-line	Non-Safety	No	Mean RMS Error	1.04m
[4]	Off-line	Non-Safety	No	Maximum RMS Error	1.5m
[6]	Off-line	Non-Safety	No	Track selectivity	94.2%
[10]	Off-line	Non-Safety	ETCS	Instantaneous Error in covered distance Instantaneous Error in speed	N/A
[11]	Off-line	Non-Safety	No	N/A	N/A
[12]	On-line	Non-Safety	No	Maximum Total Cumulative Error	27.29m
[15]	Off-line	Safety	EN50126 (RAMS and SIL)	-	-
[16]	Off-line	Non-Safety	No	Mean RMS Error Variance RMS Error	0.135m 0.136m
[30]	Off-line	Non-Safety	No	Cumulative Error in covered distance	6.4km
[36]	Off-line	Non-Safety	No	Mean RMS Error Maximum RMS Error	0.73m 1.46m
[37]	Off-line	Non-Safety	No	Track selectivity	99.7%

In Table V, the research results are analysed. Beginning with the analysis mode, it is clear that the usual analysis of the results is based on post-processed data (10 out of 11). The reasons for this can be explained by many causes: approvals from the infrastructure managers to set up equipment, computational power requirements not fulfilled by on-board equipment (since on board units are dedicated devices to protect the train but not to record such large data sources), etc. As to the application, although most of the publications do not compare their results to specific requirements, in [10] the European Train Control System (ETCS) requirements [31] are analysed in order to evaluate the architecture proposed. In another paper, local governmental requirements are presented [5]. However, almost all the literature focusses on non-safety related applications (10 out of 11). Consequently, the implementation of such research in real train scenarios has a long way to go as long as safety requirements are not analysed. The only paper, [14], that analysed the railway safety-related performance properties (RAMS) calculates the following variables. The reliability is evaluated by the mean time to failure (MTTF), with a value of approximately 185 s. In addition, the solution availability reaches 82.26%. From the safety point of view, the hazard rate (HR) is divided into forest ($HR = 5.25 \times 10^{-2} h^{-1}$) and open area ($HR = 5.25 \times 10^{-7} h^{-1}$). The solution overall achieves SIL2.

In the papers presented, each author decides on the variables to be analysed. So, it is quite complicated to evaluate these results with the same criteria. However, some similar variables are collected and commented on the in the following. The maximum root mean square (RMS) error is approximately 1.5 meters, whereas the mean RMS error has a wider range (between 0.135 and 1.04 meters). Another parameter in common use in two papers is the track selectivity (i.e. the percentage of cases in which the track selection is carried out correctly) which is higher than 94% in two cases (94.2% and 99.7%).

IV. DISCUSSION AND CONCLUSIONS

In the present paper, a survey of the most recent and relevant train positioning solutions was presented and evaluation criteria were set in order to detect research gaps for future implementations. Based on this, several conclusions will be presented in this section. Analysing the tested track characteristics, more complex simulated environments can be developed. They should cover the majority of the situations in which the odometry can fail (e.g. poor wheel–rail adhesion, GNSS signal denied areas such as urban canyons, foliage, tunnels, and bridges, changes in meteorological conditions, system power supply turn-off, sensor failures, etc.). However, these simulated environments should also be tested in real scenarios (validation). Both simulated and real environments should be very high or high speed lines because this type of track seems to be the most critical (the measurements of the IMU and GNSS are taken in the largest space section).

A GT establishment technique should also be investigated and the quality of the method evaluated. According to the algorithms used to fuse the sensor measurements, the choice criteria should be related to the ability of the algorithm to run on-line. The designed architecture should consider the computational burden of the data fusion system in order to operate in real time. The technical viability of GNSS and IMU integrated solutions for non-safety related applications has been demonstrated by the the literature surveyed here. However, research focussed on safety-critical applications is very limited, and the fulfillment of the safety requirements is not guaranteed for ATP systems.

It seems clear from the current state of research that the eventual train positioning solution will integrate a low-end GNSS receiver and customer grade IMU sensor-based solutions. The economic viability of high-end solutions is unfeasible, due to their hllarge cost (thousands of euros). In this eventual solution, the sensors currently installed on trains (tachometers, Doppler radar, and balise readers) should be included as aided navigation sensors. The research challenge will come in the construction of low-cost (hundreds of euros) architectures that can fulfill the safety requirements.

The selection and justification of the optimum data fusion algorithm as well as the standardization problem of the validation parameters intend to be the most relevant future directions. In future works sensors data (10 DOF IMU and GNSS seems

to be most novel sensors in train context) obtained from a test run should be analysed under SIL requirements in order to evaluate Bayesian framework algorithms.

ACKNOWLEDGMENTS

The authors would like to thank CAF I+D for contributions to the knowledge of trains and railways that directly motivated the writing of this paper.

REFERENCES

[1] T. Albrecht, K. Luddecke, and J. Zimmermann, "A precise and reliable train positioning system and its use for automation of train operation," in *Proc. IEEE Int. Conf. Intell. Rail Transp. (ICIRT)*, Aug./Sep. 2013, pp. 134–139. [Online]. Available: http://ieeexplore.ieee.org/abstract/document/6696282/

[2] K. Kim, S.-H. Kong, and S.-Y. Jeon, "Slip and slide detection and adaptive information sharing algorithms for high-speed train navigation systems," *IEEE Trans. Intell. Transp. Syst.*, vol. 16, no. 6, pp. 3193–3203, Dec. 2015. [Online]. Available: http://ieeexplore.ieee.org/document/7123638/

[3] M. Marinov, S. Hensel, and T. Strauß, "Eddy current sensor based velocity and distance estimation in rail vehicles," *IET Sci., Meas. Technol.*, vol. 9, no. 7, pp. 875–881, Oct. 2015. [Online]. Available: http://digital-library.theiet.org/content/journals/10.1049/iet-smt.2014.0302

[4] Z. Wei, S. Ma, Z. Hua, H. Jia, and Z. Zhao, "Train integrated positioning method based on GPS/INS/RFID," in *Proc. 35th IEEE Chin. Control Conf. (CCC)*, Jul. 2016, pp. 5858–5862. [Online]. Available: http://ieeexplore.ieee.org/abstract/document/7554274/

[5] I. Durazo-Cardenas, A. Starr, A. Tsourdos, M. Bevilacqua, and J. Morineau, "Precise vehicle location as a fundamental parameter for intelligent self-aware rail-track maintenance systems," *Procedia CIRP*, vol. 22, pp. 219–224, Dec. 2014. [Online]. Available: http://linkinghub.elsevier.com/retrieve/pii/S2212827114008154

[6] M. Lauer and D. Stein, "A train localization algorithm for train protection systems of the future," *IEEE Trans. Intell. Transp. Syst.*, vol. 16, no. 2, pp. 970–979, Apr. 2015. [Online]. Available: http://ieeexplore.ieee.org/lpdocs/epic03/wrapper.htm?arnumber=6895280

[7] A. Mirabadi, N. Mort, and F. Schmid, "Application of sensor fusion to railway systems," in *Proc. IEEE/SICE/RSJ Int. Conf. Multisensor Fusion Integr. Intell. Syst.*, Dec. 1996, pp. 185–192. [Online]. Available: http://ieeexplore.ieee.org/abstract/document/572176/

[8] O. Heirich, P. Robertson, A. C. Garcia, and T. Strang, "Bayesian train localization method extended by 3D geometric railway track observations from inertial sensors," in *Proc. 15th Int. Conf. Inf. Fusion (FUSION)*, Jul. 2012, pp. 416–423. [Online]. Available: http://ieeexplore.ieee.org/abstract/document/6289833/

[9] B. Cai and X. Wang, Eds., "Train positioning via integration and fusion of GPS and inertial sensors," in *WIT Transactions on the Built Environment*. Southampton, U.K.: WIT, 2000.

[10] M. Malvezzi, G. Vettori, B. Allotta, L. Pugi, A. Ridolfi, and A. Rindi, "A localization algorithm for railway vehicles based on sensor fusion between tachometers and inertial measurement units," *Proc. Inst. Mech. Eng., F, J. Rail Rapid Trans.*, vol. 228, no. 4, pp. 431–448, May 2014.

[11] M. Larsson. (2014). *Sensor Fusion Application to Railway Odometry*. [Online]. Available: http://www.divaportal.org/smash/record.jsf?pid=diva2:754317

[12] C. Reimer, F. J. Müuller, and E. L. V. Hinüber, "INS/GNSS/odometer data fusion in railway applications," in *Proc. DGON Intertial Sensors Syst. (ISS)*, vol. 2. Karlsruhe, Germany, 2016, pp. 1–14.

[13] F. Böhringer and A. Geistler, Eds., "Adaptation of the kinematic train model using the interacting multiple model estimator," in *Advances in Transport*, vol. 74, no. 7. Southampton, U.K.: WIT Press, 2004.

[14] D. Lu and E. Schnieder, "Performance evaluation of GNSS for train localization," *IEEE Trans. Intell. Transp. Syst.*, vol. 16, no. 2, pp. 1054–1059, Apr. 2015. [Online]. Available: http://ieeexplore.ieee.org/document/6894605/

[15] J. Liu, B.-G. Cai, and J. Wang, "Track-constrained GNSS/odometer-based train localization using a particle filter," in *Proc. IEEE Intell. Vehicles Symp. (IV)*, Jun. 2016, pp. 877–882. [Online]. Available: http://ieeexplore.ieee.org/abstract/document/7535491/

[16] O. Heirich, P. Robertson, and T. Strang, "RailSLAM—Localization of rail vehicles and mapping of geometric railway tracks," in *Proc. IEEE Int. Conf. Robot. Autom. (ICRA)*, Karlsruhe, Germany, May 2013, pp. 5212–5219.

[17] R. Mazl and L. Preucil, *Sensor Data Fusion for Inertial Navigation of Trains in GPS Dark Areas* (Mathematics in Science and Engineering). San Diego, CA, USA: Academic, 2003.

[18] P. Ernest, R. Mazl, and L. Preucil, *Train Locator Using Inertial Sensors and Odometer* (Mathematics in Science and Engineering). San Diego, CA, USA: Academic, 2004.

[19] J. Marais, J. Beugin, and M. Berbineau, "A survey of GNSS-based research and developments for the european railway signaling," *IEEE Trans. Intell. Transp. Syst.*, to be published. [Online]. Available: http://ieeexplore.ieee.org/document/7857080/

[20] S. Bedrich and X. Gu, "GNSS-based sensor fusion for safety-critical applications in rail traffic," in *Proc. Galileo EGNOS Inf. Catalogue*, 2004, p. 8.

[21] H. Köpf, "InteGrail—Publishable final activity report," UNIFE-Assoc. Eur. Railway Ind., Brussels, Belgium, Tech. Rep. IGR-P-DAP-156-07, Apr. 2010.

[22] V. Thevenot, "ECORAIL-GNSS for safe railway road cross applications," AREVA, Noordwijk, The Netherlands, Tech. Rep. TA-1031195A, Jan. 2006.

[23] M. Rousseau, F. Wilms, S. Besure, and J. Willekens, "Final presentation," LOCOLOC, Noordwijk, The Netherlands, Tech. Rep., Dec. 2004.

[24] (2020). *Horizon*. [Online]. Available: https://ec.europa.eu/programmes/horizon2020/en/background-material

[25] *Shift 2 Rail*. [Online]. Available: http://shift2rail.org/

[26] C. Economou, "Shift2rail JU update and the role of the lighthouse projects," Shift2Rail, Brussels, Belgium, Tech. Rep., May 2015.

[27] *ERSAT EAV*, InnoTrans, Berlin, Germany, 2016.

[28] *RHINOS*. Accessed: Sep. 7, 2017. [Online]. Available: https://www.gsa.europa.eu/railway-high-integrity-navigation-overlay-system

[29] *STARS*. Accessed: Sep. 7, 2017. [Online]. Available: http://www.stars-rail.eu/project/

[30] D. Veillard, F. Mailly, and P. Fraisse, "EKF-based state estimation for train localization," in *Proc. IEEE SENSORS*, Oct./Nov. 2016, pp. 1–3. [Online]. Available: http://ieeexplore.ieee.org/abstract/document/7808726/

[31] *Performance Requirements for Interoperability (Subset-041)*, UNISIG, Brussels, Belgium, 2012.

[32] B. Allotta, L. Pugi, A. Ridolfi, M. Malvezzi, G. Vettori, and A. Rindi, "Evaluation of odometry algorithm performances using a railway vehicle dynamic model," *Vehicle Syst. Dyn.*, vol. 50, no. 5, pp. 699–724, May 2012. [Online]. Available: http://www.tandfonline.com/doi/abs/10.1080/00423114.2011.628681

[33] B. Allotta, V. Colla, and M. Malvezzi, "Train position and speed estimation using wheel velocity measurements," *Proc. Inst. Mech. Eng., F, J. Rail Rapid Trans.*, vol. 216, no. 3, pp. 207–225, Jan. 2002. [Online]. Available: http://pif.sagepub.com/lookup/doi/10.1243/095440902760213639

[34] M. Malvezzi, "Odometry algorithms for railway applications," Ph.D. dissertation, Dept. Appl. Mech., Univ. Bologna, Bologna, Italy, 2003.

[35] O. Heirich, A. Lehner, P. Robertson, and T. Strang, "Measurement and analysis of train motion and railway track characteristics with inertial sensors," in *Proc. 14th Int. IEEE Conf. Intell. Transp. Syst. (ITSC)*, Oct. 2011, pp. 1995–2000. [Online]. Available: http://ieeexplore.ieee.org/abstract/document/6082908/

[36] O. G. Crespillo, O. Heirich, and A. Lehner, "Bayesian GNSS/IMU tight integration for precise railway navigation on track map," in *Proc. IEEE/ION Position, Location Navigat. Symp. (PLANS)*, May 2014, pp. 999–1007. [Online]. Available: http://ieeexplore.ieee.org/abstract/document/6851465/

[37] O. Heirich, "Bayesian train localization with particle filter, loosely coupled GNSS, IMU, and a track map," *J. Sensors*, vol. 2016, no. 12, Mar. 2016, Art. no. 2672640. [Online]. Available: http://www.hindawi.com/journals/js/2016/2672640/

[38] *Test Procedure and Specification of the On-Field Measurement Campaign*, Ansaldo STS, Genoa, Italy, 2016.

[39] *Specification of the Measurement Information*, Genoa, Italy, AZD, SIEMENS, and Ansaldo STS, 2016.

[40] *Specification of the Field Measurement Procedures*, STARS, Genoa, Italy, 2016.

[41] S. S. Saab, "A map matching approach for train positioning. I. Development and analysis," *IEEE Trans. Veh. Technol.*, vol. 49, no. 2, pp. 467–475, Mar. 2000. [Online]. Available: http://ieeexplore.ieee.org/abstract/document/832978/

[42] M. Perlmutter and S. Breit, "The future of the MEMS inertial sensor performance, design and manufacturing," in *Proc. DGON Intertial Sensors Syst. (ISS)*, Sep. 2016, pp. 1–12. [Online]. Available: http://ieeexplore.ieee.org/abstract/document/7745671/

[43] S. Tripathi, P. Wagh, and A. B. Chaudhary, "Modelling, simulation & sensitivity analysis of various types of sensor errors and its impact on tactical flight vehicle navigation," in *Proc. Int. Conf. Elect., Electron., Optim. Techn. (ICEEOT)*, Mar. 2016, pp. 938–942.

[44] J. Ruppelt and G. F. Trommer, "Stereo-camera visual odometry for outdoor areas and in dark indoor environments," *IEEE Aerosp. Electron. Syst. Mag.*, vol. 31, no. 11, pp. 4–12, Nov. 2016. [Online]. Available: http://ieeexplore.ieee.org/abstract/document/7771818/

[45] F. Abyarjoo, A. Barreto, J. Cofino, and F. R. Ortega, "Implementing a sensor fusion algorithm for 3D orientation detection with inertial/magnetic sensors," in *Innovations and Advances in Computing, Informatics, Systems Sciences, Networking and Engineering*. Cham, Germany: Springer, 2015, pp. 305–310.

[46] E. Denti, R. Galatolo, and F. Schettini, "An AHRS based on a Kalman filter for the integration of inertial, magnetometric and GPS data," in *Proc. 27th Int. Congr. Aeronautical Sci.*, 2010, pp. 1–9.

[47] M. Tanigawa, H. Luinge, L. Schipper, and P. Slycke, "Drift-free dynamic height sensor using MEMS IMU aided by MEMS pressure sensor," in *Proc. 5th Workshop IEEE Positioning, Navigat. Commun. (WPNC)*, Mar. 2008, pp. 191–196. [Online]. Available: http://ieeexplore.ieee.org/abstract/document/4510374/

[48] Z. Chen, "Bayesian filtering: From Kalman filters to particle filters, and beyond," *Statistics*, vol. 182, no. 1, pp. 1–69, 2003.

[49] H. Durrant-Whyte and T. C. Henderson, "Multisensor data fusion," in *Springer Handbook of Robotics*. Cham, Germany: Springer, 2016, pp. 867–896.

[50] E. D. Kaplan and C. J. Hegarty, Eds., *Understanding GPS: Principles and Applications* (Mobile Communications), 2nd ed. Boston, MA, USA: Artech House, 2006.

[51] S. Iwnicki, *Handbook of Railway Vehicle Dynamics*. New York, NY, USA: Taylor & Francis, 2006.

[52] R. Munguía, "A GPS-aided inertial navigation system in direct configuration," *J. Appl. Res. Technol.*, vol. 12, no. 4, pp. 803–814, 2014. [Online]. Available: http://www.sciencedirect.com/science/article/pii/S1665642314700963

[53] M. S. Grewal, L. R. Weill, and A. P. Andrews, *Global Positioning Systems, Inertial Navigation, and Integration*, 2nd ed. Hoboken, NJ, USA: Wiley, 2007.

[54] *Specification and Demonstration of Reliability, Availability, Maintainability and Security (RAMS)*, UNE-EN 50126, Aenor, Madrid, Spain, 2005.

[55] D. H. Murillas and L. Poncet, "Safe odometry for high-speed trains," in *Proc. IEEE Int. Conf. Intell. Rail Transp. (ICIRT)*, Aug. 2016, pp. 244–248. [Online]. Available: http://ieeexplore.ieee.org/abstract/document/7588739/

[56] Q. Zhang, X. Niu, H. Zhang, and C. Shi, "Algorithm improvement of the low-end GNSS/INS systems for land vehicles navigation," *Math. Problems Eng.*, vol. 2013, no. 9, Jun. 2013, Art. no. 435286. [Online]. Available: http://www.hindawi.com/journals/mpe/2013/435286/

[57] A. R. Jiménez, F. Seco, J. C. Prieto, and J. Guevara, "Indoor pedestrian navigation using an INS/EKF framework for yaw drift reduction and a foot-mounted IMU," in *Proc. 7th Workshop Positioning, Navigat., Commun. (WPNC)*, Mar. 2010, pp. 135–143. [Online]. Available: http://ieeexplore.ieee.org/abstract/document/5649300/

[58] C. Fischer, P. T. Sukumar, and M. Hazas, "Tutorial: Implementing a pedestrian tracker using inertial sensors," *IEEE Pervasive Comput.*, vol. 12, no. 2, pp. 17–27, Apr. 2013. [Online]. Available: http://ieeexplore.ieee.org/abstract/document/6127851/

[59] D. Pierce, "Incorporation of a foot-mounted IMU for multi-sensor pedestrian navigation," Ph.D. dissertation, Dept. Mech. Eng., Univ. Auburn, Auburn, AL, USA, 2016. [Online]. Available: https://holocron.lib.auburn.edu/handle/10415/5074

[60] J. L. Blanco, "A collection of outdoor robotic datasets with centimeter-accuracy ground truth," *Auto. Robots*, vol. 27, p. 327, Nov. 2009.

[61] M. S. Grewal and A. P. Andrews, *Kalman Filtering: Theory and Practice Using MATLAB*, 3rd ed. Hoboken, NJ, USA: Wiley, 2008.

Jon Otegui received the degree in industrial technologies engineering and the M.Sc. degree in industrial engineering from the University of Navarra, in 2014 and 2016, respectively. His master's thesis was carried out in CAF I+D, with a focus on validation process of GNSS positioning technology in railway environment. He is currently pursuing the Ph.D. degree with the Mobility Research Group, Deusto Institute of Technology, under the supervision of Dr. A. B. Martinez. His main research line is the development of data fusion algorithms for railway odometry. His work is focused in multisensor data (wheel speed sensor, IMU, GNSS, and Balise) and its integration in train localization system for safety critical applications.

Alfonso Bahillo received the degree in telecommunications engineering and the Ph.D. degree from the University of Valladolid, Spain, in 2006 and 2010, respectively. From 2006 to 2010, he joined CEDETEL, as a Research Engineering. From 2006 to 2011, he has been an Assistant Professor with the University of Valladolid. From 2010 to 2012, he joined LUCE Innovative Technologies, as a Product Owner. From 2013 and 2017, he held a post-doctoral position at the University of Deusto and Project Manager at DeustoTech, Bilbao, where he trains Ph.D. students and collaborates in several national and international research projects. He has worked (leading some of them) in more than 25 regional, national, and international research projects and contracts. He is currently the Director of DeustoTech. He is co-author of 20 research manuscripts published in international journals, more than 40 communications in international conferences, and three national patents. His interests include local and global positioning techniques, ambient assisted living, intelligent transport systems, wireless networking, and smart cities. He received the PMP Certification at PMI in 2014.

Iban Lopetegi received the M.Sc. degree in telecommunication engineering from the University of Mondragon and the Ph.D. degree in electronics and communications from Newcastle University, U.K. Since then, he joined the CAF Research and Development Department and has worked in various strategically key projects of the company.

Luis Enrique Díez received the B.Sc. degree in telecommunications engineering from the University of Deusto in 2005 and the M.Sc. degree in communication technologies and systems from the Polytechnic University of Madrid in 2012. He is currently pursuing the Ph.D. degree in pedestrian navigation systems with the Mobility Research Group, DeustoTech, Bilbao. From 2005 to 2011, he was with Everis, as a Senior IT Consultant. From 2013 to 2014, he was with the SOFTLAB Research Group, Charles III University of Madrid, as a Research Support Technician. His research interests include positioning systems, data fusion, and context-aware applications.

Every brilliant experiment, like every great work of art, starts with an act of imagination.

Jonah Lehrer

CHAPTER

3

Candidate Sensors Analysis

The current train positioning systems are based mainly on odometry and track circuits but they present both technical and economical limitations. The combination of GNSS and INS arise as prominent solution to overcome the current system limitations as shown in the paper I.

However, according to one of the research gaps detected on paper I, the instrumentation and measurement of the candidate sensors (GNSS and IMU) in experimental tests can be improved in order to characterize their behaviour into the train navigation context. Consequently, the analysis of both the raw-measurements and data-fused solution is considered a key work to highlight the virtues and main limitations of the candidate sensors.

In this paper a experimental test on a railway is described and it broadens the test equipment, railway description and measuring architecture information from other works. In addition, it proposes a GNSS and INS data fusion algorithm based on Septentrio AsteRx3 GNSS receiver and xSens MTi-300 IMU sensor. Then, the raw measurements of the accelerometers and gyroscopes, planimetry and altimetry solution and the estimated velocity by GNSS and INS fusion are analysed. The estimated velocity is compared statistically to the one provided by the current train navigation system. Finally, additional parameters related to the track are estimated highlighting further positioning options that arise with the utilization of the INS.

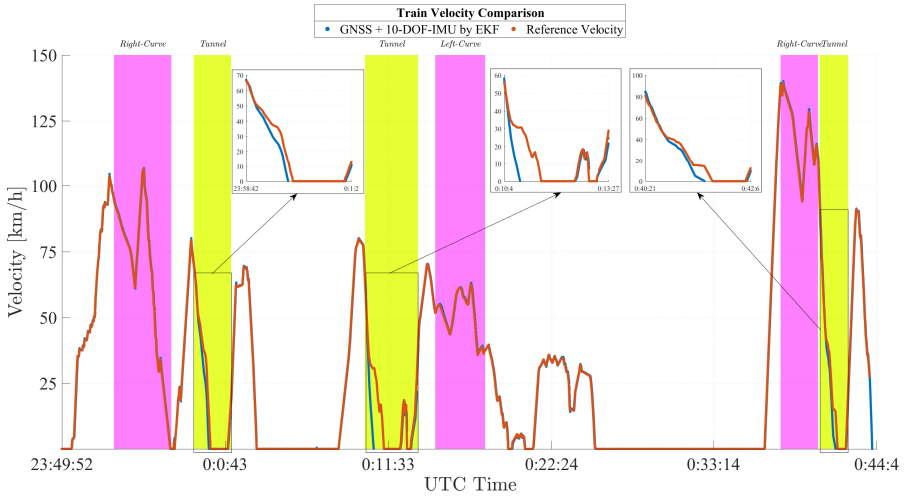

Figure 3.1: Comparative of velocity solution between GNSS+INS and current system.

In order to see the influence of the candidate sensors measurements into the velocity solution, GNSS and IMU measurements are integrated in loosely coupled configuration and fused by a 15-states-EKF (Figure 3.1). The sensors measurements are obtained from a experimental test carried out a section of high-speed track between Madrid, Valencia, and Seville (Spain). The journeys are there and back trips from Yeles station (start point) and Valdemoro station (endpoint).The train crosses a tunnel of 103.4 m (represented in yellow) and a curve of 5.4 km three times (twice in the Valdemoro direction and once in the Yeles direction, represented in pink). The GNSS signal outage zones (tunnel crossings) are zoomed-in to highlight the INS drift. According to the most exigent ERTMS accuracy requirements (i.e. maximum allowable velocity error must be 2 km/h), the proposed GNSS and INS architecture provides 2 km/h or lower error during the 93.53% of the journey.

The main contributions of this paper can be summed up as follows.

1. It provides a detailed description on the instrumentation and measuring architectures. The data acquisition, processing and time synchronization features related to the candidate and current sensors are shown.

2. It characterizes the behaviour of GNSS and IMU measurements under the

train dynamics and railway context. The measuring ranges, tunnels, cants, slopes and curves influences on candidate sensors are shown. This analysis can help to the generation of synthetic signals of candidate sensors in more accurate way.

3. It provides an accurate solution based on GNSS and INS compared to the current system (Figure 3.1): an absolute error in velocity lower than 2 km/h in more than 90% of the test duration is reached. However, the INS stand-alone dead-reckoning solution drifts when the GNSS signal is not available, as shown in the three tunnel crossings during the test.

4. It offers an enhanced solution compared to the current system: track parameters, such as curve radius, cant and slope are estimated using the IMU raw measurements and longitudinal velocity provided by GNSS. This fact makes possible the utilization of IMU in combination with external velocity (provided by any kind of sensors such as wheel speed sensor, Dopper radar, Eddy-current sensor or GNSS) for estimating instantaneous cant, slope and curve radius of the track and, actually, for map-based positioning.

Evaluation of Experimental GNSS and 10-DOF MEMS IMU Measurements for Train Positioning

Jon Otegui, Alfonso Bahillo, Iban Lopetegi, and Luis Enrique Díez

***Abstract*— Integrating new candidate sensors, such as Global Navigation Satellite System (GNSS) and inertial measurement unit (IMU), into fail-safe train positioning systems have recently become a prominent area of research. Although there are a number of contributions related to the design of data fusion algorithms, the lack of details in raw measurements analysis has directly motivated this paper. This paper aims to record data from a variety of sensors (such as GNSS, IMU, magnetometer, barometer, tachometers, and Doppler radars) to evaluate train velocity and railway features (track slope, curve cant, and radius) extending previous works in the instrumentation and measurement field. The field test designed and concisely described in this paper presents several challenging environments, such as a tunnel, which can be used to analyze the candidate sensors limitations. In addition, a demonstration of a data fusion algorithm is presented to calculate train velocity based on measurements from the candidate sensors. The results obtained by an extended Kalman filter using GNSS and IMU are compared with velocity recorded by tachometers and Doppler radars, which is considered to be the reference value. The calculated velocity by IMU and GNSS when both sensors measurements are available presents an absolute error in velocity lower than 2 km/h in more than 90% of test duration. Finally, railway features (curve radius, cant, and slope) are calculated and analyzed according to train and railway dynamics.**

***Index Terms*— Inertial sensors, Kalman filtering, railway vehicle, satellite positioning, sensor fusion, train navigation.**

I. Introduction

TRADITIONAL train navigation systems rely on a combination of track-side and vehicle-borne subsystems, which are able to calculate instantaneous speed and covered distance by train [1], [2]. Odometry sensors are commonly used for this purpose, such as wheel speed sensors (also known as tachometers, encoders, odometers or phonic wheels [3]), Doppler radars, and eddy-current sensors [2].

Manuscript received January 23, 2018; revised March 27, 2018; accepted May 8, 2018. Date of publication June 5, 2018; date of current version December 7, 2018. This work was supported in part by the Spanish Ministry of Economy and Competitiveness through ESPHIA Project under Grant TIN2014-56042-JIN and in part by the Basque Country Department of Education through BLUE Project under Grant PI-2016-0010. The Associate Editor coordinating the review process was Dr. Daniele Fontanelli. *(Corresponding author: Jon Otegui.)*

J. Otegui is with DeustoTech-Fundación Deusto, Deusto Foundation, Av. Universidades, 48007 Bilbao, Spain (e-mail: j.otegi@gmail.com).

A. Bahillo and L. E. Díez are with the Faculty of Engineering, University of Deusto, Av. Universidades, 48007 Bilbao, Spain (e-mail: alfonso.bahillo@deusto.es; luis.enrique.diez@deusto.es).

I. Lopetegi is with Construcciones y Auxiliar de Ferrocarriles Investigación y Desarrollo, CAF I+D, 20200 Beasain, Spain (e-mail: ilopetegi@caf.net).

Color versions of one or more of the figures in this paper are available online at http://ieeexplore.ieee.org.

Digital Object Identifier 10.1109/TIM.2018.2838799

However, in the last 30 years, the rapid development of telecommunication technologies and electronics has led to the emergence of new sensors. For example, Global Navigation Satellite Systems (GNSSs) and inertial measurement units (IMUs) are widely used in civilian applications.

GNSS can provide absolute positioning information when at least four satellites are visible. This presents a completely new standpoint in a train environment because relative positioning is no longer the unique method localization. However, the absence of a GNSS signal provokes availability problems (when a train is inside a tunnel for instance), which can bring the entire system into a safe state (e.g., by stopping the train) unless there are other sensors capable of providing position (i.e., an IMU). In addition, the high levels of safety that are required by railways have slowed down the inclusion of GNSS in trains [4], [5].

IMUs have been used in areas such as aviation or maritime navigation for many years. However, microelectro-mechanical systems (MEMSs) have been widely used in inexpensive applications, such as drone navigation or indoor pedestrian localization [6]. In the train positioning context, they are considered to be candidate sensors for future fail-safe train positioning systems because they can overcome the limitations of traditional sensors. For example, wheel speed sensors suffer from slip/slide phenomena when wheel and rail conditions are degraded. They are also dependent on the knowledge of the wheel diameter, which can change according to wear or instantaneous contact point (note that train wheels are conical). Doppler radars also present limitations that are caused by the weather. For example, snow can reflect the wave emitted and received by the radar. Meanwhile, the development of MEMS applied to IMU manufacturing has significantly reduced its cost. Consequently, the price drawback of Doppler radars (thousands of euros) in comparison with the IMU (hundreds of euros) is also remarkable. However, IMUs also present limitations that should be analyzed before its integration in a positioning system. The main one is related to the accumulating errors that grow over time, whose modeling and quantification have received significant scientific research attention [7], [8]. Another errors related to the IMUs are those coming from measurement, such as vibrations, atmospheric pressure changes, or electromagnetic disturbances. The analysis of magnetic effects [9], [10] and pressure sensors [11] is a prominent field of research in indoor positioning although it is rather novel in the railway context.

In order to overcome GNSS and IMU standalone respective limitations, data fusion techniques are used. Since the first publication about multisensor data fusion in railways in 1996 [12], a number of studies have researched the integration of GNSS and IMU in train positioning systems. A detailed analysis of most relevant previous works related to data fusion can be found in [13]. However, Marinov *et al.* [14] have stated that these techniques are prohibitive in railway scenarios due to forests, valleys, tunnels, heavy weather, and dirt existence. In this context, experimental data play a key role to evaluate GNSS and IMU raw data in the railway environment and highlight the main limitations of these candidate sensors.

On the one hand, the experimental data fosters the characterization of the environment in which the sensors will work to understand the performance and behavior of the sensors. The analysis of the raw data can be used to evaluate the performance of the sensors in terms of accuracy, precision, availability, etc. The performance of the sensors is related to safety and availability features and it plays a key role in reaching the safety integrity level that is required in train navigation. In the case of railways, tracks are designed to avoid train derailment, ensure passengers comfort, and optimize energy efficiency [15]. This makes the measurements recorded on the railway different from those recorded on the road. (The curve radii and tunnels length are higher in railroads than in common roads, the slope and turning maneuvers are limited, etc.) In addition, railways are often exposed to electromagnetic effects due to catenary or electric motors, temperature gradients, and heat associated with climatic issues or geographical obstacles present in the railway (valleys, urban canyons, tunnels, etc.), which can influence the measurement devices. All these features suggest that measurements recorded in a railway test will have particularities compared with indoor localization or robot positioning contexts, for instance. Based on this idea, an exhaustive analysis of accelerometers and gyroscopes is presented in [16]. In this paper, raw measurements of acceleration and angular rate are analyzed and associated with track features (i.e., cant or bank angle and curvature). However, GNSS, magnetometer, and barometer signals are not analyzed in this paper.

On the other hand, the experimental data are the most suitable way to validate a system. However, the availability of test equipment is not always a trivial issue in rolling stock. Thus, the simulation environment arises as a potential alternative when experimental tests are unfeasible (e.g., no train available, lack of permission to run on the track, and high economical cost). In this case, all of the elements involved in the test must be modeled: tracks must take into account particular characteristics of the railways (radii and cants of the curves, slope, and attitude bounds of the track, etc.), train dynamics should be fulfilled (rolling characteristics, primary and secondary suspensions, axle, and wheel rigidity, etc.) and the sensors' behavior needs to be studied (temperature influence, signal bias, and drift, etc.). Therefore, computational and programming efforts are required in simulated tests. One of the most remarkable works in the use of a simulated environment in the railway context can be found in [17]. In this paper, a localization algorithm is presented, which is fed by experimentally obtained tachometers, a tri-axial accelerometer and a tri-axial gyroscope measurements. Some preceding studies include the improvement of wheel speed sensor measurements [18], [19], a dynamic model of a train [20], [21], and an analysis of data fusion algorithms [22], [23]. In addition, covered distance and velocity solutions have been evaluated and compared with European train control system (ETCS) requirements. It is concluded that the proposed and designed system in this paper fulfill these requirements. However, the testing methodology is based on externally gathered data and, consequently, instrumentation and measurement data are not detailed.

The work presented in this paper is motivated by the lack of instrumentation and measuring architectures detail in previous works and the need of GNSS and IMU raw measurements analysis in railway environment before their integration in fail-safe train positioning systems. Similar works are published in related fields (such as aeronautical) in order to characterize the dynamics of rollators and quadrotors [24], [25].

This paper evaluates GNSS and ten DOF IMU experimental data for train positioning systems and it aims at extending the most relevant previous works in the field of instrumentation and measurement [16], [17], [23]. Based on the raw measurements evaluation, train velocity calculation method is proposed and track features are calculated. The results of this paper can help us to understand the behavior of these sensors in a railway context and, consequently, to better model the sensors in simulated environments. It can also contribute to detect the main limitations of the candidate sensors.

The rest of this paper is organized as follows. In Section II, the experimental test is described in detail. In Section III, a simple data fusion algorithm is described and the reference velocity is defined. In Section IV, raw measurements are analyzed and data fusion techniques are applied to the measurements. Finally, in Section V, the main conclusions of the work are highlighted.

II. Test Description

The experimental field test is executed in a real environment to evaluate in the most realistic way inertial sensors (accelerometers and gyroscopes), magnetometers, barometer, and satellite positioning systems in a railway context. Although the overall duration of the test run is about 4 h, the measurements used for analysis correspond to an hour record, approximately. This is done as a tradeoff between the data representativeness and ease of visualization of the measurements. The chosen section is considered the most representative section of all of the tests according to the characterization of the sensors (e.g., GNSS outages, IMU drift, and railway typical features as curves or cants). The test is executed running below 160 km/h, which is the maximum allowed velocity in the section where the test is carried out.

A. Test Equipment

The railway vehicle employed for the test is formed of four cars with distributed traction (i.e., all the cars are motorized) which are fed by 25 kV in alternative current (50 Hz). The vehicle has 920-mm nominal diameter wheels and the floor

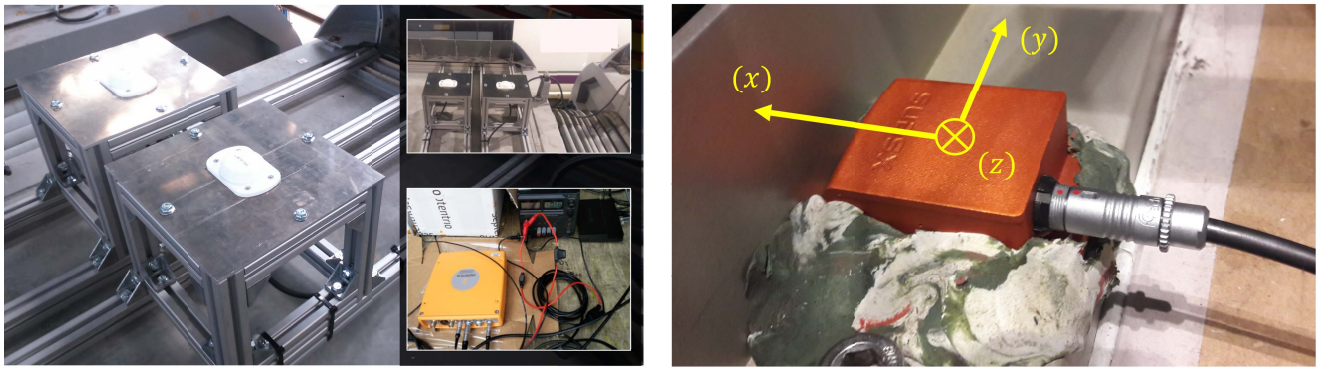

Fig. 1. Experimental setup in the train. (a) AntCom 42AT1 GNSS antennas mounted over the train roof and a Septentrio AsteRx3 GNSS receiver. (b) xSens MTi-300 Series IMU fixed with plasticine to avoid vibrations caused by wheel and rail contact. The IMU axes are aligned to the train's longitudinal direction (x, forward-positive), lateral or transversal direction (y, right-positive), and vertical direction (z, down-positive).

height is 1260-mm above rail. It is equipped with a GNSS receiver, 10 DOF IMU, four tachometers, and two Doppler radars.

A Septentrio AsteRx3 GNSS receiver is used during the test in multiconstellation and multifrequency mode. Both raw data and position, velocity, and time (PVT) data are recorded. The sampling frequency is established as 1 Hz according to the recommendations in [26] and [27]. AntCom 42AT1 GNSS antennas are used because they are certified by Septentrio for their devices. The antennas are installed over the roof of the train in a specific device built for fixing them [Fig. 1(a)]. The GNSS receiver admits double-antenna configuration to record extra measurements (e.g., attitude calculation); therefore, in this test these extra measurements are also recorded.

The IMU is an xSens MTi-300 Series model with an integrated tri-axial magnetometer and a barometer. The sampling frequency used in the accelerometer, gyroscope, and magnetometer is 100 Hz, whereas in the barometer the maximum rate it is 50 Hz. The IMU is located inside the train in the drivers cab, fixed with plasticine over the floor to avoid direct contact between metals and consequent vibrations due to train movement [Fig. 1(b)]. The lever arm phenomena is considered to be negligible because of the proximity of the IMU and GNSS antennas.

These sensors are used following the recommendations about the appropriateness of a GNSS receiver and IMU in the railway context. The GNSS receiver that we used allows a time synchronization based on pulse-per-second (PPS) electrical flag and the recording interface supports extra features recordings (multipath model, dilution of precision, signal-to-noise ratio, etc.), which are not available in most of the GNSS receivers. The IMU is a reference device and is used in different positioning contexts and also in train navigation research works [16], [28], [29].

The Doppler radar that we used is the CORREVIT R-350 Rail model that is supplied by Corrsys-Datron. The wheel speed is measured with hall-effect type sensors that are supplied by Lenord–Bauer.

A DEWESoft Minitaur and a Lenovo T400p laptop are configured as data acquisition units for the GNSS receiver and IMU. A dongle GPS (z050 Universal Serial Bus GPS Dongle) is also connected to the Lenovo T400p laptop to get GPS time from the satellites and to synchronize the measurements of the laptop with values of the DEWESoft Minitaur.

B. Railway Description

The railway that we used for the test is a section of high-speed track between Madrid, Valencia, and Seville (Spain). The test was executed between the stations of La Sagra, Valdemoro, and Los Gavilanes, with multiple there and back journeys; as shown in Fig. 2. The track has a gauge of 1435 mm (i.e., international gauge) in all of the itinerary. In high-speed operation zones, the minimum curve radius is 4000 m and the maximum slope is 1.25%, which can be considered typical for high-speed lines. The maximum speed is limited to 300 km/h, although the design of the infrastructure can be used in the future for operational speeds of up to 350 km/h.

The track that we selected covers a tunnel of 103.4 m, which will be used to evaluate GNSS signal outage and signal degraded environments. The rest of the track has an open-sky view and it can be considered a relatively flat terrain (e.g., the maximum height change is about 100 m). As the majority of high-speed lines it is far away urban regions.

C. Measuring Architecture

The measuring architecture describes how the sensors' data are recorded in data acquisition units (Fig. 3). In this test, two computers or data acquisition units were used (DEWESoft Minataur and Lenovo T400p) because they do not have enough inputs to record all of the data in the same device. When multiple data acquisition units are in use, synchronization of measurements between devices must be guaranteed. Consequently, GPS time was used. The errors derived from synchronization (about 40 ns in GPS time) are considered to be negligible according to the sampling rate used for sensors.

The recording software used for Septentrio AsteRx3 GNSS receiver was RX-Tools [30]. The output file format was a proprietary format called Septentrio binary file. In this paper,

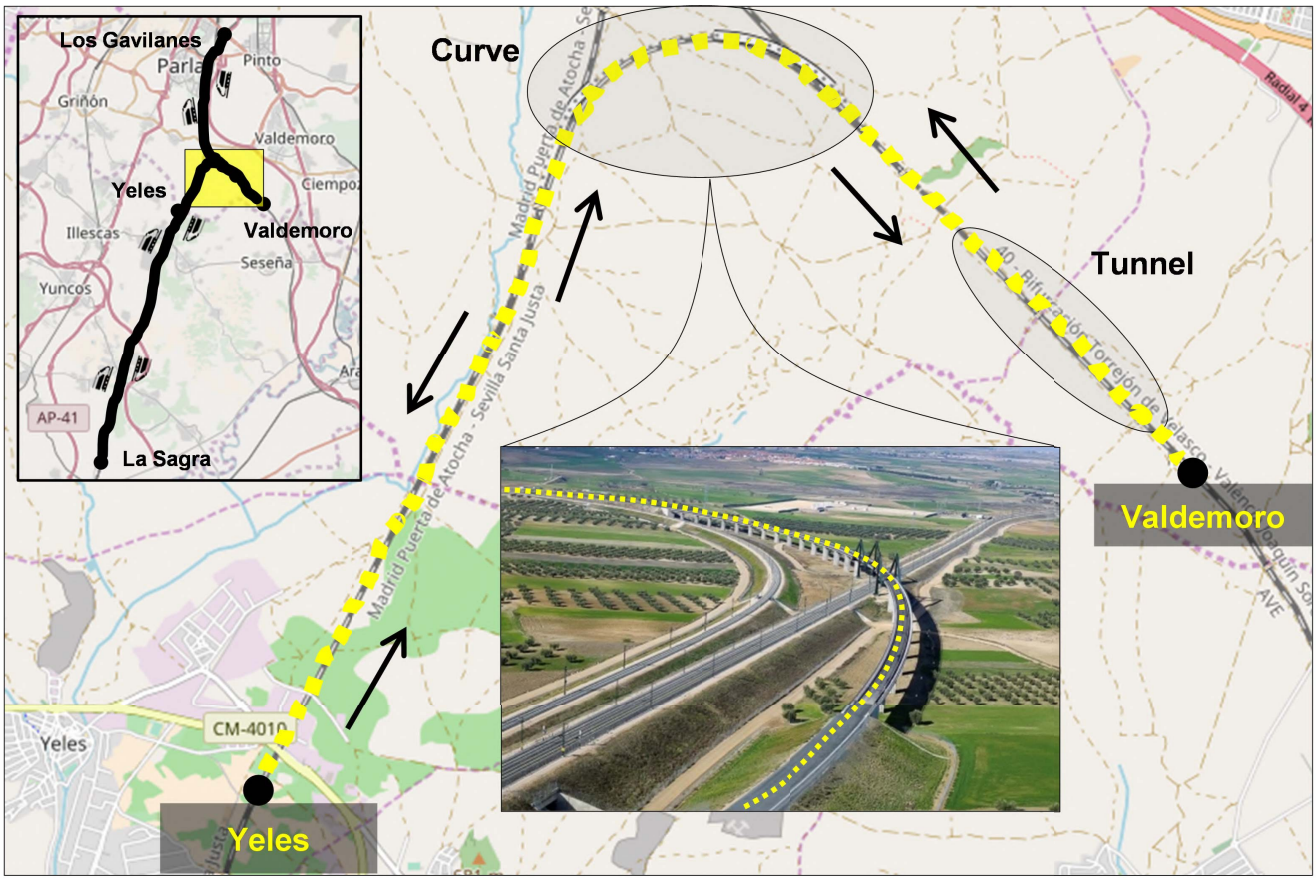

Fig. 2. Railway used for the experimental test in OSM. The journeys are there and back trips from Yeles station (start point) and Valdemoro station (endpoint). We recorded three trips: Yeles-Valdemoro, Valdemoro-Yeles, and Yeles-Valdemoro. The train crosses a tunnel of 103.4 m and a curve of 5.4 km three times (twice in the Valdemoro direction and once in the Yeles direction). The total distance covered is about 54.53 km. The photography is courtesy of Administrador de Infraestructuras Ferroviarias.

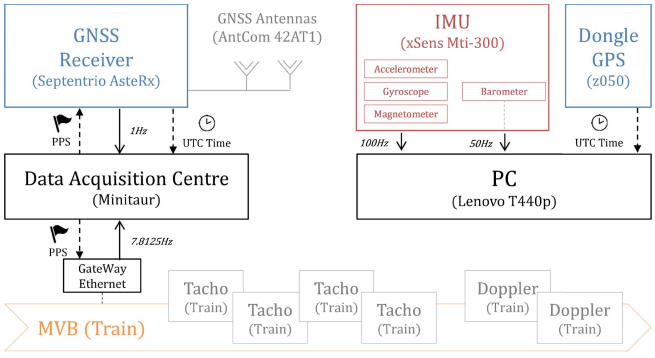

Fig. 3. Measuring architecture proposed and used during the test to record data from sensors.

conversion software supplied by Septentrio was used to obtain a text file (.txt) for ease of data treatment.

For data recorded by xSens MTi-300 IMU, we used MT-Manager software because it is the proprietary software to record and monitor the measurements of the 10-DOF IMU [31].

For tachometers and Doppler radars measurements, it is not be feasible to record the signals from the sensors directly because of the sampling frequency required; for instance, to characterize the pulse of the encoder, it is recommended to use kilohertz order sampling. To overcome this limitation, it was decided to record the velocity value that is published in the train multifunction vehicle bus (MVB) every 128 ms (7.8125 Hz). To make this measurement, a DEWESoft Minatour was connected to the MVB by Ethernet Gateway and a PPS flag was used to synchronize the starting time of both records (GNSS and MVB) as suggested in [7].

All of the measurements and data acquisition units were synchronized by GPS time converted to Coordinated Universal Time, as shown in Fig. 3. With this strategy, it is rather simple to obtain the output of the test as a merged file in text format where all of the measurements are synchronized.

III. Train Velocity Based on GNSS and IMU Data

Based on measurements recorded during the test from GNSS and IMU, train velocity is calculated using the Bayesian recursive estimation technique for data fusion; as shown in Fig. 4. This section intends to demonstrate that the candidate sensors can substitute for measurements recorded by the tachometers and Doppler radars.

A. Data Fusion Algorithm

The algorithm that we implemented is an extended Kalman filter (EKF) with 15 state variables (3-D attitude, 3-D gyro,

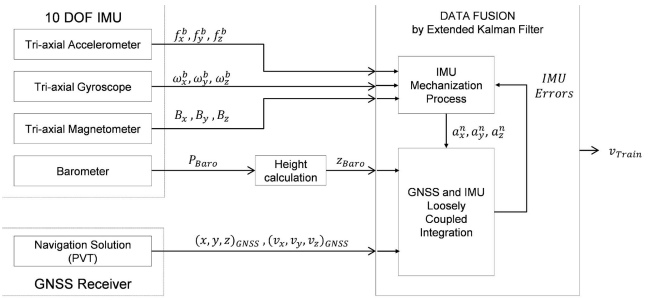

Fig. 4. Data fusion architecture for train velocity calculation. The inputs are the raw measurements from the 10-DOF-IMU and the PVT solution of GNSS receiver. The output is the calculated train velocity.

3-D position, 3-D velocity, and 3-D acceleration). These states are not directly the solution but they are error states (indirect configuration). The IMU and GNSS are integrated in a loosely coupled configuration, which is the simplest implementation scheme and only requires IMU raw measurements and GNSS PVT solution. Note that PVT solution is available in almost any GNSS receiver unlike raw GNSS data—required to tight integration—that is not available in all of them. The algorithm output is a velocity solution, which is calculated at 100 Hz. The initial value is assumed to be a reference velocity value. The other EKF states are initialized to zero.

The input parameters of the algorithm are a GNSS PVT solution provided by Septentrio AsteRx3 GNSS receiver and 10 DOF IMU raw measurements provided by xSens MTi-300 series. The data recorded by the accelerometers and gyroscopes are used in mechanization process where the rotation matrix between the body frame and navigation frame (local-level frame or geodetic) is computed by Euler angles. Once the acceleration values are represented in a navigation frame, they are passed to the EKF, and to the barometer and GNSS data.

The data processing that is described above is depicted in Fig. 4. Accelerometers and gyroscopes outputs are represented with subscripts, which refer to axes where the data are recorded (x, y or z). The superscript refers to axis frame, which can be body frame (b) or navigation frame (n). The same applies to the output variables of the mechanization process. In the case of the magnetometer, the intensities of the magnetic field in the three axes are used to calculate train heading (i.e., yaw angle). The atmospheric pressure recorded by the barometer is applied to international standard atmospheric to compute the height, as shown in (1). This model assumes constant temperature ($T_0 = 288.15$ K) and pressure ($p_0 = 1013.25$ hPa) at sea level, temperature gradient ($\lambda = -0.0065$ K/m), atmospheric gas constant ($R = 287$ m^2/s^2 K), and gravity acceleration ($g = 9.8$ m/s^2) [32]

$$h = \frac{T_0}{\lambda}\left[1 - \left(\frac{P_{\text{baro}}}{P_0}\right)^{\frac{\lambda R}{g}}\right]. \tag{1}$$

According to GNSS, only the PVT solution is used, which refers to position $(x, y, z)_{\text{GNSS}}$ and velocity $(v_x, v_y, v_z)_{\text{GNSS}}$.

The MATLAB programming framework is used because of the ease of working with matrices and mathematical libraries when implementing EKF. The data treatment process is solved once all of the measurements are recorded (i.e., in off-line configuration).

B. Reference Velocity Definition

A reference velocity is used to compare and evaluate the solution obtained by data fusion. In this paper, the velocity published in MVB is used as a reference value. This velocity calculation method is proprietary and it is used for most of applications of the train that internally requires a velocity value (e.g., vehicle control). Consequently, it is considered accurate and precise enough to be compared with the candidate sensors solution. Its value is calculated using four wheel speed sensors and two Doppler radars. The reason why redundant sensors measurements are used is justified by the limitations of each sensor individually present. If only wheel speed sensors were used to determine train velocity, then this value would be erroneous in slipping or skidding situations. Otherwise, experienced rolling stock manufactures have demonstrated by internal experimental tests Doppler radars give an erroneous value of velocity when train velocity is nearby zero. Although the limitations can be overcome with two wheel speed sensors and a Doppler radar, to guarantee safety and availability of velocity, redundant architectures are used (i.e., four wheel speed sensors and two Doppler radars).

IV. Experimental Results and Discussion

The field test covers three there and back travels between Yeles and Valdemoro stations. The recording of the measurements starts in Yeles at 23:49:52 on 18/03/2017 and ends in Valdemoro at 00:44:04 on 19/03/2017 after a 54.53 km run covered in three travels (twice in the Valdemoro direction and once in the Yeles direction), as shown in Fig. 2.

A. Sensors Raw Measurements Analysis

The raw measurements provided by accelerometer, gyroscope, magnetometer, and barometer are presented in Figs. 5–9, respectively.

The accelerometers measure specific forces in the three axes of the IMU (Fig. 1). The acceleration values recorded in the x-axis are below 1 m/s^2 value (Fig. 5), which is coherent to the dynamics of the train. Note that several studies have demonstrated that the maximum values of longitudinal acceleration are around 1.14 m/s^2, although in some exceptional situations (e.g., emergency brake) -3.0 m/s^2 deceleration values can be reached [33], [34].

Analysis of the y-axis acceleration values shows that the curved section of the trips can be clearly distinguished. The acceleration recorded in the y-axis is the normal acceleration due to curving section subtracted by the gravity acceleration projection on the y-axis caused by the cant of the curve. In automotive roads, the cant is usually designed to void the normal acceleration but in railways the cants do not have enough inclination (because of passenger comfort, derailment

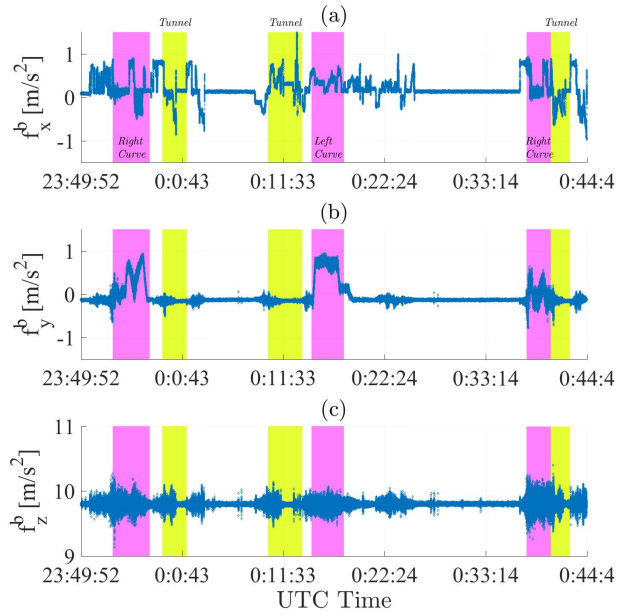

Fig. 5. Tri-axial accelerometer raw measurements.

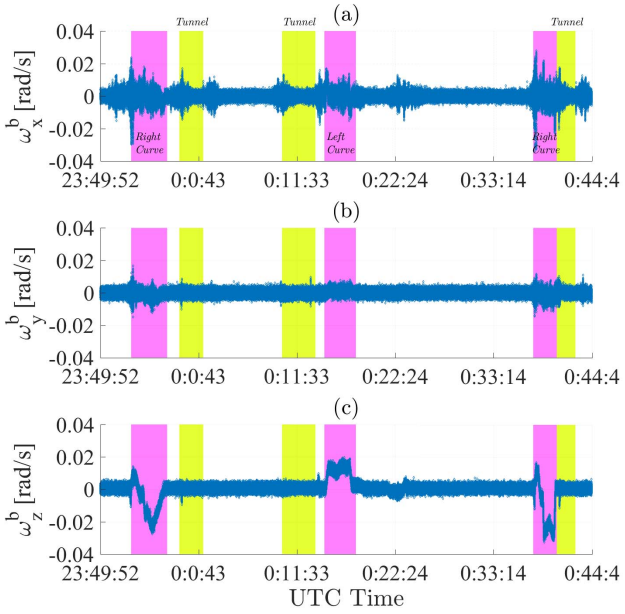

Fig. 6. Tri-axial gyroscope raw measurements.

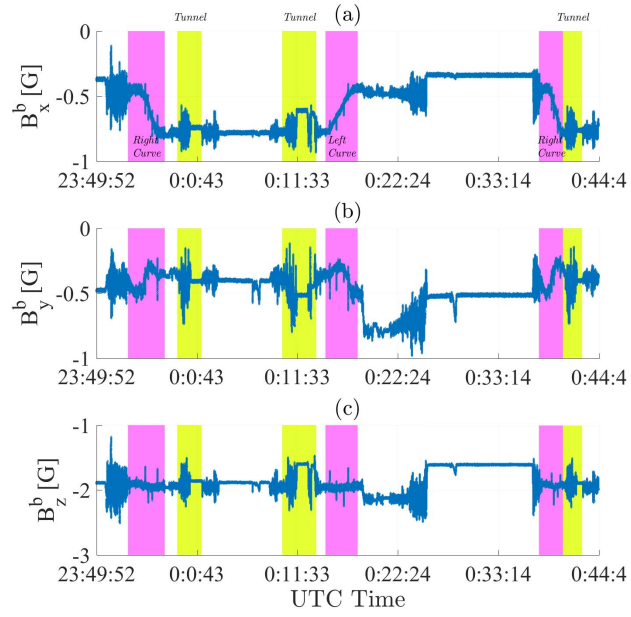

Fig. 7. Tri-axial magnetometer raw measurements.

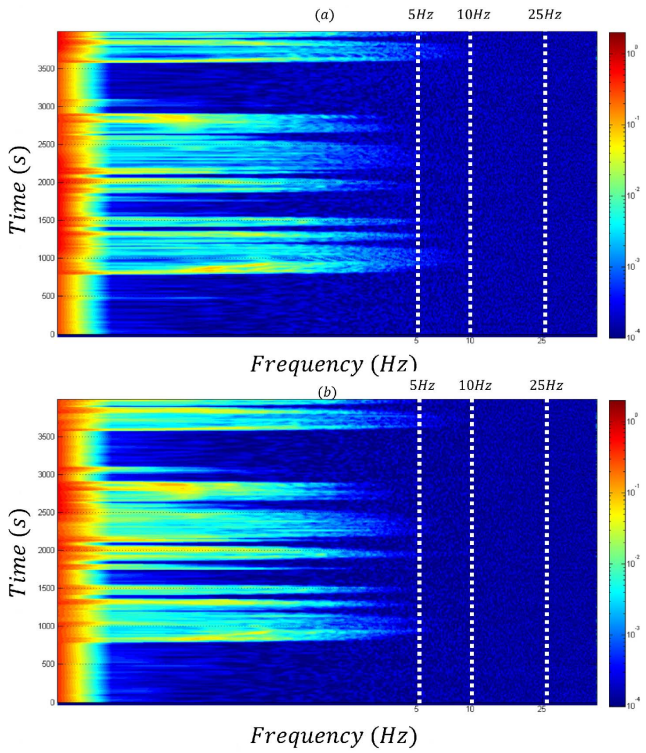

Fig. 8. Countour plot of (a) x-axis and (b) y-axis magnetometer measurements after applying the FFT.

risk, wheel, and rail contact, etc.) and a noncompensated lateral acceleration arises. This noncompensated lateral acceleration is the measured value on the y-axis and it presents typical values around 0.65 m/s^2 [35].

Acceleration values in the z-axis are near 10 m/s^2 according to the gravity acceleration present in raw measurements (body frame). The acceleration recorded in the z-axis presents significant changes when the train is running inside the curve or the height is varying. This behavior is related to the gravity acceleration projection in the z-axis: when a train is in a curve the cant angle provokes a change in roll angle (x-axis rotation) and gravity acceleration is projected onto z-axis and y-axis. When a height change is present, a rotation in the y-axis (pitch) occurs and the gravity acceleration is projected onto z-axis and x-axis. This is the reason why the acceleration values on the z-axis are noisy and the acceleration values on x-axis and y-axis are affected in the described zones.

According to gyroscope measurements, very smooth changes are present (all of the measurements are below 0.03 rad/s) and this makes it difficult to distinguish the angular

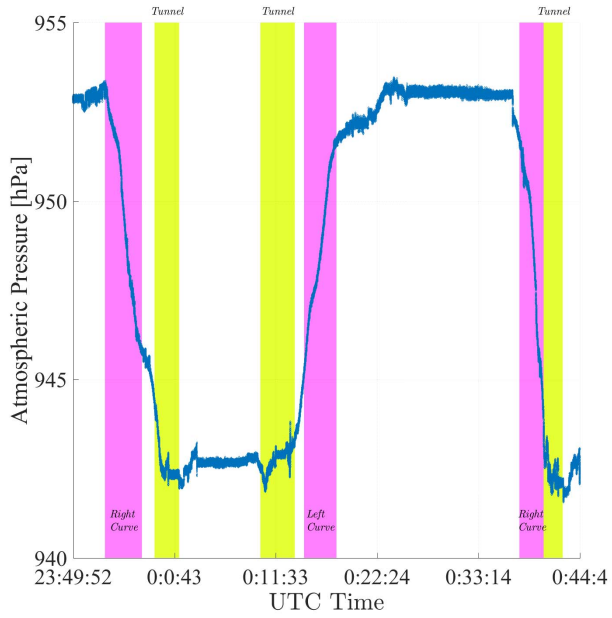

Fig. 9. Barometer raw measurements.

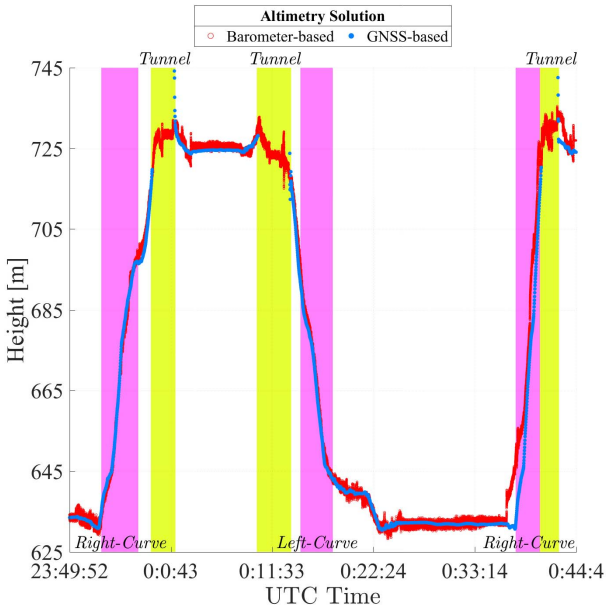

Fig. 11. Altimetry solution comparative between barometer-based calculated and GNSS recorded values.

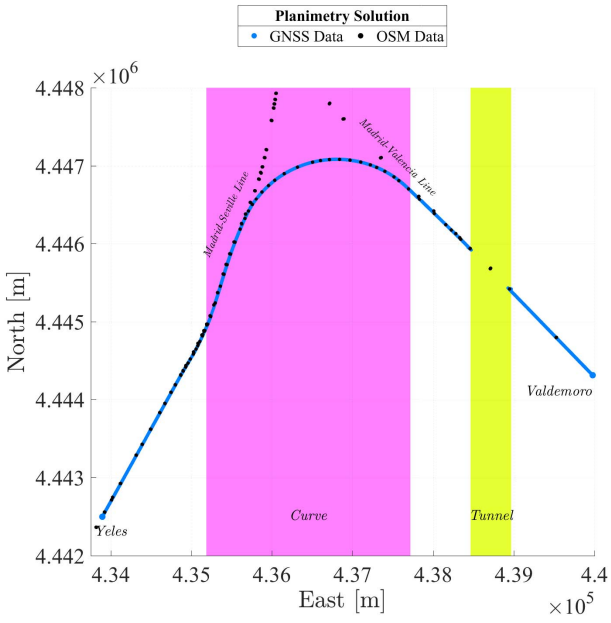

Fig. 10. Planimetry solution comparative between GNSS PVT and OSM nodes.

rates values from the noise (Fig. 6). However, by focusing the analysis on the z-axis angular rates, three curves can be detected easily. A curve presents a change in heading angle and the gyroscope located in the z-axis is able to detect this change. Heading change also provides the direction of the curve when analyzing the sign of the measurement (i.e., it is negative when the train goes to the right and positive otherwise). Note that the curve is the same in the three cases but the z-axis angular rate differs because the velocity of the train on every travel is different.

The curve not only affects in the rotations on the z-axis but the x-axis and y-axis gyroscopes also present relevant measurements. As stated previously, a railway curve is built with a cant angle and, consequently, a height change (slope). The cant angle provokes a roll angle change and it is measured on the x-axis angular rate. The slope change is measured on the y-axis angular rate because it is a pitch angle change. Note that the height change is comparatively smaller than the cant, so the angular rates in the x-axis are approximately two times higher than in the y-axis.

The magnetometer measures looks rather chaotic, although the behavior of the sensor in three axes is analogous and it can be explained in several ways (Fig. 7). First, the magnetometers in the x-axis and y-axis show how the heading angle changes when the train is on a curve. A heading angle change provokes a change of the projection of earth magnetic field intensity in the x-axis and y-axis. These phenomena can be seen from Fig. 7(a) and (b). These measurements can also discriminate the direction of the curve and unlike the z-axis angular rate measurements the magnetic field intensity change is independent of external variables. When a heading change occurs—when a train is negotiating a curve—gyroscope-based heading calculation depends on train velocity (Fig. 7) but magnetometer-based heading always should present the same magnitude independent of velocity (Fig. 6). Second, a relationship between acceleration in the x-axis and magnetic field intensity can be seen. For example, when significant traction or brake is applied to the train (higher than 0.5 m/s^2 acceleration or lower than -0.5 m/s^2 deceleration), the magnetometer records in the three axis are affected enhancing the noise of the magnetic field intensity measurements (e.g., before the train negotiates the first curve $-$23:52:20$-$ and after negotiating the second curve $-$00:23:24$-$). Although this correlation can be seen in the results, after analyzing the fast Fourier

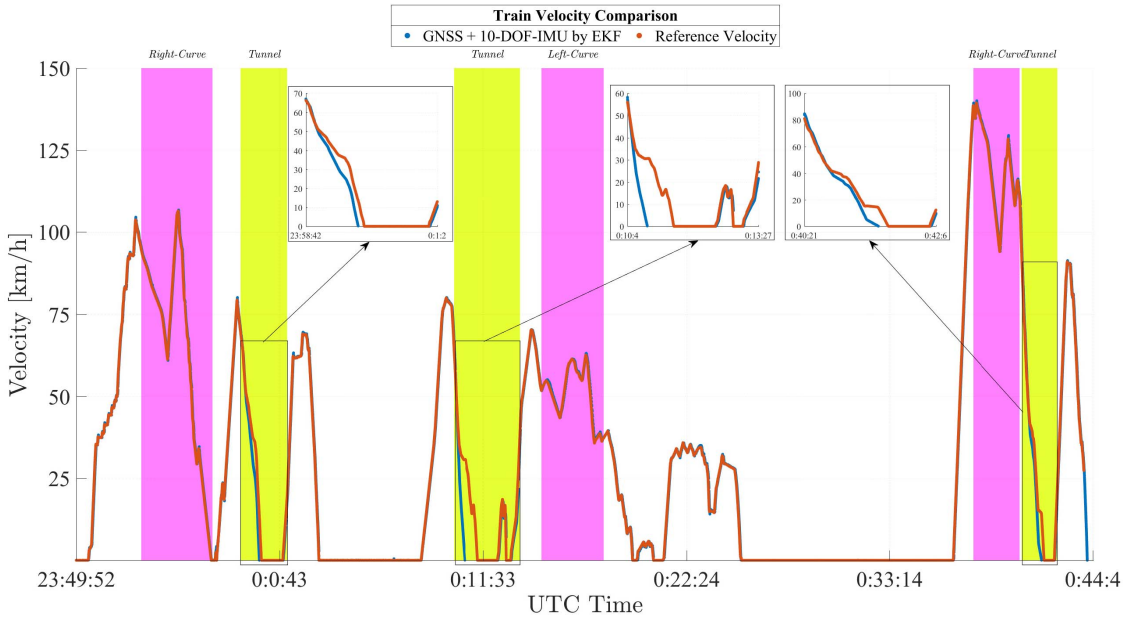

Fig. 12. EKF solution for train velocity and comparative with reference velocity values.

transform (FFT) of the signals and comparing our results with other spectrograms in the train context, it can be concluded that neither the train motors nor the braking resistor magnetic fields have an influence (Fig. 8). Finally, noisy measurements in the section between 23:58:42–00:01:02, 00:10:04–00:13:27, and 00:40:21–00:42:06, can be explained by the tunnel crossing, during which the magnetic field intensity is affected. Although the main behavior of magnetometers is characterized with the recorded measurements, further research should be carried out to evaluate, for instance, the influence of the high-voltage catenary or the train metallic box. This would allow us to more precisely characterize the magnetometer measurements.

The last measurements related to the 10 DOF IMU is the atmospheric pressure recorded by the barometer (Fig. 9). The maximum pressure registered is 953 hPa and the minimum 942 hPa. These measurements only make sense if they are applied to atmospheric models to compute altitude over the sea. In this paper, the international standard atmosphere model is used to compute height from the barometer raw measurements. As shown in height calculated in Fig. 11, only 100 m of height difference is measured in 17 km, approximately, which is coherent to the smooth altitude changes of railway topography. The main height changes (almost 100 m) occur on the curves, enhanced by cant and slope of the curve. The tunnel section also presents an incongruence near 00:11:33 instant, where it seems to make a transition of slope from positive to negative. This erroneous height computation is a consequence of using the raw measurements of the atmospheric pressure without applying any smoothing or filtering technique. The measurement of atmospheric pressure is affected by the column of air that is over the barometer; so, when the train is inside the tunnel, the pressure head is lower than outside the tunnel and, consequently, the atmospheric pressure measurement is erroneous.

In the GNSS solution, the signal outage is highlighted in planimetry (Fig. 10) and altimetry solutions (Fig. 11). During the trip, three GNSS signal outages occur because of the tunnel crossing. On every crossing, the duration of the outage is intentionally designed to be different by modifying the train's velocity during the test. The first outage duration is 2 min and 18 s, the second is 3 min and 21 s, and the third is 1 min and 45 s. This is done intentionally to simulate a large period of GNSS outage and to show the drift of the IMU when it is working stand alone. Extrapolating this outage time to a scenario where the train is running at maximum velocity (300 km/h), the tunnel lengths would be about 11.5, 16.9, and 8.75 km. These scenarios are considered to be feasible in a railway context, unlike, for instance, roads.

The planimetry solution given by the GNSS PVT solution and the nodes downloaded from open street map (OSM) database are compared in Fig. 10. GNSS solution provides a node each second in the sections where the signal is available, so the number of nodes given by GNSS is higher than the nodes provided by OSM. In this railway database, only one node is available inside the tunnel which can be considered insufficient to evaluate the solution when GNSS signal outage occurs.

Motivated by the lack of precision of height in GNSS, a comparison between the computed height from barometer and the provided by GNSS receiver is presented in Fig. 11. The barometer raw measurements (Fig. 9) present noise that is propagated to the height calculation whereas the GNSS height computation is noise free. However, the GNSS solution is given in a lower sampling rate (1 Hz) and the signal outage provokes solution unavailability.

B. Train Velocity Comparison

To see the influence of the candidate sensors measurements into the velocity solution, GNSS, and IMU measurements are

TABLE I
ANALYSIS OF THE RAILWAY'S FEATURES

	Calculated	Normative [35]
Lateral acceleration	<1 m/s^2	0.65 m/s^2
Slope	2%	Conventional lines: 1.25–2%
		High-speed lines: 1.5–2.5%
Cant	100mm	Conventional lines: 150mm
		High-speed lines: 180–200mm
Curve Radius	1800m	Iberian gauge (1668mm) (140–200 km/h): 1000–2000m (minimum)
		International gauge (1435mm) (200–300 km/h): 2100–4700m (minimum)

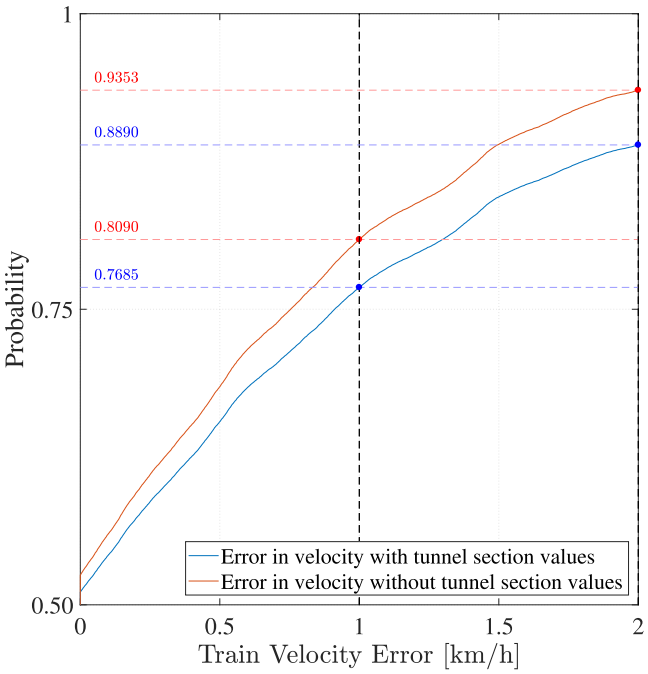

Fig. 13. CDF of velocity difference between reference value and GNSS + 10 DOF IMU data fusion.

fused by an EKF (Fig. 12). The GNSS signal outage zones (tunnel crossings) are zoomed-in to highlight the IMU drift.

The velocity calculated by GNSS and IMU data fusion is evaluated using the empirical cumulative distribution function (CDF). The highest value of velocity error (i.e., 2 km/h) is set according to the most exigent ETCS requirement, which states that the maximum allowable velocity error must be 2 km/h.

According to the CDF calculated in this paper (Fig. 13), it is concluded that the probability of finding a difference between the fused solution and the reference velocity (i.e., velocity error) below 1 km/h is 80.90% (Fig. 13). The probability rises to 93.53% if the error in velocity is 2 km/h. The probabilities values are reduced when the tunnel section velocity solution is added: 1 km/h or lower error are 76.85% whereas 2 km/h or lower errors decreases up to 88.90%.

C. Track Features Calculation

The velocity obtained by data fusion can be combined with the accelerometers' and gyroscopes' measurements to calculate railway features, such as the radius and cant of the curve that is crossed during the test. According to the mathematical formulas developed in this paper, the relationship between the candidate sensors raw measurements and track features is presented in this section.

The curve radius (R) is related to the train's instantaneous velocity (v_{train}) and the heading angle change (i.e., gyroscope measurement in the z-axis). The cant of the curve is used to compute the noncompensated lateral acceleration (i.e., accelerometer measurement in the y-axis). The noncompensated lateral acceleration is the resultant acceleration due to the lack of cant to compensate the centripetal acceleration. The track parameters, such as the track gauge (s) and curve radius (R), and also dynamic variables (train velocity) plays a key role in the lack of cant (also known as Cant deficiency). The approximated formulas for calculation of curve radius and cant are given in the following equations [16], [17]:

$$R = \frac{v_{\text{train}}}{\omega_z^b} \tag{2}$$

$$h_{\text{cant}} = \left(\frac{v_{\text{train}}^2}{R} - f_y^b\right)\frac{s}{g}. \tag{3}$$

With the measurements recorded in the field test and the velocity calculated by the described data fusion algorithm, an approximated calculation of curve radius and cant height is carried out. The left curve is selected for the calculation because it presents the closest dynamics of constant velocity (i.e., minimum longitudinal acceleration). These are calculated by taking the mean values of the velocity in the curved section. The curve radius calculated value is 1800 m and the cant value is 100 mm, approximately (Table I).

Note that the curve radius is small in comparison with the high-speed line's typical values (over 4000 m [35]). However, this value explains why the velocity of the track section where the test is executed is limited to 160 km/h (below high-speed requirements). Higher speeds would provoke the noncompensated lateral acceleration to grow and the centripetal force acting in the train would increase, with a consequent risk of derailment.

The cant value can also be considered to be small (typical values of 160 mm are considered in high speed lines [35]). However, many trains incorporate tilting technologies that are able to incline the train box on curves to add acceleration in the direction of gravity projection. If these technologies are applied, then the railway cants can be designed to be lower.

If we know the altimetry of the railway, then the instantaneous slope can be calculated based on the velocity obtained by GNSS and 10 DOF IMU data fusion. However, the covered distance between two height-known-points (Δh) is required, which is computable with train velocity (v_{train}) and sampling

rate $(1/\Delta t)$. The formulation for slope calculation is given in the following equation:

$$\text{slope} = \frac{\Delta h}{v_{\text{train}} \Delta t} 100. \tag{4}$$

High-speed railways are built with very smooth height changes so as not to introduce vertical accelerations in the train and provoke uncomfortable movements for the passengers (slope values near to 1.5% are considered typical but maximum values of 2.5% cannot be exceeded in high-speed lines [35]). This makes it challenging to measure the altitude changes with barometers because the signal-to-noise ratio plays an important role. With the raw measurements recorded by the 10 DOF IMU, it is not possible to compute a valid slope; therefore, a local regression method is used based on weighted linear least squares and a second-degree polynomial model. This method is implemented in MATLAB by *loess* function. With this technique, a slope value of approximately 2% is determined by taking the mean value of the three evaluations of the same curve.

V. Conclusion

In this paper, experimental measurements of GNSS and 10 DOF IMU are analyzed in the railway context. After a detailed explanation and justification of the field test, the measurements are evaluated by highlighting the particular features of the train's dynamics. Finally, a data fusion algorithm is proposed to obtain train velocity with candidate sensors and to calculate the railway's track parameters (cant, slope, and curve radius). Based on this paper, our main conclusions are presented in this section.

The measurements recorded in this paper combine GNSS and 10 DOF IMU sensors and compare them to a reference velocity obtained from tachometer and Doppler radar readings. The measurements are carried out using a synchronized recording system based on GPS time and they are stored in a text file. The railway that we used for our experimental test presents several challenging scenarios for validating train navigation algorithms, such as multiple GNSS signal outages.

By analyzing the measurements obtained in the field test, the usability of IMU and GNSS candidate sensors in railway domain can be concluded. Even with a simple data fusion algorithm that fuses IMU and GNSS measurements, the solution that we have calculated is able to reach very similar values of velocity to higher cost sensors, such as Doppler radars: below 2 km/h difference between both velocity solutions is reached by 93.53% of probability. However, when the IMU needs to work standalone (i.e., GNSS signal outage) it is concluded that additional information is required to guarantee solution validity. The use of standardized digital maps and information provided by beacons installed on the track could provide the data needed to support the candidate sensors in GNSS signal degraded environments.

Finally, railway features such as cant, slope, and curve radius are obtained using raw measurements from the candidate sensors and velocity is obtained by data fusion. This analysis can contribute to help us better model the simulation environments because once the railway that will be simulated is known, the ideal measurements of angular rate in the z-axis, acceleration on the y-axis, and barometer values can be calculated.

Acknowledgment

The authors would like to thank CAF $I + D$ and CETEST for contributions to the knowledge of trains and railways, and also for their expertise in the testing methodology that directly motivated the writing of this paper.

References

[1] T. Albrecht, K. Luddecke, and J. Zimmermann, "A precise and reliable train positioning system and its use for automation of train operation," in *Proc. IEEE Int. Conf. Intell. Rail Transp. (ICIRT)*, Sep. 2013, pp. 134–139. [Online]. Available: http://ieeexplore.ieee.org/abstract/document/6696282/

[2] M. Lauer and D. Stein, "A train localization algorithm for train protection systems of the future," *IEEE Trans. Intell. Transp. Syst.*, vol. 16, no. 2, pp. 970–979, Apr. 2015. [Online]. Available: http://ieeexplore.ieee.org/lpdocs/epic03/wrapper.htm?arnumber=6895280

[3] K. Kim, S.-H. Kong, and S.-Y. Jeon, "Slip and slide detection and adaptive information sharing algorithms for high-speed train navigation systems," *IEEE Trans. Intell. Transp. Syst.*, vol. 16, no. 6, pp. 3193–3203, Dec. 2015. [Online]. Available: http://ieeexplore.ieee.org/document/7123638/

[4] J. Marais, J. Beugin, and M. Berbineau, "A survey of GNSS-based research and developments for the European railway signaling," *IEEE Trans. Intell. Transp. Syst.*, vol. 18, no. 10, pp. 2602–2618, Oct. 2017. [Online]. Available: http://ieeexplore.ieee.org/document/7857080/

[5] D. Lu and E. Schnieder, "Performance evaluation of GNSS for train localization," *IEEE Trans. Intell. Transp. Syst.*, vol. 16, no. 2, pp. 1054–1059, Apr. 2015. [Online]. Available: http://ieeexplore.ieee.org/document/6894605/

[6] M. S. Grewal, L. R. Weill, and A. P. Andrews, *Global Positioning Systems, Inertial Navigation, and Integration*, 2nd ed. Hoboken, NJ, USA: Wiley, 2007.

[7] Y. Stebler, S. Guerrier, and J. Skaloud, "An approach for observing and modeling errors in MEMS-based inertial sensors under vehicle dynamic," *IEEE Trans. Instrum. Meas.*, vol. 64, no. 11, pp. 2926–2936, Nov. 2015. [Online]. Available: http://ieeexplore.ieee.org/document/7159103/

[8] N. El-Sheimy, H. Hou, and X. Niu, "Analysis and modeling of inertial sensors using Allan variance," *IEEE Trans. Instrum. Meas.*, vol. 57, no. 1, pp. 140–149, Jan. 2008. [Online]. Available: http://ieeexplore.ieee.org/document/4404126/

[9] V. Pasku, A. De Angelis, M. Dionigi, A. Moschitta, G. De Angelis, and P. Carbone, "Analysis of nonideal effects and performance in magnetic positioning systems," *IEEE Trans. Instrum. Meas.*, vol. 65, no. 12, pp. 2816–2827, Dec. 2016. [Online]. Available: http://ieeexplore.ieee.org/document/7581032/

[10] V. Pasku, A. de Angelis, G. de Angelis, A. Moschitta, and P. Carbone, "Magnetic field analysis for 3-D positioning applications," *IEEE Trans. Instrum. Meas.*, vol. 66, no. 5, pp. 935–943, May 2017. [Online]. Available: http://ieeexplore.ieee.org/document/7890423/

[11] S. Zihajehzadeh, T. J. Lee, J. K. Lee, R. Hoskinson, and E. J. Park, "Integration of MEMS inertial and pressure sensors for vertical trajectory determination," *IEEE Trans. Instrum. Meas.*, vol. 64, no. 3, pp. 804–814, Mar. 2015. [Online]. Available: http://ieeexplore.ieee.org/document/6922538/

[12] A. Mirabadi, N. Mort, and F. Schmid, "Application of sensor fusion to railway systems," in *Proc. IEEE/SICE/RSJ Int. Conf. Multisensor Fusion Integr. Intell. Syst.*, Dec. 1996, pp. 185–192. [Online]. Available: http://ieeexplore.ieee.org/abstract/document/572176/

[13] J. Otegui, A. Bahillo, I. Lopetegi, and L. E. Díez, "A survey of train positioning solutions," *IEEE Sensors J.*, vol. 17, no. 20, pp. 6788–6797, Oct. 2017. [Online]. Available: http://ieeexplore.ieee.org/document/8022861/

[14] M. Marinov, S. Hensel, and T. Strauß, "Eddy current sensor based velocity and distance estimation in rail vehicles," *IET Sci., Meas. Technol.*, vol. 9, no. 7, pp. 875–881, Oct. 2015. [Online]. Available: http://digital-library.theiet.org/content/journals/10.1049/iet-smt.2014%.0302

[15] S. Iwnicki, *Handbook of Railway Vehicle Dynamics*. New York, NY, USA: Taylor & Francis, 2006.

[16] O. Heirich, A. Lehner, P. Robertson, and T. Strang, "Measurement and analysis of train motion and railway track characteristics with inertial sensors," in *Proc. 14th Int. IEEE Conf. Intell. Transp. Syst. (ITSC)*, Oct. 2011, pp. 1995–2000. [Online]. Available: http://ieeexplore.ieee.org/abstract/document/6082908/

[17] M. Malvezzi, G. Vettori, B. Allotta, L. Pugi, A. Ridolfi, and A. Rindi, "A localization algorithm for railway vehicles based on sensor fusion between tachometers and inertial measurement units," *Proc. School Mech. Eng. F, J. Rail Rapid Transit*, vol. 228, no. 4, pp. 431–448, 2014, doi: 10.1177/0954409713481769.

[18] M. Malvezzi, P. Toni, B. Allotta, and V. Colla, "Train speed and position evaluation using wheel velocity measurements," in *Proc. IEEE/ASME Int. Conf. Adv. Intell. Mechatronics*, vol. 1, Jul. 2001, pp. 220–224. [Online]. Available: http://ieeexplore.ieee.org/abstract/document/936457/

[19] B. Allotta, V. Colla, and M. Malvezzi, "Train position and speed estimation using wheel velocity measurements," *Proc. School Mech. Eng. F, J. Rail Rapid Transit*, vol. 216, no. 3, pp. 207–225, 2002, doi: 10.1243/095440902760213639.

[20] B. Allotta, L. Pugi, A. Ridolfi, M. Malvezzi, G. Vettori, and A. Rindi, "Evaluation of odometry algorithm performances using a railway vehicle dynamic model," *Vehicle Syst. Dyn.*, vol. 50, no. 5, pp. 699–724, May 2012, doi: 10.1080/00423114.2011.628681.

[21] E. Meli, M. Malvezzi, S. Papini, L. Pugi, M. Rinchi, and A. Rindi, "A railway vehicle multibody model for real-time applications," *Vehicle Syst. Dyn.*, vol. 46, no. 12, pp. 1083–1105, Dec. 2008, doi: 10.1080/00423110701790756.

[22] M. Malvezzi, "Odometry algorithms for railway applications," Ph.D. dissertation, Dept. Appl. Mech., Univ. Stud. Bologna, Bologna, Italy, 2003.

[23] B. Allotta, P. D'Adamio, M. Malvezzi, L. Pugi, A. Ridolfi, and G. Vettori, "A localization algorithm for railway vehicles," in *Proc. IEEE Int. Instrum. Meas. Technol. Conf. (I2MTC)*, May 2015, pp. 681–686.

[24] T.-J. Cheng *et al.*, "Characterisation of rollator use using inertial sensors," *Healthcare Technol. Lett.*, vol. 3, no. 4, pp. 303–309, Dec. 2016. [Online]. Available: http://digital-library.theiet.org/content/journals/10.1049/htl.2016.006% 1

[25] M. Tailanian, S. Paternain, R. Rosa, and R. Canetti, "Design and implementation of sensor data fusion for an autonomous quadrotor," in *Proc. IEEE Int. Instrum. Meas. Technol. Conf. (I2MTC)*, May 2014, pp. 1431–1436.

[26] O. Heirich, "Bayesian train localization with particle filter, loosely coupled GNSS, IMU, and a track map," *J. Sensors*, vol. 2016, no. 12, pp. 1–15, Mar. 2016, Art. no. 2672640.

[27] O. G. Crespillo, O. Heirich, and A. Lehner, "Bayesian GNSS/IMU tight integration for precise railway navigation on track map," in *Proc. IEEE/ION Position, Location Navigat. Symp. (PLANS)*, May 2014, pp. 999–1007. [Online]. Available: http://ieeexplore.ieee.org/abstract/document/6851465/

[28] A. R. Jiménez, F. Seco, J. C. Prieto, and J. Guevara, "Indoor pedestrian navigation using an INS/EKF framework for yaw drift reduction and a foot-mounted IMU," in *Proc. 7th Workshop Positioning Navigat. Commun. (WPNC)*, Mar. 2010, pp. 135–143. [Online]. Available: http://ieeexplore.ieee.org/abstract/document/5649300/

[29] U. Qureshi and F. Golnaraghi, "An algorithm for the in-field calibration of a MEMS IMU," *IEEE Sensors J.*, vol. 17, no. 22, pp. 7479–7486, Nov. 2017.

[30] *RxTools Manual*, Septentrio, Leuven, Belgium, Mar. 2016.

[31] *MT Manager User Manual*, xSens, Enschede, The Netherlands, Feb. 2015.

[32] H. Fernández, "Aplicación Android para localizacion de personas en entornos de interior mediante señales WiFi y barométricas," Ph.D. dissertation, Dept. Signal Commun. Theory Telematics Eng., Univ. Valladolid, Valladolid, Spain, 2012.

[33] J. P. Powell and R. Palacín, "Passenger stability within moving railway vehicles: Limits on maximum longitudinal acceleration," *Urban Rail Transit*, vol. 1, no. 2, pp. 95–103, 2015. [Online]. Available: http://link.springer.com/10.1007/s40864-015-0012-y

[34] S. K. Sharma and S. Chaturvedi, "Jerk analysis in rail vehicle dynamics," *Perspect. Sci.*, vol. 8, pp. 648–650, Sep. 2016. [Online]. Available: http://linkinghub.elsevier.com/retrieve/pii/S2213020916301860

[35] A. R. Gómez, "Las líneas de Alta Velocidad frente a las convencionales. Adaptación de las líneas convencionales a Velocidad Alta," Ph.D. dissertation, Dept. High-Speed Train, Trens D'alta Velocitat, Polytech. Univ. Catalonia, Barcelona, Spain, 2007. [Online]. Available: http://hdl.handle.net/2099.1/5938

Jon Otegui received the B.Sc. degree in industrial technologies engineering and the M.Sc. degree in industrial engineering from the University of Navarra, Pamplona, Spain, in 2014 and 2016, respectively. His master's thesis was focused on the experimental validation process of GNSS positioning technology in railway environment and it was carried out in CAF Research and Development Department. He is currently pursuing the Ph.D. degree with the Mobility Research Group, DeustoTech, Bilbao, Spain, under the supervision of Dr. Bahillo.

His current research interests include the development of data fusion algorithms for train positioning and navigation, multiple sensors (wheel speed sensor, IMU, GNSS, and track balises) data fusion and its integration in train localization system for safety critical applications.

Alfonso Bahillo received the Telecommunications Engineering and Ph.D. degrees from the University of Valladolid, Valladolid, Spain, in 2006 and 2010, respectively.

He got the PMP certification at the PMI in 2014. From 2006 to 2010, he was a Research Engineer with CEDETEL. From 2006 to 2011, he was an Assistant Professor with the University of Valladolid. From 2010 to 2012, he was a Product Owner with LUCE Innovative Technologies, Valladolid. From 2013 and 2017, he was a Post-Doctoral Researcher with the University of Deusto, Bilbao, Spain, and the Project Manager with DeustoTech, Bilbao, where he trains Ph.D. students and collaborates in several national and international research projects. He is currently the Director of DeustoTech. He has worked (leading some of them) in more than 25 regional, national, and international research projects and contracts. He has coauthored over 20 research manuscripts published in international journals and over 40 communications in international conferences, and holds three national patents. His current research interests include local and global positioning techniques, ambient assisted living, intelligent transport systems, wireless networking, and smart cities.

Iban Lopetegi received the M.Sc. degree in telecommunication engineering from the University of Mondragon, Mondragón, Spain, in 2007, and the Ph.D. degree in electronics and communications from Newcastle University, Newcastle Upon Tyne, U.K., in 2011.

He is currently with the CAF Research and Development Department, Beasain, Spain, where he is involved in various strategically key projects of the company.

Luis Enrique Díez received the B.Sc. degree in telecommunications engineering from the University of Deusto, Bilbao, Spain, in 2005, and the M.Sc. degree in communication technologies and systems from the Polytechnic University of Madrid, Madrid, Spain, in 2012. He is currently pursuing the Ph.D. degree in pedestrian navigation systems with the Mobility Research Group, DeustoTech, Bilbao.

From 2005 to 2011, he was a Senior IT Consultant with Everis, Madrid. From 2013 to 2014, he was a Research Support Technician with the SOFTLAB Research Group, Carlos III University of Madrid, Getafe, Spain. His current research interests include positioning systems, data fusion, and context-aware applications.

Evaluation of Experimental GNSS and 10-DOF MEMS IMU Measurements for Train Positioning

Jon Otegui[1], Alfonso Bahillo[1], Iban Lopetegi[2], and Luis Enrique Díez[1]

[1] *Faculty of Engineering, University of Deusto, Av. Universidades, 48007 Bilbao, Spain*

[2] *Construcciones y Auxiliar de Ferrocarriles Investigación y Desarrollo, CAF I+D, 20200 Beasain, Spain*

jon.otegui@deusto.es

Introduction

Integrating new candidate sensors, such as Global Navigation Satellite System (GNSS) and inertial measurement unit (IMU), into fail-safe train positioning systems have recently become a prominent area of research.

MEMS | Fail-safe | φ θ h

The work presented in this paper is motivated by the lack of instrumentation and measuring architectures and the need of GNSS and IMU raw measurements analysis in railway environment before their integration in fail-safe train positioning systems. The main **research contributions** are:

- To **extend** the most relevant previous works in the field of instrumentation and measurement.
- To **understand** the behavior of these sensors in a railway context and, consequently, to better model the sensors in simulated environments.
- To **detect** main limitations of candidate sensors when measuring track features (cant, slope, …).

Do you know…

that, nowadays, no train is positioned safely in an absolute reference frame such as WGS84?

Materials and methods

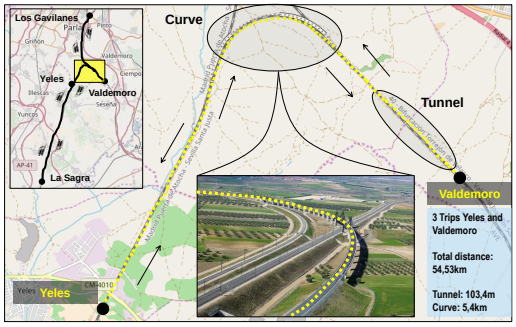

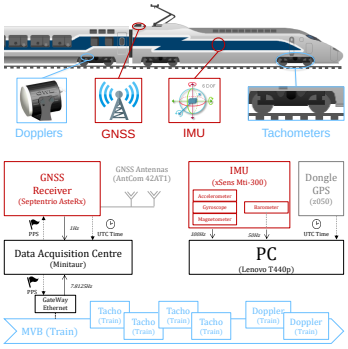

Dopper radar

GNSS receiver and antennas

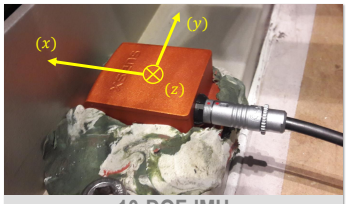

10-DOF-IMU

Results

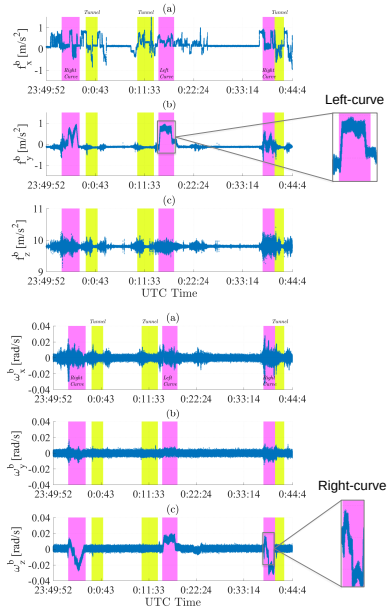

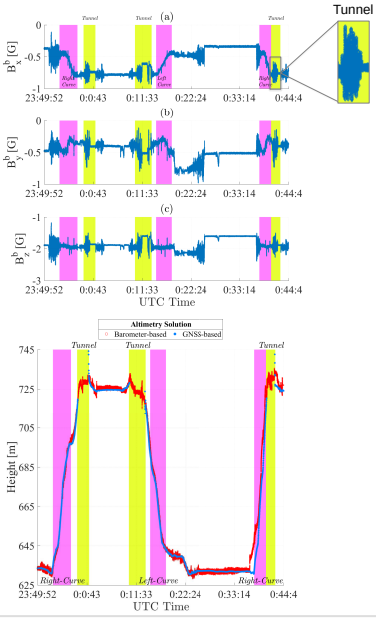

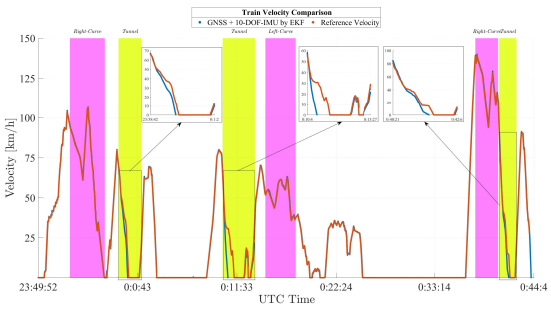

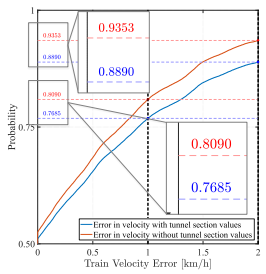

	Calc.	Normative
Lateral accel.	< 1m/s²	0.65 m/s²
Slope	2%	Conventional: 1.25-2%
		High-speed: 1.5-2.5%
Cant	100mm	Conventional: 150mm
		High-speed: 180-200mm
Curve radius	1800m	Iberian gauge: 1000-2000m
		International gauge: 2100-4700m

Conclusions

- This work demonstrates the usability of IMU and GNSS in railway domain: the solution we have calculated by EKF is able to reach very similar values of velocity to higher cost sensors, such as Doppler radars: below 2 km/h difference between both velocity solutions is reached by 93.53% of probability.
- When the IMU needs to work standalone (i.e., GNSS signal outage) it is concluded additional data (digital maps or beacons) is required to guarantee solution validity.
- The knowledge of track cant, curve radius and slope (in addition to IMU and velocity measurements) beforehand can help positioning accurately and safely a train.

Acknowledgment

The authors would like to thank CAF I + D and CETEST for contributions to the knowledge of trains and railways, and also for their expertise in the testing methodology that directly motivated the writing of this paper.

CAF

DeustoTech Mobility

The logic of validation allows us to move between the two limits of dogmatism and skepticism.

Paul Ricoeur

CHAPTER

4

Simulation Framework

The survey about train positioning solutions (paper I) highlighted the few simulation frameworks to test train navigation algorithms under different conditions. Eventually, it has directly motivated the design, development and validation of a one-stop simulation framework presented in this paper.

According to the experimental evaluation of GNSS and IMU (paper II), these candidate sensors arise as prominent solution, especially the IMU due its trade-off between cost and functionality in railways. However, the lack of agreement of the main research works about GNSS integration into the train positioning system, has set it aside for short-term solutions.

The simulation framework presented is focused on the integration of the INS and wheel speed sensor as an alternative to the actual system (wheel speed sensor and Doppler radar). Under the technical point of view, the INS can be able to overcome the wheel speed sensors limitations (slip/skid, wear, conicity, pure-rolling conditions). In addition, it can provide additional information related to railway features that can broad the positioning techniques (e.g. using digital maps and map-matching algorithms). It can substitute Doppler radar lowering the cost of the system but the accuracy and precision of the positioning solution is in part subject to IMU quality (low-, medium- or high-end inertial sensors can be used).

Table 4.1: A comparison of the simulation frameworks.

		Simulation Frameworks				
		Prev. (1)	Prev. (2)	Prev. (3)	Prev. (4)	Proposed
Input files	Train characteristics	No	Yes	Yes	No	Yes
	Sensors characteristics	No	Yes	No	No	Yes
	Speed profile	Yes	Yes	Yes	No	Yes
	Track profile	Yes	Yes	Yes	Yes	Yes
Sensors	Accelerometers	Yes	No	Yes	Yes	Yes
	Gyroscopes	Yes	No	Yes	Yes	Yes
	Magnetometers	No	No	No	No	Yes
	Tachometers	Yes	No	Yes	No	Yes
Signal Generation	Synthetic signals	Yes	Yes	Yes	No	Yes
	• Sensors error models	No	No	No	No	Yes
	• Degraded scenarios	Yes	Yes	Yes	No	Yes
	• Vehicle dynamic model	No	No	Yes	No	Yes
	Experimental signals	No	Yes	No	Yes	Yes
Navigation algorithms	IMU mechanization methods	No	No	Yes*	Yes*	Yes**
	Data fusion methods	Yes*	Yes*	Yes*	Yes*	Yes**
	Performance evaluation methods	No	Yes	Yes*	Yes*	Yes*

Acronyms: Only one method (*) or more than one methods (**) are presented and tested. Prev. = Previously done.

Under the safety point of view, train positioning systems are required to be tested in different and multiple scenarios, especially, in those scenarios where sensors provide erroneous measurements; so, the flexibility for testing different trains, along different tracks, equipped with different sensors and running under different speed profiles plays a key role in the design of a simulation framework.

The simulation framework presented in this paper has been deployed to test the performance of train navigation algorithms based on IMU and wheel speed sensors (Figure 4.1). The overall functioning of the simulation framework presented in this work can be outlined as follows: first, all of the data required as input are loaded to the simulation framework. An overall testing configuration file sets the global variables (output data rate, train navigation algorithm, INS mechanization method, etc.). The input files block includes information about the velocity profile, digital map, train parameters, sensors characteristics, and so on. Once the input data is loaded, the sensor signals are built based on synthetic or experimental procedures. The signal generation process is gathered in the synthetic and experimental signal simulator. After the sensor signals are generated, the train navigation algorithm processes them to get the train navigation solution (i.e., train position, velocity,

heading, etc.). Finally, the performance of the solution is evaluated by comparing the estimated results to the reference values. Both algorithms are gathered in the Train Navigation Algorithms and Solution Performance Evaluation Algorithms.

As use case, the simulated train, track, sensors and speed profile has been built based on the experimental tests presented in paper II. Consequently, the train and track features, as well as, sensors data-sheet parameters are close to reality. This paper shows two mechanization methods and two data fusion algorithms and evaluates their performance according to orientation and velocity values.

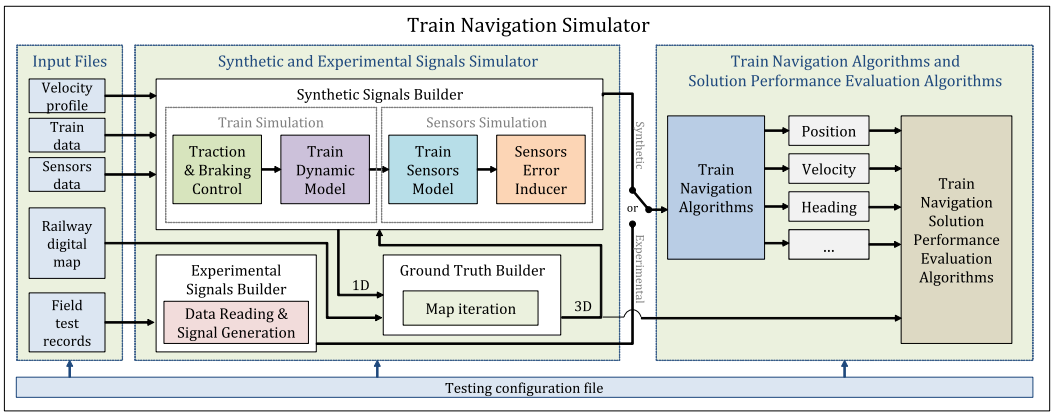

Figure 4.1: The proposed simulation framework for testing train navigation algorithms.

The main contributions of this paper can be summed up as follows.

1. It provides functionalities that previous simulation frameworks do not deal with, making it a one-stop flexible simulation framework: one of the most relevant contributions is related to the signals generation, where synthetic and experimental signals can be used. The main enhanced functionalities over the state-of-the-art simulation frameworks can be found in Table 4.1.

2. The synthetic signals can be generated in flexible way based on train characteristics (mechanical, electrical and electronic issues), track features (curve radius, cant, slope, heading, etc.), sensors data (sampling rate, error sources, etc.) and speed profiles (commanded velocity, acceleration and jerk) defined in the initialization files. This is concluded to be the most flexible way to test train navigation algorithms.

3. Different mechanization methods (such as reduced mechanization and gyro-based mechanization techniques), data fusion algorithms (such as decision rules based and EKF based algorithms) and performance evaluation methods can be used to evaluate the same sensors measurements.

Further developments of this work shall cover the integration of GNSS and digital maps for positioning purposes.

Simulation Framework for Testing Train Navigation Algorithms based on 9-DOF-IMU and Tachometers

Jon Otegui, Alfonso Bahillo, Iban Lopetegi and Luis Enrique Diez

***Abstract*—The integration of candidate sensors such as a microelectromechanical system-based inertial measurement unit (MEMS IMU) for localization and navigation has been widely explored for vehicular, pedestrian and robotics applications. They also arise as candidate sensors in the train navigation context and their integration in safety relevant applications has become a prominent area of interest. This requires sensor modelling in a specific context, the search of new information sources (e.g., digital maps), development of navigation algorithms, and testing of the system. In this context, this work proposes a one-stop simulation framework for testing train navigation algorithms that uses a 9 degrees of freedom (DOF) IMU and tachometers. The simulation framework can generate synthetic signals based on the dynamic model of a train, digital maps, speed profiles and sensor error model. It also uses real signals recorded from experimental measuring campaigns. Train navigation algorithms are then executed. Finally, the performance of the obtained results is evaluated. The main contribution made by this framework is its flexibility when used to evaluate different sensors, train configurations, tracks, mechanization methods, navigation algorithms, and so on during different stages of the development process. Simulation framework use cases are presented in this work, where several mechanization methods and train navigation algorithms are tested. Finally, experimental data is recorded and included in the presented simulation framework to evaluate an example of a train navigation algorithm based on a 9-DOF-IMU and tachometers. The mean differences in the synthetic and experimental IMU signals are around 3.52% in accelerometers, below 0.01% in gyroscopes, and 10.16% in magnetometers in the acceleration sections (i.e. when train is applying torque).**

***Index Terms*—simulation, tachometers, inertial sensors, train navigation, sensor fusion, digital maps**

I. Introduction

THE development of train localization and navigation systems is a prominent field of research, especially when they are focused on relevant safety applications. Both the enhancement of the functionality of current systems and the integration of new candidate sensors (e.g., GNSS or IMU) contribute to this promising area of research in the train and railways context. In addition, the standardization and interoperability issues set in the European Railway Train Management System (ERTMS) and European Train Control System (ETCS) have led the EU to promote this research field through projects such as NGTC [1], STARS [2], ERSAT GGC [3], and so on.

Although it has almost been 20 years since the design of the first architectures in which multisensor data fusion was integrated, the proposals of candidate sensors and the development of train positioning algorithms have only recently become a relevant research topic, particularly in the last 5 years. The majority of these studies are focused on developing data fusion algorithms that are fed by different sources, such as GNSS, IMU, tachometers (a.k.a. wheel speed sensors or encoders), Doppler radars, Eddy-current sensors or track beacons (a.k.a. balises). The most relevant works dealing with this issue are gathered and analyzed in [4].

The integration of the proposed solution in a train navigation system requires exhaustive testing procedures to guarantee the high safety requirements related to train positioning [5]. This obliges the performance of the proposed algorithms to be tested under many different scenarios where the sensors are expected to give erroneous measurements. For example, when slipping occurs due to lack of adherence between wheel and rail, the tachometer will tend the overestimate the angular rate of the wheelset. Meanwhile, the IMU will present a bias drift problem that can accumulate substantial error over time, especially for velocity and distance calculation. Although the most realistic scenarios are experimental tests, they are expensive because they require a large number of scenarios to be tested. Consequently, simulation frameworks have become a popular alternative to test train navigation algorithms.

A concise description of a simulation framework in which different sensors and train parameters, as well as track and speed profiles are characterized can help us to better understand the behaviour of candidate sensors (such as IMU) under multiple scenarios without making use of costly experimental tests on railways. In addition, a simulation framework can be a very useful tool to evaluate the train navigation algorithms that have already been developed, while using different criteria to find the specific cases where they work best.

This work is motivated by the few complete simulation frameworks that are currently available to flexibly test the performance of train navigation algorithm. The lack of frameworks on which the train navigation algorithms

Manuscript received May 30, 2019; revised August 28, 2019; accepted May 30, 2019. Date of publication May 30, 2019; date of current version May 30, 2019.

J. Otegui, A. Bahillo and L. E. Díez are with Faculty of Engineering, University of Deusto, Av. Universidades, 24, 48007, Bilbao, Spain (e-mail: jon.otegui@deusto.es; alfonso.bahillo@deusto.es; luis.enrique.diez@deusto.es).

I. Lopetegi is with Construcciones y Auxiliar de Ferrocarriles Investigación y Desarrollo, CAF I+D, Calle José Miguel Iturrioz 26, 20200 Beasain, Spain (e-mail: ilopetegi@caf.net).

Digital Object Identifier

This article has been accepted for publication in a future issue of this journal, but has not been fully edited. Content may change prior to final publication. Citation information: DOI 10.1109/TIM.2019.2957892, IEEE Transactions on Instrumentation and Measurement

Table I: A comparison of the simulation frameworks.

		Simulation Frameworks				
		[8]	[9]	[10],[11]	[12]	Proposed
Input files	Train characteristics	No	Yes	Yes	No	Yes
	Sensors characteristics	No	Yes	No	No	Yes
	Speed profile	Yes	Yes	Yes	No	Yes
	Track profile	Yes	Yes	Yes	Yes	Yes
Sensors	Accelerometers	Yes	No	Yes	Yes	Yes
	Gyroscopes	Yes	No	Yes	Yes	Yes
	Magnetometers	No	No	No	No	Yes
	Tachometers	Yes	No	Yes	No	Yes
Signal Generation	Synthetic signals	Yes	Yes	Yes	No	Yes
	• Sensors error models	No	No	No	No	Yes
	• Degraded scenarios	Yes	Yes	Yes	No	Yes
	• Vehicle dynamic model	No	No	Yes	No	Yes
	Experimental signals	No	Yes	No	Yes	Yes
Navigation algorithms	IMU mechanization methods	No	No	Yes*	Yes*	Yes**
	Data fusion methods	Yes*	Yes*	Yes*	Yes*	Yes**
	Performance evaluation methods	No	Yes	Yes*	Yes*	Yes*

Acronyms: Only one method (*) or more than one methods (**) are presented and tested.

could be tested by both synthetic and experimental signals is considered to be a research gap, which this work aims to address. This can reduce the testing time of train navigation algorithms because the same simulation framework can be used in different stages of the development process (e.g., for design, test, and validation purposes).

The present paper aims to describe a complete simulation framework. Its potential deployment will be used to test the performance of train navigation algorithms. This work encompasses the most recent and validated IMU models, and it makes use of the knowledge of the rolling stock manufacturers to build a tachometer model. This may overcome the lack of detail about the synthetic sensor signals that are used in the current simulation frameworks. It also allows us to work with both synthetic (generated by mathematical models) and actual (recorded in experimental tests) sensor signals, making it completely flexible. In addition, the presented framework can work with different types of IMUs, tachometers, train configurations, railway tracks and velocity profiles, which can be configured with initialization files. Finally, this framework has been adapted—but is not limited—to evaluate train navigation algorithms under the ERTMS/ETCS accuracy criteria.

The rest of this paper is organized as follows. Section II gathers an exhaustive analysis of the current simulation frameworks and summarises their main limitations. Section III covers the description of the proposed simulation framework and it highlights the potential uses of this work. In Section IV, synthetic and experimental signal generation stages are described in detail. Meanwhile, the train navigation and solution performance evaluation algorithms are described in Section V. In Section VI, the case studies of the simulation framework are shown and they are compared to experimental data, while discussing the obtained results. In Section VII, two different mechanization methods and data fusion techniques are proposed as test cases of the simulation framework. Finally, the main conclusions and some areas for future research are drawn in Section VIII.

II. Simulation Frameworks: An Overview

The utilization of simulation frameworks to evaluate positioning and navigation systems is quite extended in aviation [6], [7] which can be considered close to the train navigation context because of its high safety requirements and costly experimental tests. In contrast, in the train navigation context, there are very few works that enclose all of the stages required to build an one-stop simulation framework. The very first work dealing with train navigation was presented 15 years ago, in which the conception of a train position locator simulator was described, including GNSS, IMU and tachometers [8]. However, this work is limited to the synthetic generation of signals (i.e., no experimental data are used to validate the accuracy and precision of the synthetic signals) and it is not used to test train navigation algorithms. The most intensive work carried out on train navigation simulation frameworks was published over 10 years later. This framework is called ATLAS (Advanced Train Location Simulator) [9] and is focused on on-board railway location using wireless communication technologies, such as GNSS, Global System for Mobile communications in Railway (GSM-R) and Universal Mobile Telecommunications System (UMTS). Its main limitations are the lack of IMU and tachometers for train navigation, while the sensor's signals are not validated using experimental data.

Apart from complete simulation frameworks, several works have used particular-use test frameworks (e.g., for evaluating algorithms accuracy or safety level). Although these frameworks enable the authors to test and analyze their own design of a particular system, the flexibility to

This article has been accepted for publication in a future issue of this journal, but has not been fully edited. Content may change prior to final publication. Citation information: DOI 10.1109/TIM.2019.2957892, IEEE Transactions on Instrumentation and Measurement

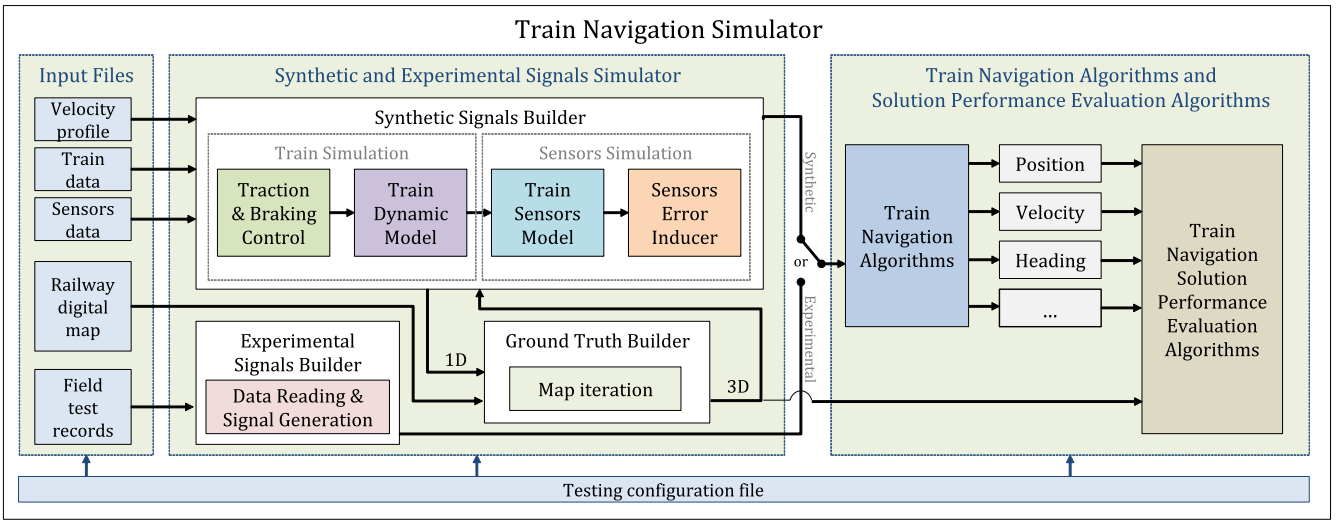

Figure 1: The complete proposed simulation framework for testing train navigation algorithms.

test other architectures (i.e., with different sensors, trains, tracks or navigation algorithms) is rather limited. The most significant works on this topic evaluate a specific odometry algorithm based on tachometers and IMU using a train dynamic model ([10], [11]). However, these works do not implement error models of the sensors and the synthetic signals are not compared against experimental ones. Furthermore, other works only use experimental tests to obtain sensors measurements, which are then fed to the proposed train navigation algorithms but are only tested in a few scenarios [12]. These works are limited in most cases to the architecture designed and, consequently, they are less flexible when including new candidate sensors, modifying the characteristic of the current sensors, or when changing the train and track parameters.

Another framework for the certification and safety authorization process for a location determination system based on the GNSS integrated into the ERTMS is presented in [13]. Finally, although there are many simulation frameworks related to railway networks, logistics management, timetable assessments or gaming purposes, they have been omitted from this literature review because they do not discuss train navigation.

The simulation frameworks described previously are gathered in Table I, where their main limitations are highlighted. Note that the presented simulation framework overcomes some of the main limitations presented by previous works, making it one of the most flexible options to design, evaluate and validate train navigation algorithms.

III. Description of the Simulation Framework

The simulation framework that is presented in this work was developed in Matlab-Simulink, due to ease of representation and integration of different simulation blocks and the integration of mathematical libraries. This is bounded but not limited to 9 DOF IMU (i.e., tri-axial accelerometers, gyroscopes and magnetometers) and tachometers because short-term train navigation is expected to be based on enhanced odometry systems [14].

The overall functioning of the simulation framework presented in this work can be outlined as follows (Fig. 1): first, all of the data required as input are loaded to the simulation framework. An overall *testing configuration file* (Fig. 1) sets the global variables (output data rate, train navigation algorithm, IMU mechanization method, etc.). *The input files* (Fig. 1) block includes information about the velocity profile, digital map, train parameters, sensors characteristics, and so on. Once the input data is loaded, the sensor signals are built based on synthetic or experimental procedures. The signal generation process is gathered in the *synthetic and experimental signal simulator* (Fig. 1). After the sensor signals are generated, the train navigation algorithm processes them to get the train navigation solution (i.e., train position, velocity, heading, etc.). Finally, the performance of the solution is evaluated by comparing the estimated results to the reference values. Both algorithms are gathered in the *Train Navigation Algorithms and Solution Performance Evaluation Algorithms* (Fig. 1). Further details of the boxes shown in Fig. 1 are given in Sections IV and V.

As stated previously, proposed simulation framework both generates synthetic sensor signals (theoretical scenario) and loads them from a previously recorded file (experimental scenario), or even both synthetic and experimental signals can be mixed. This makes the framework flexible for theoretical or experimental purposes. Note that the synthetic signal generation shows the potential uses of utmost relevance during the testing procedure for train navigation algorithms. They can then be used to evaluate the maximum performance, and even to control the error sources and their magnitude on the simulated sensor signals. In addition, all of the synthetic signals can be compared to the experimental records, if they are available, by simply modifying the initialization files. In the following sections, the synthetic signal generation and experimental signal generation stages are described.

This article has been accepted for publication in a future issue of this journal, but has not been fully edited. Content may change prior to final publication. Citation information: DOI 10.1109/TIM.2019.2957892, IEEE Transactions on Instrumentation and Measurement

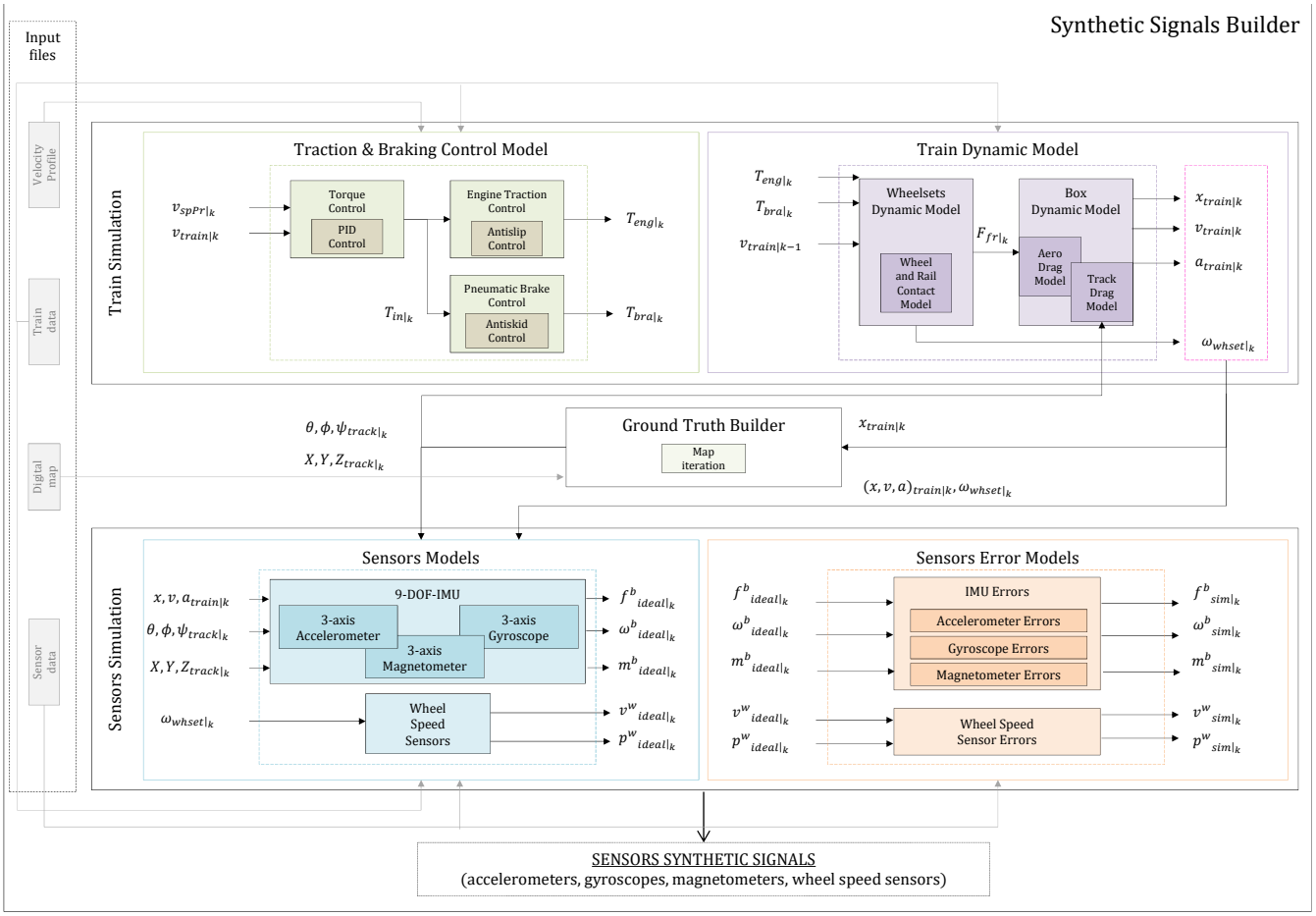

Figure 2: Synthetic signal generation procedure.

IV. Synthetic and Experimental Signal Generation

The simulation framework is able to build sensor signals from either experimental files or to generate synthetic signals. The experimental file can be obtained from any field test record with a time stamp. The simulation framework reads data and then generates a signal, which is further used in train navigation algorithms. For both cases, a reference value set (named here as Ground Truth) is required to evaluate the performance of the train navigation algorithms, which can be generated from experimental file or generated synthetically (Fig. 2).

To build synthetic signals, a simulation framework requires contextual information about the train and railway that are expected to be simulated. Consequently, it is fed by a testing configuration file, which selects a velocity profile, a digital map, sensors parameters, train characteristics, and a series of global variables (e.g., output data rate, simulation time-step, etc.) as shown in Fig. 1 and Fig. 2.

The *velocity profile* (Fig. 2) is a dataset, in which the velocity commanded to the train control is referred to the covered distance or time. Although time-referred profiles are easier to get experimentally, it is more accurate in the train navigation context to find distance-referred profiles to define stations, level crossings and curved sections. Distance-referred velocity profiles have previously been designed, hence they are known before a train starts moving and they are usually optimized to reduce operational energy consumption [15]. This is the main reason why the velocity profile defined for the simulation framework is distance-referred. The velocity profile is used in the *Traction & Braking Control* block to estimate the engine and braking torques (Fig. 2).

A *digital map* (Fig. 2) is a collection of track features (e.g., cant, heading and slope angles, curve radius, geodetic position, balises and stations location, etc.) that is compiled and formatted for multiple purposes. Digital maps provide the representation of both geometry and topology of the railway tracks, and they also create the connection between three-dimensional position coordinates and one-dimension track-defined location for the train [16]. In contrast, typical railway maps provided by railway operators only give cant, curve radius and height information (neither longitude or latitude is given). However, the latest scientific contributions are making great efforts to provide absolute positioning to the current maps [17], [18]. This simulator makes use of a digital map as the main source

This article has been accepted for publication in a future issue of this journal, but has not been fully edited. Content may change prior to final publication. Citation information: DOI 10.1109/TIM.2019.2957892, IEEE Transactions on Instrumentation and Measurement

for generating the 3D Ground Truth (see *Ground Truth Builder* in Fig. 2) based on a configurable train simulator of the 1D velocity and position (Fig. 1). The flexibility for defining an adhoc digital map and the configuration parameters of a particular train provides an accurate and adaptable Ground Truth generator that is able to feed any candidate sensor for train navigation algorithms.

The *train data* file (Fig. 2) contains information about the train box (a.k.a. carbody), bogies, wheelsets, engine traction and pneumatic brake control parameters, aerodynamic coefficients, wheel and rail contact model variables, and so on. All of the parameters given in this file are described and justified in Section IV.A of this article.

The *sensor data* file (Fig. 2) gathers all of the parameters given in sensors' datasheets, which will be used to generate synthetic signals. In the case of tachometers, the resolution and sampling rate are required. In case of 9-DOF-IMU static bias, bias linearity with temperature, scale-factor, scale-factor dependability of temperature and noise parameters are some of the typical parameters that are given in the datasheets. All of the parameters given in this file are described and justified in Section IV.B of this article.

The simulation framework first loads all of the files that will play a key role in synthetic sensors signal generation process (Fig. 2). This process begins with train simulator block, which is responsible for calculating the train's kinematic (e.g., accelerations, velocity, covered distance, angular rates, rotating angles, etc.) and dynamic (e.g., engine and braking torque, friction and aerodynamic forces, etc.) variables based on the *Input Files* block. Once the train's movement is defined, the simulation framework is able to generate the reference values (Ground Truth) by iterating the position of the train along a given map named as *Map Iteration* in Fig. 1 and Fig. 2. Then, 9-DOF-IMU and tachometers signals are generated from the digital map and train movement variables (*Sensors Model* in Fig. 2). Errors are then induced to ideal signals (*Sensors Error Model*, see Fig. 2). The train simulator and sensor simulator are described in detail in the following subsections.

A. Train Simulator

The train simulator presented in this work is mainly based on mechanical features. For ease of understanding, its implementation is divided into the *Traction and Brake Control Model* and the *Train Dynamic Model* (Fig. 2). The first model determines the engine and brake torque required to reach the commanded velocity profile. The second model estimates train's kinematics based on the torque applied to the wheelsets.

1) Traction and Brake Control Model: The *Torque Control* (Fig. 2) reads the commanded velocity ($v_{spPr|k}$) to a train, which is given by the velocity profile. Depending on the train's velocity, ($v_{train|k}$), it sets the input torque ($T_{in|k}$) based on a Proportional-Integrator-Derivative (PID) control. The input torque ($T_{in|k}$) can be either positive (i.e., traction) or negative (i.e., braking), depending on the velocity profile designed by the author.

Table II: Train's characteristics

Parameters	***Value***	***Unit***
Mass (Tare)	15000	kg
Mass (Load)	20000	kg
Axle mass	2200	kg
Motor inertia	4.35	$kg \cdot m^2$
Wheelset inertia	120	$kg \cdot m^2$
Inertia factor	0.6	-
Max. traction effort of the train engine	161000	N
Axle linear velocity for max. traction	108.1	km/h
Max. pneumatic brake torque	4600	$N \cdot m$
Distance between axle 1 and 2	3	m
Distance between axle 1 and 3	18.7	m
Distance between axle 1 and 4	21.7	m
Axles' wheel diameter	0.92	m
Gearbox ratio	2.69	-
Aerodynamic drag constant	0.05	$daN/(km/h)^2$

The input torque ($T_{in|k}$) is used to calculate the engine torque ($T_{eng|k}$) that is required to reach the commanded velocity ($v_{spPr|k}$). Note that electric engines are able to accelerate or decelerate the wheelsets, so the engine torque values ($T_{eng|k}$) can either be positive or negative. However, their traction and braking ability is limited due to engine power, efficiency, and wheel and rail adhesion conditions. To make it more realistic or precise when reading slipping phenomena while tractioning, anti-slip control has been included. This control allows us to simulate different adhesion conditions (e.g., modifying dry friction coefficient for any section of the map) and it allows us to adapt the torque applied to the wheelsets. This is one of the reasons, on top of the PID, that makes the Ground Truth velocity ($v_{train|k}$) different from the commanded velocity ($v_{spPr|k}$).

In addition to electric engines, trains are equipped with pneumatic brakes that are used when the engines are unable to reduce the train's velocity themselves. In this train simulator, they are modelled as braking torque ($T_{bra|k}$), so their values will always be negative or zero. The braking ability of pneumatic brakes is also limited until the wheelsets are locked. However, this scenario can damage the shape of the wheels, thus affecting the wheel thread and causing vibrations. In order to avoid this phenomena, anti-skid control is used.

The torque control models that are implemented in this work are based on longitudinal train dynamics described in [19]. Each rolling stock manufacturer usually designs these systems with proprietary blocks and they can vary from one train to another. Consequently, the simulation framework has been designed to be adaptable, as long as the interface is kept.

2) Train Dynamic Model: The train dynamic model block calculates the kinematic variables (train acceleration -$a_{train|k}$-, velocity -$v_{train|k}$-, covered distance -$x_{train|k}$- and the wheelsets' angular rate -$\omega_{whset|k}$-) based on the forces acting on the vehicle making use of Newton's 2nd law and time-integration techniques. The train model build is composed of a *Wheelset Dynamic Model* and *Box Dynamic Model* (Fig. 2).

The *Wheelset Dynamic Model* (Fig. 2) is based on the torques applied to the wheelsets and the reaction torques that appear in the contact zone between the wheel and rail. In the first stage, the maximum allowable force is estimated based on the information given by the traction and brake control (i.e. traction -$T_{eng|k}$- and braking -$T_{bra|k}$- torques). According to the adhesion between wheels and rail, maximum allowable forces in the wheelset are calculated (a.k.a. contact forces -$F_{fr|k}$-). Note that these forces will always be lower than or equal to the forces calculated from tractioning and braking torques. Kalker's simplified theory is used to calculate the contact forces, assuming a Herzian contact, which is considered to be the most contrasted hypothesis in wheel-rail contact theory [20].

The *Box Dynamic Model* (Fig. 2) makes use of the contact force calculated previously in *Wheelset Dynamic Model* ($F_{fr|k}$) and it adds drag effects to the train box. On the one hand, aerodynamic drag for air evolving around the train is calculated using a quadratic function of the velocity based on Davis equation (*Aero Drag Model* in Fig. 2) [21]. The validation of the model used can be found in [22]. On the other hand, the track drag model is built based on digital map information, such as curve radius, cant and slope angles (*Track Drag Model* in Fig. 2). The formulation and on-field tests can be found in [23] and [24].

By subtracting the drag forces from the contact force, Newton's 2nd law can be applied to obtain train accelerations on tri-axial body frame [25]. By integrating over time, the longitudinal acceleration ($a_{train|k}$), train speed ($v_{train|k}$) and covered distance ($x_{train|k}$) can be obtained numerically. The wheelset's angular rate ($\omega_{whset|k}$) is given by the *Wheelset Dynamic Model*.

Note that the implemented train simulator is non-linear, as shown in Fig. 2: train velocity ($v_{train|k}$) is used to estimate the covered distance ($x_{train|k}$). The covered distance is used to iterate into the map, which provides the cant ($\phi_{track|k}$), slope ($\theta_{track|k}$) and heading ($\psi_{track|k}$) angles that are required in track drag model to estimate train velocity ($v_{train|k}$). The map iteration process carried out in *Ground Truth Builder* also provides absolute position values ($X, Y, Z_{track|k}$) in the local coordinate frame.

B. Sensor Simulator

The sensors simulated in this work are a tachometer and a 9-DOF-IMU (with tri-axial accelerometers, gyroscopes and magnetometers). The tachometer is a well-known sensor in the train navigation context and it is able to provide accurate measurements in nominal conditions. However, it must deal with wheel-rail contact, so accuracy can be degraded in low adhesion conditions or when the wheel is worn [26]. To overcome this limitation, an IMU plays a key role when estimating the velocity and covered distance because it does not depend on the wheel-rail contact. Many of the proposed train navigation systems are based on the same sensors simulated in this work (e.g., [10] and [27]).

Table III: Sensor characteristics

Parameters	***Value***	***Unit***
Tachometers		
Number of teeth	80	-
Maximum time-out for stopping	2	s
Accelerometers		
Static bias	0.25	m/s^2
Static bias drift with temperature	0.01	(m/s^2)/K
Scale-factor or sensitivity	0.61e-3	(m/s^2)/LSB
Scale-factor drift with temperature	0.03	%/K
Cross-axis sensitivity	0.01	-
Noise power spectral density	1.8e-3	$(m/s^2)/Hz^{1/2}$
Gyroscopes		
Static bias	3	deg/s
Static bias drift with temperature	0.05	(deg/s)/K
Scale-factor or sensitivity	0.1	(dps)/LSB
Scale-factor drift with temperature	0.02	%/K
Cross-axis sensitivity	0.02	-
Noise power spectral density	1.8e-3	$(deg/s)/Hz^{1/2}$
Gravity sensitivity (a.k.a. g-sensitivity)	0.18e-3	$(rad/s)/(m/s^2)$
Magnetometers		
Static bias	0.06	G
Static bias drift with temperature	0.3e-3	G/K
Scale-factor or sensitivity	1.5e-3	G/LSB
Scale-factor drift with temperature	0.03	%/K
Cross-axis sensitivity	0	-
Noise power spectral density	3.0e-3	$G/Hz^{1/2}$

1) Tachometer: The tachometer measures the spikes of a rotatory gear and it gives the revolutions per time unit of the wheelset. The rotation of the sensor is proportional to the covered roll off distance of the wheel along the rail head; hence, the distance and the velocity can be estimated by taking into account the revolution per time unit and the diameter of the wheel [28].

The measurement physics of the simulated tachometers are based on the Hall Effect. A gear tooth is detected due to the air gap between the sensor and the gear. This generates an electrical pulse sequence, which is read by a field-programmable gate array (FPGA). The total number of pulses are counted and the time between flanges is measured. This makes the signals more challenging to measure at high rotation rates. In addition, at low rotation rates, the time between flanges can be large, so the time-out parameters are generally used to consider zero velocity. Depending on the application and the velocity ranges wanted to measure, the number of teeth of rotatory gear changes [29]. This parameter is usually called the encoder's resolution.

The tachometer signal is built based on the wheelset angular rate obtained from train simulator ($\omega_{whset|k}$) and configuration file information (encoder's resolution, time-out parameter and wheel radius). The outputted signals from *Sensors Models* (Fig. 2) are the linear velocity ($v^w_{ideal|k}$) and the counter that accumulates measured pulses ($p^w_{ideal|k}$).

The main error source induced in the tachometers is related to the simulation of wheel slip or skid phenomena, which makes the sensor overestimate or underestimate rotation rate measurements. In addition, the train wheel's rolling radius difference from nominal value (e.g., due to wear) infers measurements errors. White noise is

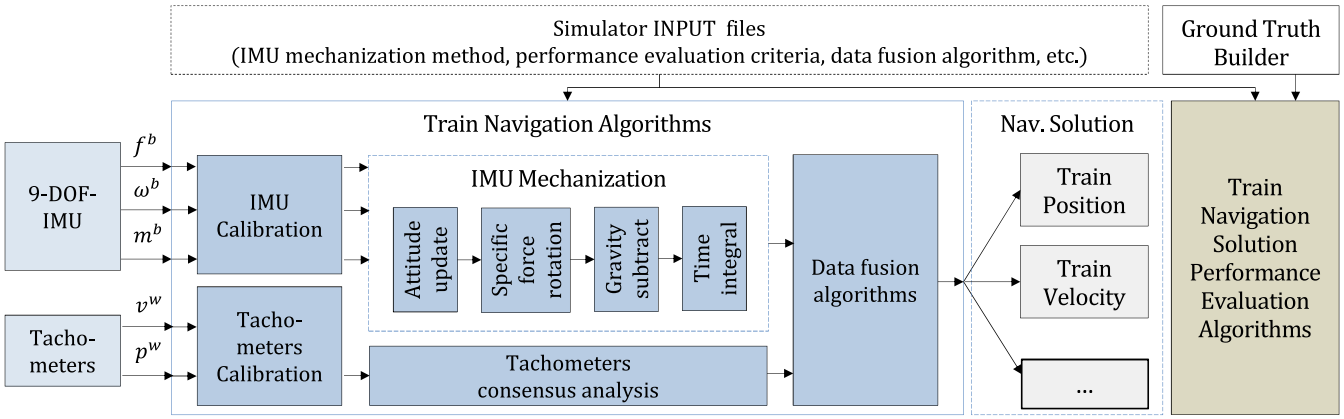

Figure 3: Train navigation algorithms for 9-DOF-IMU and tachometers.

added to original signal to simulate the time measured between spikes can include discretization errors. After the error models are included, the outputted signals from the *Sensors Error Models* (Fig. 2) are the linear velocity ($v^w_{sim|k}$) and the counter that accumulates measured pulses ($p^w_{sim|k}$).

2) Inertial Measurement Unit: The IMU signals simulated in this work consist of tri-axial accelerometers, gyroscopes and magnetometers that measure the train's accelerations, angular rates and magnetic field intensity, respectively.

The measuring technology of the simulated IMU is based on microelectromechanical systems (MEMS) but the configuration file is adaptable to simulate other kind of technologies as long as the error sources are the same. MEMS sensors can be low cost and low powered systems, which make them attractive to mass-market applications. However, their measurements are not accurate compared to their tactical grade counterparts and they suffer from bias, noise, scaling errors, non-linearity, temperature based variations and misalignment errors [30]. In addition to deterministic errors, these kind of sensors also suffer from stochastic errors [31].

Extensive studies of accelerometer and gyroscope models for vehicles can be found in the literature. In this work, two particular conclusions from previous works have been considered: first, accelerometers and gyroscopes measurements are modelled according to track features and vehicle kinematics, as stated in [23]; and second, railway cant deficiency and its influence on lateral accelerometer measurements are considered, as stated in [10]. These facts have been considered when ideal accelerometers ($f^b_{ideal|k}$), gyroscopes ($\omega^b_{ideal|k}$) and magnetometers ($m^b_{ideal|k}$) signals are generated in the *Sensors Model* (Fig. 2).

All types of accelerometers and gyroscopes exhibit biases, scale factor, and cross-coupling errors, and random noise to a certain extent [32]. In addition, previous errors can be influenced by temperature changes that can be usual in train navigation context in contrast to indoor positioning, for instance. Consequently, the error model designed in this work considers the error behaviour of low-cost inertial sensors in dynamic conditions [33], bias, scale-factor [34] and noise characteristics [30], [35], [36] and temperature influence [37]. Simulated accelerometers ($f^b_{sim|k}$) and gyroscopes ($\omega^b_{sim|k}$) signals in *Sensors Error Model* (Fig. 2) includes these facts over ideal signals.

The magnetometers measure the magnetic field intensity around the sensor. Consequently, the simulator is required to have a model that could provide these data. In this work the World Magnetic Model (WMM) developed by National Oceanic and Atmospheric Administration (NOAA) has been used because it is considered to be the most contrasted and refuted model [38].

In an ideal situation, the magnetometers would measure the terrestrial magnetic field for a given point. However, biases and scale-factor errors are induced in real scenarios. In addition, magnetic disturbances due to catenary, electronics, and signal interference are very usual in a railway context. Consequently, a specific error model is required for the simulation framework, which gathers biases, scale factor, cross-coupling errors, noise, and so on [39], [40]. Simulated magnetometers ($m^b_{sim|k}$) signals in *Sensors Error Model* (Fig. 2) includes these facts over ideal signals.

V. Train Navigation Algorithms and Solution Performance Evaluation Methodology

Once the sensor signals are built (either synthetic signals or experimental signals), they are used as inputs for train navigation algorithms. General purpose navigation algorithms aim to estimate the position and derived variables (e.g., velocity, acceleration, orientation, etc.) but train navigation is focused on calculating vehicle velocity and covered distance (also known as odometry) [11]. Consequently, the simulation frameworks have been designed focused on but not limited to odometry, which allows us to estimate complementary variables (e.g., orientation).

Navigation algorithms are usually made up of multiple stages or sub-algorithms, which are used for dynamic calibration of sensors, IMU mechanization, tachometers consensus analysis and data fusion. These stages are depicted in Fig. 3 and implemented in the simulation framework; further details are given later in this section.

This article has been accepted for publication in a future issue of this journal, but has not been fully edited. Content may change prior to final publication. Citation information: DOI 10.1109/TIM.2019.2957892, IEEE Transactions on Instrumentation and Measurement

Dynamic calibration or compensation model of sensors is a common technique to estimate recursively error terms in measurements. In case of tachometers, it is usual to update the wheel radius value; whereas in case of IMU, measurements biases are estimated in static scenarios or making use of additional sensors.

IMU mechanization is the process in which sensor's orientation, acceleration, velocity and position are estimated. First, orientation angles are calculated to compensate for the gravity term in accelerometers. Generally speaking, it requires an attitude update on each iteration to transform the current measurement frame (body frame) to navigation frame where the gravity vector is known. Once the acceleration is obtained, the velocity and covered distance can be calculated by time integration. The simulation framework also allows different type of mechanization methods, which allow reduced mechanization methods to be implemented [41], [42].

It is very usual to install more than one tachomete a train alternating driving and trailing axles. Some slip and skid phenomena can be compensated by taking the maximum or minimum measurements in a processing stage called sensor consensus [29].

Data fusion is the last stage of the train navigation algorithms. They are usually based on Kalman Filter and derived architectures but in some cases simpler algorithms can be found (especially for fail-safe purposes). The data fusion algorithms output so-called states, which are used to calculate the train navigation solution.

The final part of the simulation framework evaluates the performance of the estimated train navigation solution against Ground Truth. In most cases, the solution is evaluated in terms of accuracy and precision using root mean square error, hypothesis tests, and so on [9]. In addition, different mechanization techniques or train navigation algorithms can be compared to each other.

VI. Synthetic and Experimental Signal: Tests and Results

The potential of the simulation framework is shown through two use cases presented in this section. On the one hand, synthetic signals have been generated for a high speed train that can reach over 250 km/h, which travels on previously designed track and velocity profile. On the other hand, experimental signals have been used from a measurement campaign. In this section, a comparison between synthetic and experimental signals is presented.

A. Synthetic Signals

The utilization of synthetic signals is the main part of the simulation framework because it allows us to simulate different trains, sensors, tracks and train navigation algorithms, leading to a flexible working framework. In this section, a representative use case is presented on which a complete analysis is carried out.

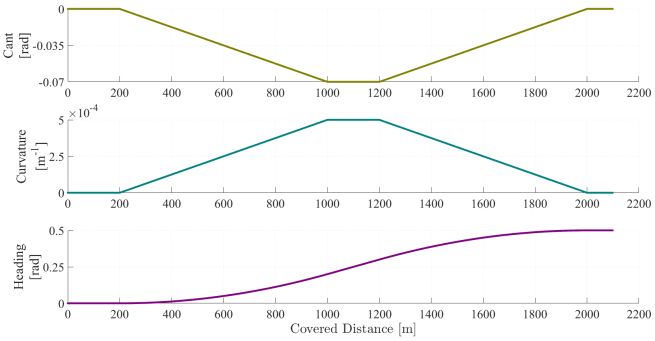

Figure 4: Digital Map for generating synthetic signals.

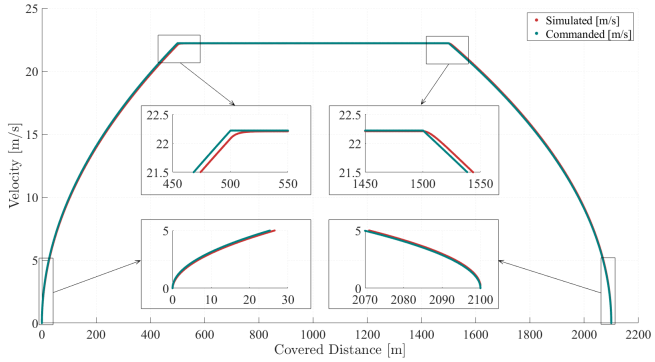

Figure 5: Commanded ($v_{spPr|k}$) and train simulated velocity ($v_{train|k}$).

1) Settings: The train dynamics simulated in the simulation framework corresponds to a high speed train model, whose main mechanical characteristics are gathered in Table II. The values shown there are given by datasheets (e.g., maximum traction effort, axle linear velocity for maximum traction or maximum pneumatic brake) or measured in previous experimental tests (e.g., axle's wheel diameter, distance between axles, masses, etc.).

The characteristics of the simulated tachometers and 9-DOF-IMU can be seen in Table III. The number of teeth on the tachometers' rotatory wheel is a trade-off design between the minimum and maximum measurable rotation rates. The 9-DOF-IMU data corresponds to a low-end IMU that could be integrated in a train navigation system due to ease of installation and reduced economic cost (few euros).

The simulated track can be any digital map defined as an input of the simulation framework. The example presented here covers 2000 m and it has straight and curved sections, as well as transition curves (modelled as clothoids). The curve radius designed for this simulation has 2000 m, which can be considered a typical value for high speed lines according to track design criteria. The curved section has a cant of 100 mm to compensate in part the lateral acceleration. The track designed is plotted in Fig. 4.

The commanded velocity to the train has accelerating, coasting, and decelerating sections. The maximum

This article has been accepted for publication in a future issue of this journal, but has not been fully edited. Content may change prior to final publication. Citation information: DOI 10.1109/TIM.2019.2957892, IEEE Transactions on Instrumentation and Measurement

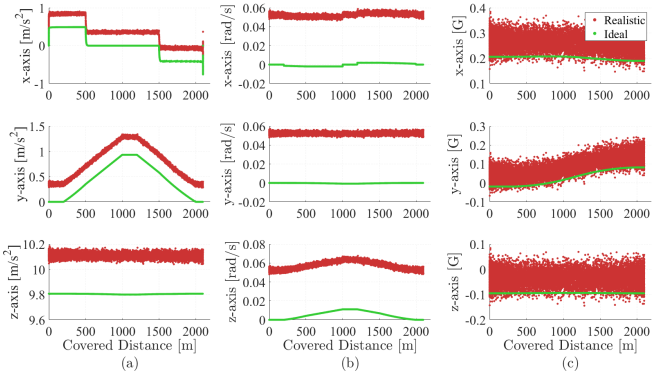

Figure 6: 9-DOF-IMU ideal ($f^b_{ideal|k}$, $\omega^b_{ideal|k}$, $m^b_{ideal|k}$) and realistic ($f^b_{sim|k}$, $\omega^b_{sim|k}$, $m^b_{sim|k}$) synthetic signals. Tri-axial specific-forces (a), angular rates (b) and magnetic field intensities (c) of the simulated signals.

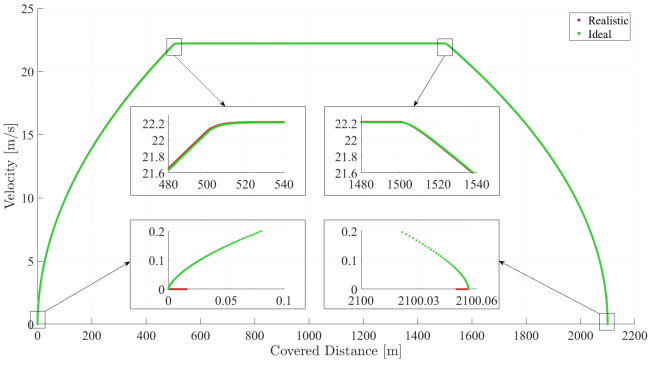

Figure 7: Tachometer ideal ($v^w_{ideal|k}$, $p^w_{ideal|k}$) and realistic ($v^w_{sim|k}$, $p^w_{sim|k}$) synthetic signals.

simulated velocity is 80 km/h (i.e. 22.2 m/s), which is considered to be easily reachable by train characteristics (note that the train model simulated can reach higher velocities when operating in high speed mode) and to fulfill safety criteria for derailment in 2000 m curved section. The commanded velocity profile is plotted in Fig. 5.

2) Results: Let us recall Fig. 2 to analyze the synthetic signals. The very first analysis represented in Fig. 5 shows the difference between the commanded velocity to the train (input file) and the simulated train velocity (constrained by the train dynamics). Although there seems to be few differences in the overall plot, the zoomed areas enable us to see the delay that is inferred in simulated train velocity over the commanded velocity. The reason why two curves are not exactly the same is due to the train control, which needs some time to reach the commanded value. At 500m, the velocity difference is about 0.14 m/s (0.62% difference) and at 1525m the velocity difference is reduced to 0.094 m/s (0.43% difference) because in the coasting zone the train has reached the commanded value. The maximum value (0.26 m/s) is given at the final part of the travel (2100 m), where the train is commanded to stop and several meters are covered before the train goes standstill. The mean difference is around 0.1 m/s, which is equivalent to a 10% difference when a train is running at 360 km/h. Therefore, it is shown that modeling the train dynamics can play a key role when designing high precision (e.g., 1% relative velocity difference) train navigation systems making the Ground Truth more accurate than considering the commanded values. Consequently, the difference between commanded and simulated values are a design constraint but not a problem to correctly evaluate the algorithms.

According to the sensor signals, remarkable differences can be observed between the ideal signals (given by the train dynamics) and realistic signals (added error models to tachometers and 9-DOF-IMU based on [33]). The synthetic signals generated for the 9-DOF-IMU can be observed in Fig. 6, where both realistic and ideal signals are represented. IMU specific-forces gathers the accelerations measured in train box and gravity acceleration projection. Train acceleration, coasting, and deceleration sections can be shown in x-axis specific-forces, where 0.5 m/s^2 magnitude is in concordance with the simulated train velocity profile. The curving zone is reflected on y-axis specific-force due to the lateral acceleration that arises when the train is negotiating a curve. In addition, the z-axis gyroscope measures the heading change (up to 0.01 rad/s), the y-axis magnetometer also senses a variation on the magnetic-field intensity (about 0.1 G) due to a variation of the magnetic north direction. The measurements are affected in the lower part by the track cant, which is reflected on z-axis specific force (0.01 m/s^2 is projected into train vertical axis when it tilts inside the curve) and x-axis angular rate (0.002 rad/s is the rotation rate during the tilting). Regarding the errors induced by the error models used for generating synthetic signals, the major contribution is given by the static bias: note that the mean difference between realistic and ideal signals in x-axis specific-force is 0.35 m/s^2 where the static bias (0.25 m/s^2) represents almost 70.95% of the total error. In case of the x-axis angular-rate, the mean difference is about 0.053 rad/s, where the static bias encompass almost all the error budget (99.73%).

The tachometer signals are analyzed in Fig. 7. The main difference between realistic ($v^w_{sim|k}$, $p^w_{sim|k}$) and ideal ($v^w_{ideal|k}$, $p^w_{ideal|k}$) signals is shown in the initial and final section of the velocity profile; that is, when the train starts moving and when it stops. The time-out (2s as shown in Table III) set to consider null velocity is represented in these sections and the velocity difference is explained as follows: an ideal tachometer can wait an infinite time until a new tooth of the rotatory gear is detected but, in a realistic scenario, a time-out is required to consider that the train is not moving.

According to the results shown in Fig. 6 and Fig. 7, some differences between the tachometer and IMU signals can be distinguished: the tachometers simulated in this work measure the linear velocity ($v^w_{sim|k}$) of the train based on the angular rate of the train's wheelset ($\omega^b_{sim|k}$). The internal logic of the tachometers multiplies the angular rate of the train's wheelset by the wheel radius to provide the

This article has been accepted for publication in a future issue of this journal, but has not been fully edited. Content may change prior to final publication. Citation information: DOI 10.1109/TIM.2019.2957892, IEEE Transactions on Instrumentation and Measurement

linear velocity. This assumption is accurate when the train runs in a straight line, the wheels radii are close to nominal values and pure rolling conditions are fulfilled. When the train is negotiating a curve, for instance, the rolling radius changes (note that train's wheels are conical) and some discrepancies can arise between $v^w_{sim|k}$ and $\omega^b_{sim|k}$. The accelerometers and gyroscopes are not influenced by the angular rates of the train's wheelsets and their signals correspond to the movement of the train box. The main discrepancies that can arise between the sensors utilized are related to the different movement that are measuring: the tachometers deals with wheelsets dynamics and IMU deals with box dynamics. This reason explains why the Train Dynamic Model (Fig. 2) includes Wheelset Dynamic Model and Box Dynamic Model.

B. Experimental Signals

As stated earlier, the simulation framework has been designed to test train navigation algorithms with experimental data. This functionality allows the framework to operate as a record and playback system, which is very common in navigation systems [43]. In this section, a use case of these feature is described based on the measuring campaign carried out by [24]. This section aims to evaluate the experimental errors in signal measurements and compare them to IMU synthetic signals generated in the simulation framework. This work is focused on IMU signals, due to the lack of characterization of these kind of sensors in train navigation context in contrast to tachometers, which are widely explored and used for this purpose.

1) Settings: The train used in measuring campaign is the same high speed model that has been simulated previously and the IMU sensor is a MEMS sensor with the same specification values as defined by Tables II and III. The velocity recorded is based on tachometers and Doppler radars to avoid low-velocity errors due to time-out restriction of the tachometers, and to overcome the slip and skid phenomena.

The railway track that is used corresponds to a straight section of 1500 m, which is covered in approximately 150 s. Note that the simulated track length is similar to the experimental. The velocity profile commanded to the train was not available when recording data but the train operation covers accelerating, coasting, and decelerating sections, as simulated earlier. The track characteristics are estimated as stated in [23] and [24].

2) Results: The measurements recorded by the 9-DOF-IMU (tri-axial specific-forces, angular-rates and magnetic-field intensities) are presented in Fig. 8. To analyze the IMU measurements, three different sections (accelerating, coasting and decelerating) have been chosen (Fig. 9) and the square root of quadratic sum of accelerometers, gyroscopes and magnetometers has been calculated. The obtained results are compared to the three simulated sections by synthetic signals and the comparison is given in Table IV. Note that generated synthetic signals are required to

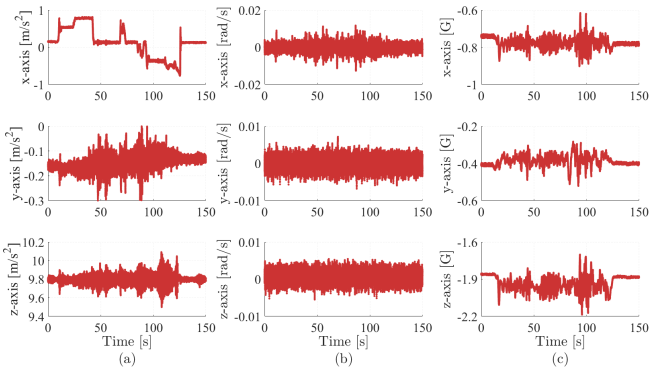

Figure 8: 9-DOF-IMU experimental signals. Tri-axial specific-forces (a), angular rates (b) and magnetic field intensities (c) of the experimental signals.

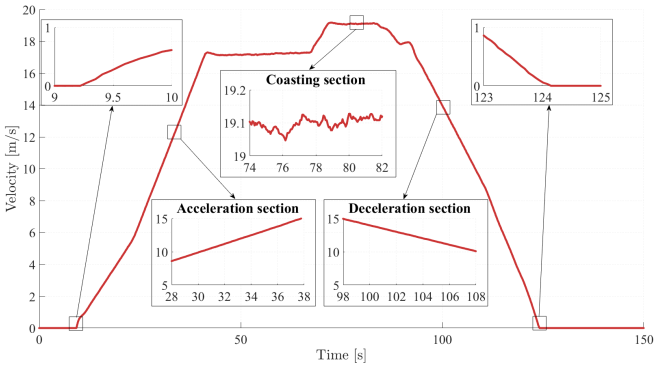

Figure 9: Tachometer experimental signal.

be calibrated (in this work, static bias is removed based on [44]) before comparing to the experimental signals because the utilized IMU provides calibrated and normalized measurements.

The accelerometer signals show a mean difference between raw synthetic signal and experimental signals of about 0.36 m/s^2 (3.52%) in the accelerating section. After static bias is compensated in synthetic signals (note that the simulated signals assume maximum bias given in the datasheet), the difference has dropped to 0.016 m/s^2 (0.16%). The difference between calibrated signals is 0.27% and 0.051% for coasting and decelerating sections, respectively.

The gyroscope's raw signals are strongly affected by the static bias (3 deg/s or 0.052 rad/s), which can be considered rather high for a train navigation context that rarely records 12 deg/s (i.e. 0.21 rad/s) or higher angular rates. However, when it is removed from the synthetic signals (calibration stage), the errors are lowered to almost zero in accelerating and decelerating sections (in coasting section the difference between synthetic and experimental signals is about 0.0076 rad/s).

The magnetometer signals show larger differences than accelerometers and gyroscopes. The main reason for this is the difficulty to model all of the magnetic fields inside a train with magnetometers. In the worst case (coasting

Table IV: Synthetic and experimental 9-DOF-IMU signals comparative.

	IMU accelerometers $[m/s^2]$			IMU gyroscopes $[rad/s]$			IMU magnetometers $[G]$		
	Syn.		Exp.	Syn.		Exp.	Syn.		Exp.
	Raw	Cal.	Cal.	Raw	Cal.	Cal.	Raw	Cal.	Cal.
Accelerating section	10.16	9.81	9.79	0.09	0.0019	0.0019	1.20	1.03	1.00
Coasting section	10.18	9.83	9.80	0.09	0.0100	0.0019	1.14	1.11	0.99
Decelerating section	10.12	9.81	9.81	0.09	0.0028	0.0029	1.02	1.03	1.00

Acronyms: Synthetic signals (Syn.) and experimental data (Exp.). Static bias calibrated (Cal.).

section), a 0.11 G (10.16%) difference is obtained. In accelerating and decelerating sections, the difference is about 3.05% and 2.65%, respectively.

Regarding the velocity measurement recorded in the measuring campaign, a significant difference can be observed below 1m/s velocities (Fig. 9). When generating the synthetic signals, a time-out need has been stated to provide null velocity for higher waiting times. However, in the experimental records, all of the range velocities can be observed. This happens when the tachometer's signals are recorded through Multi-function Vehicle Bus (MVB), where Doppler radar can support tachometers at low velocities.

The comparison of the synthetic (Fig. 7) and experimental (Fig. 9) signals of the tachometers highlights the limitations of the track information. The experimental test carried out in this work deals with the fact that the track information is not available. This is usual where railways are not digitalized or the railway operator only provide topological data of the track. Although some track parameters (e.g. curve radius, slope and cant) can be obtained with additional sensors (e.g. GNSS, Doppler radar, etc.), the transition curves are not known beforehand, so the track characteristics are not fully defined. Consequently, the speed profile measured by the tachometers and the synthetic signal generated are not completely identical. In order to overcome this limitation, the analysis carried out in this work is limited to those sections where track is correctly characterized. This is the reason why different sections (acceleration, coasting and deceleration) are defined in Fig. 7 and the results in Table IV are limited to those sections.

VII. Simulation Framework Use Case: Testing of Multiple Train Navigation Algorithms

Focusing now on train navigation algorithms, two different mechanization techniques are compared to evaluate the orientation estimation from an IMU (Fig. 10). The first method is based on gyroscope measurement integration over time [24], whereas the second method is based on the so called gyroscope-reduced inertial navigation that makes use of external velocity values (from the tachometer in this case) to estimate the orientation angles [41], [42]. The first method is able to calculate these angles using IMU measurements stand-alone; that is, no extra measurements apart from gyroscopes and accelerometers are required, so an independent solution can be obtained. The second method does not use all the IMU measurements but it adds new sensors measurements, so its solution cannot be considered independent for an IMU. Note that when the these angles' accuracy is higher, the gravity acceleration influence on the final solution will be lower. Consequently, the velocity will be lower and the covered distance will drift over time. The results gathered in Fig. 10 show a comparison between two mechanization methods results and the digital map provided values. No correction is applied to the signals (e.g., obtained from calibration or error states) to purely analyze the mechanization method. For gyro-based mechanization, drift phenomena is observed (especially on roll angle whose error at the end of the trip is about 0.02 rad), which is caused by signal errors that are integrated over time. In contrast, the gyro-reduced mechanization shows lower errors along the track, especially in roll and pitch angles estimation: the mean difference of gyro-based roll estimation is 0.012 rad whereas the mean difference of gyro-reduced roll estimation has dropped to 0.00065 rad. In pitch estimation, the mean differences are 0.0021 rad and 0.00054 rad, respectively.

Finally, the estimated velocities by a Decision Rules algorithm and an Extended Kalman Filter (EKF) are compared to the train velocity (given by the train dynamics), as shown in Fig. 11. The Decision Rules algorithm is based on a series of rules defined by expertise on each sensor behaviour that allows us to choose an output solution combining the IMU and tachometer measurements. The EKF can produce estimates of unknown variables, called states, using a series of measurements that provide a sub-optimal solution for non-linear systems (optimal solution is reserved for linear systems and Gaussian distributed noise). In this work, an EKF has been implemented (indirect implementation with error-states based on [11]) to analyze the contribution of these kind of algorithms in inertial systems, and to find its virtues when estimating and correcting measurements errors. The mechanization used for both algorithms is the same and it uses gyroscopes measurements integration over time [24]. The results in Fig. 11 show that in the initial stages, both algorithms are similar and rather accurate to simulated train velocity (approximately 0.0001 m/s error has been computed). However, once the train starts the trip, the errors in orientation are propagated in Decision Rules algorithm, reaching 0.53 m/s error (2.39% error w.r.t. train velocity) at 520 m (similar to 0.5 m/s error presented in [11]). It takes the maximum value of 0.95 m/s at 1152 m.

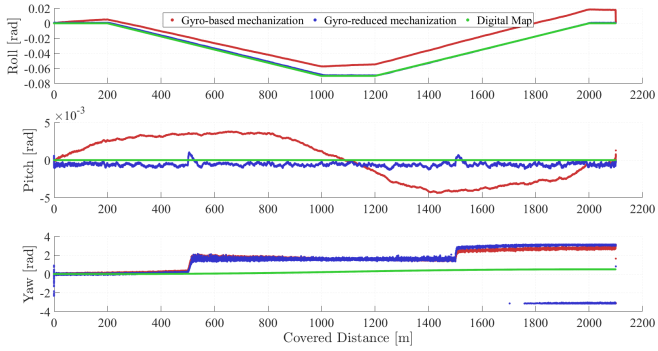

Figure 10: Orientation angles estimation by two different mechanization methods.

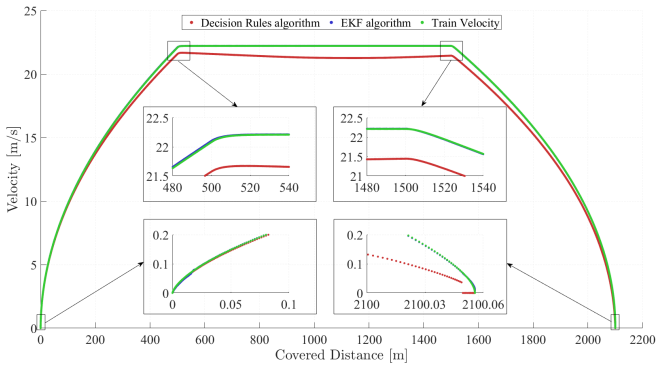

Figure 11: Train velocity estimation by two different data fusion algorithms.

The EKF algorithm is able to compensate IMU errors and orientation angles errors are corrected by tachometers measurements thanks to error-states. The results show a 0.0057 m/s error at 520 m and a maximum error of 0.02 m/s at 498 m.

VIII. Conclusions

In the present paper, a one-stop simulation framework for testing train navigation algorithms is described. The simulation framework broadens the previous works, overcomes the main limitations, and provides a flexible tool to test train navigation algorithms in different stages of development process (i.e., design, test and validation), thereby reducing the overall time.

The flexibility of the presented simulation framework relies on the possibility of using different train and sensor configurations, as well as track and speed profiles for testing train navigation algorithms. Additionally, train navigation algorithms can be fed by either synthetic or experimental signals.

The addition of train dynamic model and sensors error models to the synthetic signal generation has overcame the accuracy limitations cited in previous works. Considering the simulated train velocity instead of commanded velocity allows us to generate more realistic sensors measurements and avoids inferring errors in synthetic signals generation that can condition the performance for high accuracy (e.g., 1% relative error in velocity) train navigation algorithms.

The experimental data recorded in a measuring campaign has propitiated a comparison between 9-DOF-IMU synthetic and experimental signals. The larger differences of the analyzed sections are around 3.52% in accelerometers, below 0.01% in gyroscopes, and 10.16% in magnetometers. The use cases of the simulation framework presented in this work have demonstrated that different mechanization methods for a 9-DOF-IMU and different train navigation algorithms can be analyzed and their performance can be obtained. According to the test procedure discussion, a gyro-reduced mechanization technique and EKF-based train navigation algorithms arise as prominent techniques.

The utilization of additional sensors, such as, high-end IMU and GNSS for characterizing the track should help to improve the track data and it would help to make a comparison of the whole speed profile but it deals with the experimental data recording process (it is independent of the synthetic signals generation and it does not influence the flexibility of the simulation framework).

Acknowledgements

The authors would like to thank CAF Research and Development Department for contributions to the knowledge of trains and railways, and also for their expertise in the rolling stock modeling that directly motivated the writing of this paper.

References

[1] P. Gurník, "Next Generation Train Control (NGTC): More Effective Railways through the Convergence of Main-line and Urban Train Control Systems," *Transportation Research Procedia*, vol. 14, pp. 1855–1864, 2016. [Online]. Available: https://linkinghub.elsevier.com/retrieve/pii/S2352146516301533

[2] J. Marais, J. Beugin, J. Poumailloux, and M. Gandara, "EGNOS service evaluation in railway environment for safety- critical operations," in *7th Transport Research Arena TRA 2018 (TRA 2018)*, Vienna, Apr. 2018, p. 10.

[3] O. G. Crespillo, A. Konovaltsev, J. Marais, and S. Sabina, "Local GNSS Threat Detection Methods for Virtual Balise Placement in Railway Applications," in *2018 16th International Conference on Intelligent Transportation Systems Telecommunications (ITST)*, Lisbon, Portugal, Oct. 2018, p. 7.

[4] J. Otegui, A. Bahillo, I. Lopetegi, and L. E. Diaz, "A Survey of Train Positioning Solutions," *IEEE Sensors Journal*, vol. 17, no. 20, pp. 6788–6797, Aug. 2017. [Online]. Available: http://ieeexplore.ieee.org/document/8022861/

[5] J. Beugin, C. Legrand, J. Marais, M. Berbineau, and E.-M. El-Koursi, "Safety Appraisal of GNSS-Based Localization Systems Used in Train Spacing Control," *IEEE Access*, vol. 6, pp. 9898–9916, 2018. [Online]. Available: http://ieeexplore.ieee.org/document/8293773/

[6] J. G. McAnanama and G. Marsden, "An open source flight dynamics model and IMU signal simulator," in *2018 IEEE/ION Position, Location and Navigation Symposium (PLANS)*. Monterey, CA: IEEE, Apr. 2018, pp. 874–881. [Online]. Available: https://ieeexplore.ieee.org/document/8373465/

[7] Y. Sui, P. Kang, D. Cheng, and J. Lin, "Analysis and Simulation of Flight Effects on an Airborne Magnetic Gradient Tensor Measurement System," *IEEE Transactions on Instrumentation and Measurement*, vol. 64, no. 10, pp. 2657–2665, Oct. 2015. [Online]. Available: http://ieeexplore.ieee.org/document/7097712/

[8] V. Maixner, H. Mocek, J. Taufer, L. Bažant, and A. Filip, "The Simulator of Train Position Locator," in *Computers in railways IX, J. Allan, C. A. Brebbia, R. J. Hill, G. Sciutto, S. Sone, and Wessex Institute of Technology.* Eds. Southampton, England: WIT Press, 2004, p. 1015.

[9] J. Goya, L. Zamora-Cadenas, S. Arrizabalaga, A. Brazález, J. Meléndez, and J. Mendizabal, "Advanced Train Location Simulator (ATLAS) for developing, testing and validating on-board railway location systems," *European Transport Research Review*, vol. 7, no. 3, Sep. 2015. [Online]. Available: http://link.springer.com/10.1007/s12544-015-0173-5

[10] B. Allotta, L. Pugi, A. Ridolfi, M. Malvezzi, G. Vettori, and A. Rindi, "Evaluation of odometry algorithm performances using a railway vehicle dynamic model," *Vehicle System Dynamics*, vol. 50, no. 5, pp. 699–724, May 2012. [Online]. Available: http://www.tandfonline.com/doi/abs/10.1080/00423114.2011.628681

[11] B. Allotta, P. D'Adamio, M. Malvezzi, L. Pugi, A. Ridolfi, and G. Vettori, "A localization algorithm for railway vehicles," in *IEEE International Instrumentation and Measurement Technology Conference (I2MTC)*, Pisa, Italy, 2015, pp. 681–686.

[12] O. Heirich, "Bayesian Train Localization with Particle Filter, Loosely Coupled GNSS, IMU, and a Track Map," *Journal of Sensors*, vol. 2016, pp. 1–15, 2016. [Online]. Available: http://www.hindawi.com/journals/js/2016/2672640/

[13] A. Filip, S. Sabina, and F. Rispoli, "A framework for certification of train location determination system based on GNSS for ERMTS/ETCS," *International Journal of Transport Development and Integration*, vol. 2, no. 3, pp. 284–297, Jan. 2017. [Online]. Available: http://www.witpress.com/doi/journals/TDI-V2-N3-284-297

[14] J. Marais, J. Beugin, and M. Berbineau, "A Survey of GNSS-Based Research and Developments for the European Railway Signaling," *IEEE Transactions on Intelligent Transportation Systems*, vol. 18, no. 10, pp. 2602–2618, Oct. 2017. [Online]. Available: http://ieeexplore.ieee.org/document/7857080/

[15] Y. Huang, L. Yang, T. Tang, Z. Gao, F. Cao, and K. Li, "Train speed profile optimization with on-board energy storage devices: A dynamic programming based approach," *Computers & Industrial Engineering*, vol. 126, pp. 149–164, Dec. 2018. [Online]. Available: https://linkinghub.elsevier.com/retrieve/pii/S0360835218304406

[16] Wei-Jie, Tao, Baigen, Cai, Jian, Wang, Jian, Liu, and Wei, Shan-guan, "Digital Track Map Generation for Safety-Critical Railway Applications," in *Proceedings of the 30th International Technical Meeting of the Satellite Division of The Institute of Navigation (ION GNSS+ 2017),*, Portland, Oregon, USA, Sep. 2017, pp. 1978–1987.

[17] C. Rahmig and A. Kluge, "Digital maps for railway applications based on OpenStreetMap data," in *16th International IEEE Conference on Intelligent Transportation Systems (ITSC)*. The Hague, Netherlands: IEEE, 2013, pp. 1322–1327. [Online]. Available: http://ieeexplore.ieee.org/abstract/document/6728414/

[18] H. Winter, S. Luthardt, V. Willert, and J. Adamy, "Generating Compact Geometric Track-Maps for Train Positioning Applications," *arXiv:1903.05014 [cs]*, Mar. 2019, arXiv: 1903.05014. [Online]. Available: http://arxiv.org/abs/1903.05014

[19] C. Uyulan, "Adaptive Slip&Slide Control System Design in Railway Applications," *Advances in Science and Technology Research Journal*, vol. 12, no. 1, pp. 207–220, Mar. 2018. [Online]. Available: http://www.journalssystem.com/astrj/Adaptive-Slip-Slide-Control-System-Design-in-Railway-Applications,85870,0,2.html

[20] S. Z. Meymand, A. Keylin, and M. Ahmadian, "A survey of wheel–rail contact models for rail vehicles," *Vehicle System Dynamics*, vol. 54, no. 3, pp. 386–428, Mar. 2016.

[21] H. S. Hansen, M. U. Nawaz, and N. Olsson, "Using operational data to estimate the running resistance of trains. Estimation of the resistance in a set of Norwegian tunnels," *Journal of Rail Transport Planning & Management*, vol. 7, no. 1-2, pp. 62–76, Jun. 2017. [Online]. Available: http://linkinghub.elsevier.com/retrieve/pii/S2210970616300415

[22] C. J. Baker, "A review of train aerodynamics Part 1 – Fundamentals," *The Aeronautical Journal*, vol. 118, no. 1201, pp. 201–228, Mar. 2014.

[23] O. Heirich, A. Lehner, P. Robertson, and T. Strang, "Measurement and analysis of train motion and railway track characteristics with inertial sensors," in *2011 14th International IEEE Conference on Intelligent Transportation Systems (ITSC)*. Washington, DC, USA: IEEE, 2011, pp. 1995–2000. [Online]. Available: http://ieeexplore.ieee.org/abstract/document/6082908/

[24] J. Otegui, A. Bahillo, I. Lopetegi, and L. E. Diez, "Evaluation of Experimental GNSS and 10-DOF MEMS IMU Measurements for Train Positioning," *IEEE Transactions on Instrumentation and Measurement*, vol. 68, no. 1, pp. 269–279, Jan. 2019. [Online]. Available: https://ieeexplore.ieee.org/document/8372929/

[25] G. Muniandi and E. Deenadayalan, "Train distance and speed estimation using multi sensor data fusion," *IET Radar, Sonar & Navigation*, Nov. 2018. [Online]. Available: https://digital-library.theiet.org/content/journals/10.1049/iet-rsn.2018.5359

[26] K. Kim, S.-H. Kong, and S.-Y. Jeon, "Slip and Slide Detection and Adaptive Information Sharing Algorithms for High-Speed Train Navigation Systems," *IEEE Transactions on Intelligent Transportation Systems*, vol. 16, no. 6, pp. 3193–3203, Dec. 2015. [Online]. Available: http://ieeexplore.ieee.org/document/7123638/

[27] M. Malvezzi, G. Vettori, B. Allotta, L. Pugi, A. Ridolfi, and A. Rindi, "A localization algorithm for railway vehicles based on sensor fusion between tachometers and inertial measurement units," *Proceedings of the Institution of Mechanical Engineers, Part F: Journal of Rail and Rapid Transit*, vol. 228, no. 4, pp. 431–448, May 2014. [Online]. Available: http://pif.sagepub.com/lookup/doi/10.1177/0954409713481769

[28] M. Spindler, D. Stein, and M. Lauer, "Low power and low cost sensor for train velocity estimation," in *2016 IEEE International Conference on Intelligent Rail Transportation (ICIRT)*. Birmingham, United Kingdom: IEEE, Aug. 2016, pp. 259–264.

[29] A. W. Palmer and N. Nourani-Vatani, "Robust Odometry using Sensor Consensus Analysis," in *IEEE/RSJ International Conference on Intelligent Robots and Systems (IROS)*, Madrid, Spain, 2018, pp. 3167–3173.

[30] U. Qureshi and F. Golnaraghi, "An Algorithm for the In-Field Calibration of a MEMS IMU," *IEEE Sensors Journal*, vol. 17, no. 22, pp. 7479–7486, Nov. 2017.

[31] N. El-Sheimy, H. Hou, and X. Niu, "Analysis and Modeling of Inertial Sensors Using Allan Variance," *IEEE Transactions on Instrumentation and Measurement*, vol. 57, no. 1, pp. 140–149, Jan. 2008. [Online]. Available: http://ieeexplore.ieee.org/document/4404126/

[32] P. Groves, "Navigation Using Inertial Sensors," *IEEE Aerospace and Electronic Systems Magazine*, vol. 30, no. 2, pp. 42–69, Feb. 2015. [Online]. Available: http://ieeexplore.ieee.org/xpl/articleDetails.jsp?arnumber=7081494

[33] Y. Stebler, S. Guerrier, and J. Skaloud, "An Approach for Observing and Modeling Errors in MEMS-Based Inertial Sensors Under Vehicle Dynamic," *IEEE Transactions on Instrumentation and Measurement*, vol. 64, no. 11, pp. 2926–2936, Nov. 2015. [Online]. Available: http://ieeexplore.ieee.org/document/7159103/

[34] J. Guo and M. Zhong, "Calibration and Compensation of the Scale Factor Errors in DTG POS," *IEEE Transactions on Instrumentation and Measurement*, vol. 62, no. 10, pp. 2784–2794, Oct. 2013. [Online]. Available: http://ieeexplore.ieee.org/document/6564423/

[35] A. Quinchia, G. Falco, E. Falletti, F. Dovis, and C. Ferrer, "A Comparison between Different Error Modeling of MEMS Applied to GPS/INS Integrated Systems," *Sensors*, vol. 13, no. 8, pp. 9549–9588, Jul. 2013. [Online]. Available: http://www.mdpi.com/1424-8220/13/8/9549

[36] R. J. Vaccaro and A. S. Zaki, "Statistical Modeling of Rate Gyros," *IEEE Transactions on Instrumentation and Measurement*, vol. 61, no. 3, pp. 673–684, Mar. 2012. [Online]. Available: http://ieeexplore.ieee.org/document/6068252/

[37] B. Altinoz and D. Unsal, "Determining efficient temperature test points for IMU calibration," in *2018 IEEE/ION Position, Location and Navigation Symposium (PLANS)*. Monterey, CA: IEEE, Apr. 2018, pp. 552–556. [Online]. Available: https://ieeexplore.ieee.org/document/8373426/

[38] A. Chulliat, S. Macmillan, P. Alken, C. Beggan, M. Nair, B. Hamilton, A. Woods, V. Ridley, S. Maus, and A. Thomson, "The US/UK World Magnetic Model for 2015-2020. Technical Report." *NOAA National Geophysical Data Center, Boulder,*

CO, 2015. [Online]. Available: https://data.nodc.noaa.gov/cgi-bin/iso?id=gov.noaa.ngdc:WMM2015$_{T}echnical_{R}eport$

[39] Y. Mu, C. Wang, X. Zhang, and W. Xie, "A Novel Calibration Method for Magnetometer Array in Nonuniform Background Field," *IEEE Transactions on Instrumentation and Measurement*, vol. 68, no. 10, pp. 3677–3685, 2018. [Online]. Available: https://ieeexplore.ieee.org/document/8542734/

[40] M. Muraccini, A. Mangia, M. Lannocca, and A. Cappello, "Magnetometer Calibration and Field Mapping through Thin Plate Splines," *Sensors*, vol. 19, no. 2, p. 280, Jan. 2019. [Online]. Available: http://www.mdpi.com/1424-8220/19/2/280

[41] U. Iqbal, A. F. Okou, and A. Noureldin, "An integrated reduced inertial sensor system (RISS) and GPS for land vehicle," in *2008 IEEE/ION Position, Location and Navigation Symposium*. Monterey, CA, USA: IEEE, 2008, pp. 1014–1021. [Online]. Available: http://ieeexplore.ieee.org/document/4570075/

[42] L. Wang, A. Noureldin, U. Iqbal, and A. M. Osman, "A Reduced Inertial Sensor System Based on MEMS for Wellbore Continuous Surveying While Horizontal Drilling," *IEEE Sensors Journal*, vol. 18, no. 14, pp. 5662–5673, Jul. 2018. [Online]. Available: https://ieeexplore.ieee.org/document/8364565/

[43] D. N. Aloi, M. Alsliety, and D. M. Akos, "A Methodology for the Evaluation of a GPS Receiver Performance in Telematics Applications," *IEEE Transactions on Instrumentation and Measurement*, vol. 56, no. 1, pp. 11–24, Feb. 2007. [Online]. Available: http://ieeexplore.ieee.org/document/4061069/

[44] M. Tailanian, S. Paternain, R. Rosa, and R. Canetti, "Design and implementation of sensor data fusion for an autonomous quadrotor," in *2014 IEEE International Instrumentation and Measurement Technology Conference (I2MTC)*, Montevideo, Uruguay, May 2014, pp. 1431–1436.

Jon Otegui received a B.Sc. degree in Industrial Technologies Engineering and a M.Sc. degree in Industrial Engineering from the University of Navarra-Tecnun, Donostia, Spain, in 2014 and 2016, respectively. His Master's thesis was focused on the experimental validation process of GNSS positioning technology in railway environment and it was carried out in CAF Research and Development Department. He is currently pursuing a Ph.D. degree with the Mobility Research Group, DeustoTech, Bilbao, Spain, under the supervision of Dr. Bahillo. He has coauthored four research manuscripts published in international journals. His current research interests include the development of data fusion algorithms for train positioning and navigation, IMU and GNSS characterization in railway context and their integration in train localization system for safety critical applications.

Alfonso Bahillo received Telecommunications Engineering and Ph.D. degrees from the University of Valladolid, Valladolid, Spain, in 2006 and 2010, respectively. He received the PMP certification at the PMI in 2014. From 2006 to 2010, he was a Research Engineer with CEDETEL. From 2006 to 2011, he was an Assistant Professor with the University of Valladolid. From 2010 to 2012, he was a Product Owner with LUCE Innovative Technologies, Valladolid. From 2013 and 2017, he was a Post-Doctoral Researcher with the University of Deusto, Bilbao, Spain, and the Project Manager with DeustoTech, Bilbao, where he trains Ph.D. students and collaborates in several national and international research projects. He is currently the Director of DeustoTech. He has worked (leading some of them) in more than 25 regional, national, and international research projects and contracts. He has coauthored over 20 research manuscripts published in international journals and over 40 communications in international conferences, and holds three national patents. His current research interests include local and global positioning techniques and intelligent transport systems.

Iban Lopetegi received a M.Sc. degree in Telecommunication Engineering from the University of Mondragon, Mondragón, Spain, in 2007, and a Ph.D. degree in Electronics and Communications from Newcastle University, Newcastle Upon Tyne, U.K., in 2011. Since 2011, he has been company representative for NGTC of WP7 and for STARS with the CAF Research and Development Department, Beasain, Spain. His current research interests include fail-safe train navigation, global positioning systems and digital maps in railways.

Luis Enrique Díez received a B.Sc. degree in Telecommunications Engineering from the University of Deusto, Bilbao, Spain, in 2005, the M.Sc. degree in Communication Technologies and Systems from the Polytechnic University of Madrid, Madrid, Spain, in 2012 and a Ph.D. degree from University of Deusto, Bilbao, Spain, in 2019. From 2005 to 2011, he was a Senior IT Consultant with Everis, Madrid. From 2013 to 2014, he was a Research Support Technician with the SOFTLAB Research Group, Carlos III University of Madrid, Getafe, Spain. Since 2014, he has worked within the Mobility Research Group, DeustoTech, Bilbao, Spain. His current research interests include positioning systems, data fusion techniques and context-aware applications.

Exploration is the engine that drives innovation. Innovation drives economic growth.

Edith Widder

CHAPTER

5

Comparative of IMU

The survey of train positioning solutions (paper I) has shown the high amount of alternatives proposed up to date that make difficult to chose the best trade-off between required performance and the system cost. Particularly in IMU selection, the approximate price ranges are between 3 and 30.000 euros.

The experimental evaluation of GNSS and IMU presented previously (paper II) is limited to a specific model of an IMU, which is considered one of the most used for vehicular and pedestrian positioning purposes by the scientific community. However, lower cost alternatives has arisen last years in the market, especially those sold in OEM format without hardware/software support.

As stated in previous sections, the short-term train navigation systems are focused on enhancing the odometry information without the integration of GNSS. The architecture proposed in this thesis is based on the INS utilization to overcome wheel speed sensors limitations (paper III) and to provide enhanced information about track features and navigation states (e.g. roll, pitch and yaw angles).

Consequently, there is a need to justify the extra cost of different IMUs against lower cost alternatives evaluating their performance in the land-vehicular context. This analysis can optimize the cost of the IMU before its integration into the train navigation system.

Table 5.1: IMU's characteristics

		H-end	M-end	L-end
Manufacturer		KVH	xSens	Bosch
Model		GEO FOG	MTi 300	BMI 160
Cost		30.000€	3.000€	3€
Gyroscopes				
Full range	$[deg/s]$	490	450	125
Initial bias	[deg/s]	N/A	0.2	3
In-run bias	[deg/h]	0.05	10	N/A
Noise density	[(deg/s)/$\sqrt{Hz}$]	0.0002	0.01	0.007
g-sensitivity	[(deg/s)/g]	N/A	0.003	0.1
Non-orthogonality	[deg]	N/A	0.05	N/A
Non-linearity	[%]	0.005	0.01	0.1
Accelerometers				
Full range	$[m/s^2]$	98.1	200	19.6
Initial bias	$[m/s^2]$	N/A	0.05	1.47
In-run bias	$[\mu g]$	0.0005	15	N/A
Noise density	[$\mu g/\sqrt{Hz}$]	0.0012	60	300
Non-orthogonality	[deg]	N/A	0.05	N/A
Non-linearity	[%]	0.03	0.1	0.5

Table 5.2: Euler angles statistical analysis

M-end	Mean error $[rad]$	Std. Dev. $[rad]$	**L-end**	Mean error $[rad]$	Std. Dev. $[rad]$	**L-end**[1]	Mean error $[rad]$	Std. Dev. $[rad]$
Roll	0.046	0.037	Roll	0.251	0.320	Roll	0.165	0.198
Pitch	0.037	0.048	Pitch	0.251	0.293	Pitch	0.186	0.179
Yaw	0.215	0.958	Yaw	0.519	2.137	Yaw	0.168	0.938

M-end = Medium-end. L-end = Low-end. L-end[1] = Low-end calibrated measurements.

This paper compares a medium-end (xSens MTi-300) and a low-end (Bosch BMI160) IMUs in a experimental test and the performance is evaluated against high-end INS (KVH GEO-FOG). The lack of availability of a train to test in a challenging railway (with tunnels, curves, slopes and cants) has conditioned the experimental test to be carried out in an automobile. This fact, presents a more challenging environment than the railway context because there are no lateral displacement constrains, the angular rates and specific forces are higher and the pure-rolling conditions are more easier to fulfill.

The safety requirements and new research proposals promotes INS stand-alone solution in train navigation. In order to compensate the drift over time associated to dead-reckoning, calibration techniques and data fusion algorithms can be used. In this work, low-end IMU calibration technique has been proposed based on previous work in the field. Finally, the raw measurements, the estimators of attitude and heading, and the main kinematic variables (acceleration, velocity and position) are statistically evaluated.

The main contributions of this paper can be summed up as follows.

1. It provides a comparison of different grade IMUs evaluating their performance in terms of raw measurements (specific forces and angular rates), orientation values and tri-axial accelerations. Note that the characteristics and the purchase cost are significantly different as shown in Table 5.1. The main difference can be observed in the orders of magnitude of the purchase cost which is directly related to the cost-efficiency requirements.

2. It proposes a calibration method to improve the low-end INS solution. The accuracy reached with the calibrated low-end INS solution is comparable to medium-end INS solution, specially in yaw angle estimation (Table 5.2); the yaw estimation by calibrated low-end IMU can be concluded to be comparable to high-end and medium-end IMUs. In future works, map-aided solutions shall be proposed by using yaw angle estimation and track information. This kind of solutions can be propitious for track-constrained positioning solution (e.g. railways) where low-cost IMUs can provide enhanced navigation data (e.g. absolute position, orientation, etc.). Consequently, it is

concluded lower cost IMU can be proposed in order to optimize the cost-efficiency of the positioning systems.

IEEE Access
Multidisciplinary ⋮ Rapid Review ⋮ Open Access Journal

Date of publication xxxx 00, 0000, date of current version xxxx 00, 0000.

Digital Object Identifier 10.1109/ACCESS.2017.DOI

Performance Evaluation of Different Grade IMUs for Land Vehicular Attitude and Accelerations Estimation

JON OTEGUI[1], ALFONSO BAHILLO[1], IBAN LOPETEGI[2], LUIS ENRIQUE DÍEZ[1]

[1]Faculty of Engineering, University of Deusto, Av. Universidades, 24, 48007, Bilbao, Spain
(e-mail: jon.otegui@deusto.es; alfonso.bahillo@deusto.es; luis.enrique.diez@deusto.es).
[2]Construcciones y Auxiliar de Ferrocarriles Investigación y Desarrollo, CAF I+D, Calle José Miguel Iturrioz 26, 20200 Beasain, Spain
(e-mail: ilopetegi@caf.net).

Corresponding author: Jon Otegui (e-mail: jon.otegui@deusto.es).

ABSTRACT Vehicular positioning systems are necessary for the development of autonomous vehicles and advanced driver assistance systems. In recent years, micro-electromechanical systems (MEMS) based Inertial Measurement Units (IMU) are being included in proposals for multi-sensor positioning system architectures in order to take advantage of their cost and size. However, the lack of criteria on the most appropriate IMU selection for each application has led to provide cost-inefficient solutions. This work compares medium-end (xSens MTi-100) and low-end (Bosch BMI160) grade MEMS-based IMUs in a experimental road-test using a fusion of high-end IMU (KVH GEO-FOG), GNSS and wheel speed sensor as reference value. In addition, a calibration technique is proposed and applied to the low-end IMU. The raw measurements (angular rates and specific-forces) and navigation states (tri-axial attitude and accelerations) are statistically compared to evaluate the performance of each IMU. It is concluded that the calibration technique proposed makes the low-end IMU performance to be similar to the medium-end one. Consequently, this work contributes to optimize the cost of land vehicular positioning systems when choosing the most appropriate sensor based on the accuracy and precision required for the application.

INDEX TERMS inertial sensors, vehicular navigation, dead reckoning, accelerometers, gyroscopes, calibration

I. INTRODUCTION

THE development of micro-electromechanical systems (MEMS) based inertial measurement units (IMU), thanks to their low-power consumption, small size, light weight, and low cost, has propitiated its utilization in broad areas: vehicular navigation in automotive [1], aerial [2] and railway [3] contexts, pedestrian positioning [4] and robotics [5] are the main research areas where MEMS-based IMUs are used.

The vehicular navigation is a prominent field because fail-safe positioning system plays a key role on autonomous vehicle as well as in driver assistance systems [6] [7]. The fail-safe positioning systems must fulfill very demanding requirements in terms of accuracy, precision, availability and integrity because its failure can cause accidents. Up to date, there is no unique sensor nor technology able to reach those requirements, so multi-sensor architectures are proposed. The multi-sensor architectures arise as prominent solution for complementing each individual sensor limitations. The most used multi-sensor combination of technologies in land vehicular context is the composition of Global Navigation Satellite System (GNSS) and IMU [8]. In addition, odometers (a.k.a. wheel speed sensors or tachometers) and LiDAR (Light Detection and Ranging) are proposed to enhance the robustness of the positioning solution [9]. In land-vehicular context, the IMU can also be combined with digital maps regarding the uniqueness of the tracks [10].

The IMU is one of the most used candidate sensors for fail-safe positioning systems because it is very cost-efficient according to the functionality it offers: it can complement other sensors limitations such as GNSS signal loss or wheel speed sensors overestimation when slipping whereas the purchase and maintenance cost, specially for MEMS-based IMUs, is lower. When IMUs are used to provide navigation data it is usually based on dead-reckoning (DR). Unlike satellite-based navigation where the absolute position is given on every measurement, DR estimates current position by using a previously determined one. Consequently, previous estima-

tion errors are propagated over time. Thus, rotation-rate and specific-force errors are propagated to vehicle accelerations, velocity and position estimation. Last years researches have proposed different quality IMUs depending on the performance required and, consequently, there have arisen different cost range solutions.

For IMUs based on the same technology, most of the cost range is related to the calibration of accelerometers and gyroscopes carried out by the manufacturers. The calibration is a process where detectable systematic errors (e.g. static-bias or offset, scale-factor, axes misalignment, etc.) are estimated in order to correct the raw measurements given by these sensors. According to the calibration techniques proposed up to date, they can be classified under different criteria. We can distinguish calibration methods depending on the error nature they mitigate: so, we can find methods for deterministic [11] [12] and for stochastic [13] errors. Another classification is related to the movements required during the calibration: we can find methods for static [14] or dynamic [15] scenarios. Last criterion deals with the required equipment for carrying out the calibration procedure: there are methods to perform the IMU calibration with additional sensors [16] or without them [17], [18]. In addition, thermal tests are proposed to evaluate the sensors bias and scale-factor stability over temperature [19], [20]. An exhaustive comparison of the last published calibration methods is gathered in [21]. The development of calibration techniques has arise as prominent field to mitigate low-end IMU errors, making these kind of IMUs comparable in performance to higher-end solutions.

For the autonomous navigation, an accurate navigation solution, which can provide a stable solution for more than 5 minutes during GNSS outages such as underground parking lot or tunnel, is necessary because autonomous land vehicles require seamless navigation [7]. For that aim, the IMU standalone solution plays a key role because it provides continuous measurements (independent of tunnels, urban canyons, etc.), do not require neither additional equipment (e.g. antennas, radars, etc.) nor specific installation in the vehicle (it can be mounted on the roof, inside the vehicle, on the front or on the rear part).

The balance between the application requirements, expected performance and the system cost is the main research gap to optimize the fail-safe positioning systems and it is the motivation of this work. An exhaustive work has been published about the fusion of ultra low-cost MEMS inertial devices with GNSS [22]. It points out attitude and position errors seem to be sensitive to GNSS sensor and the solution performance can be improved by IMUs calibration. It also concludes the long-term solution cannot be provided by low-cost MEMS IMUs standalone, but they can be used as diagnosis measurements in multi-sensor architectures. This fact can be increasingly useful in such contexts where tri-axial attitude and accelerations can be indicators of curves, slopes, cants, etc (e.g. in land-vehicles such as automobiles or trains).

This work aims at comparing the performance of different grade IMUs, according to the data-sheet parameters and purchase cost, in an experimental road test including the raw measurements (specific forces and rotation rates) and the main navigation states (tri-axial attitude and accelerations). In addition, a calibration technique is proposed in order to evaluate the accuracy improvement of low-end MEMS IMU compared to a medium-end. In order not to be influenced by additional sensors, the analysis is focused on IMU standalone dead-reckoning solution and tri-axial attitude and accelerations are statistically evaluated.

The paper is organized as follows. In section II, the IMU mathematical model is described. In section III, the calibration and mechanization models are defined. The experimental tests description is given in section IV. The results and discussion are presented in section V and, finally, the main conclusions of this work are summed up in section VI.

II. IMU MODEL

An IMU is usually a composition of tri-axial accelerometers and gyroscopes. The gyroscopes and the accelerometers mounted on the vehicle are sensor triplets with perpendicular sensitivity axes (named x,y,z) [23].

The IMU is usually used as strapdown system, i.e. the sensors are attached rigidly to the body of the vehicle. Furthermore, the sensors' axes are usually aligned with the body-frame, thus their output is expressed in body-frame. The potential benefits of this approach are lower cost, reduced size and greater reliability compared with equivalent platform systems [24].

A. SENSOR MODEL FOR LAND VEHICLES

As stated previously, the gyroscopes and the accelerometers output the measurements in sensor-frame which coincides with the body-frame. So, the vehicle's translation and rotation movements are expressed in terms of specific forces (measured by accelerometers) and rotation rates (measured by gyroscopes).

The gyroscopes measure the instantaneous rotation rate around three axes. The three rotations can be represented using gimbal angles (roll -ϕ-, pitch -θ- and yaw -ψ-) for representing the vehicle's attitude and heading. The relationship between the gimbal rates $(\dot{\phi}, \dot{\theta}, \dot{\psi})$ and the body rates $(\omega_x^b, \omega_y^b, \omega_z^b)$ are given by equations (1)-(3) where s, c and t corresponds to sine, cosine and tangent operators respectively.

$$\omega_x^b = \dot{\phi} - \dot{\psi} s\theta \tag{1}$$

$$\omega_y^b = \dot{\psi} s\phi c\theta + \dot{\theta} c\phi \tag{2}$$

$$\omega_z^b = \dot{\psi} c\phi c\theta - \dot{\theta} s\phi \tag{3}$$

The accelerometers model is based on the measurement of specific forces of the vehicle, that is, the sum of tri-axial accelerations and gravity term. In addition, Coriolis term due to the Earth rotation rate can be considered, but for short distance cases, it can be omitted [24]. Note that

horizontal (c_h) and vertical (c_v) curvature of the road and gimbal angles produces dynamic and gravity accelerations on measurements. If Earth-fixed coordinate frame tangent to the Earth's surface is used (North is aligned with the longitudinal axis), the accelerations of the vehicle (a_x, a_y, a_z) and specific forces measured by the accelerometers (f_x^b, f_y^b, f_z^b) can be related by equations (4)-(6).

$$f_x^b = a_x - gs\theta \tag{4}$$

$$f_y^b = gs\phi c\theta + a_y = gs\phi c\theta + c_h v_x^2 c\phi - c_v v_x^2 s\phi \tag{5}$$

$$f_z^b = gc\phi cs\theta + a_z = gc\phi cs\theta + c_h v_x^2 s\phi - c_v v_x^2 c\phi \tag{6}$$

The vehicle longitudinal velocity (v_x) and acceleration (a_x) can be observed in the previous equations. Gravity acceleration (g) is considered the local value on the Earth's surface.

B. SENSOR ERROR MODEL

The gyroscopes and accelerometers models shown in previous section deals only with the vehicle motion. However, the IMUs encompass different nature errors. They usually are classified into deterministic and stochastic errors [25], [26], [27].

Deterministic errors are related to the physical way the magnitudes are measured. The relationship between the electrical and physical magnitudes tend to vary and consequently, these kind of error arise. The main deterministic error sources are the static bias (a.k.a. offset), the scale factor and the axes misalignment (a.k.a. non-orthogonality). In case of gyroscopes, g-sensitivity is also considered [12].

Stochastic errors are the random errors that occur due to random variations of bias or scale factor drift over time and random sensor noise. General stochastic error sources existing in inertial sensors can be modelled as quantization noise, random walk, bias instability (a.k.a. in-run bias), rate random walk and rate ramp [28], [29].

The error models of gyroscopes and accelerometers proposed in this work are assumed to have the same terms according to the deterministic and stochastic source. The gyroscopes and accelerometers error models are given in equation (7) and (8) respectively.

$$\begin{bmatrix}\tilde{\omega}_x^b\\ \tilde{\omega}_y^b\\ \tilde{\omega}_z^b\end{bmatrix} = M_g S_g\left(\begin{bmatrix}\omega_x^b\\ \omega_y^b\\ \omega_z^b\end{bmatrix} + \begin{bmatrix}b_x^g\\ b_y^g\\ b_z^g\end{bmatrix} + w^g\right) \tag{7}$$

$$\begin{bmatrix}\tilde{f}_x^b\\ \tilde{f}_y^b\\ \tilde{f}_z^b\end{bmatrix} = M_a S_a\left(\begin{bmatrix}f_x^b\\ f_y^b\\ f_z^b\end{bmatrix} + \begin{bmatrix}b_x^a\\ b_y^a\\ b_z^a\end{bmatrix} + w^a\right) \tag{8}$$

The static bias is given by the bias array for gyroscopes ($[b_x^g, b_y^g, b_z^g]^T$) and accelerometers ($[b_x^a, b_y^a, b_z^a]^T$). The misalignment (M_a, M_g) and scale-factor (S_a, S_g) errors are gathered in 3x3 matrices. The sensors noise is represented by w^a, w^g. The realistic ($[\tilde{f}_x^b, \tilde{f}_y^b, \tilde{f}_z^b]^T$,$[\tilde{\omega}_x^b, \tilde{\omega}_y^b, \tilde{\omega}_z^b]^T$) and ideal ($[f_x^b, f_y^b, f_z^b]^T$,$[\omega_x^b, \omega_y^b, \omega_z^b]^T$) measurements can be distinguished.

III. IMU MECHANIZATION AND CALIBRATION

The navigation states estimation from the raw measurements requires two stages: first, the raw measurements are corrected by calibration parameters (calibration) and then, they are processed to estimate the attitude angles and vehicle accelerations (mechanization).

A. CALIBRATION METHOD

One of the most used technique to mitigate the error growth in IMU mechanization is the raw measurements calibration. As far as the raw measurements errors are characterized, the main error sources such as bias or scale-factor can be modelled. Consequently, the magnitude that is integrated over time is minimized.

The calibration technique proposed in this work is focused on both gyroscopes and accelerometers, using calibration parameters to correct the raw measurements. The calibration parameters are estimated comparing instrument outputs with known reference information and determining the coefficients (i.e. calibration parameters) that force the output to agree with the reference information. The calibration technique proposed aims to be a flexible, easy and economic to apply to any grade accelerometers and gyroscopes. Consequently, the technique proposed can be considered a simplification of more extended works that are cited in the following section.

In order to calibrate the gyroscopes, we can assume the measurements as bias-free simply averaging the static gyroscope signals over a suitable initial period of no motion (30 s approximately). The accelerometer calibration is done similarly to the gyro calibration, but there is an added difficulty. Determination of the bias of the gyros was easily done by observing the gyro measurements when the IMU was at rest. In the case of the accelerometers there is no unloaded state because the response to gravity is always present. However, when the IMU is at rest, the magnitude of the static acceleration measured must equal that local value of the gravity. The use of gravity excitation is very common for calibration purposes [21].

Based on the accelerometers error model, it can be particularized to the static scenarios where the total sum of the specific forces should coincide to the gravity acceleration. This way, static bias ($[b_x^a, b_y^a, b_z^a]^T$), scale factor (s_x^a, s_y^a, s_z^a) and misalignment ($m_{xy}^a, m_{xz}^a, m_{yz}^a, m_{yx}^a, m_{zx}^a, m_{zy}^a$) terms can be identified in equation (9).

$$\begin{bmatrix}s_x^a & m_{xy}^a & m_{xz}^a\\ m_{yx}^a & s_y^a & m_{yz}^a\\ m_{zx}^a & m_{yz}^a & s_z^a\end{bmatrix}\begin{bmatrix}\tilde{f}_x^b\\ \tilde{f}_y^b\\ \tilde{f}_z^b\end{bmatrix} - \begin{bmatrix}b_x^a\\ b_y^a\\ b_z^a\end{bmatrix} = \boldsymbol{g} \tag{9}$$

According to equation (9) and defining the modulus of the resulting vector, a cost function can be defined where the error terms are unknowns (12 at all) [30]. These error terms are grouped in calibration parameters of the accelerometers ($\boldsymbol{\Theta}^a$), shown in equation (10).

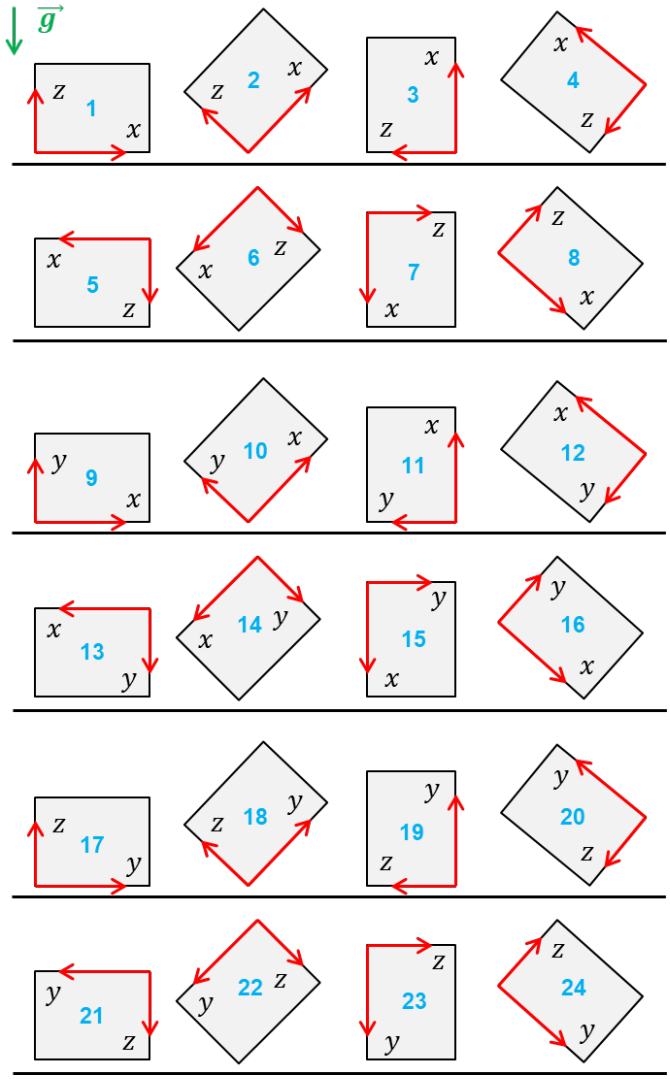

Figure 1: Calibration procedure static positions.

$$\boldsymbol{\Theta^a} = [s_x^a, s_y^a, s_z^a, m_{xy}^a, m_{xz}^a, m_{yz}^a, m_{yx}^a, m_{zx}^a, m_{zy}^a, b_x^a, b_y^a, b_z^a] \tag{10}$$

The cost function of the accelerometers ($\boldsymbol{F}(\boldsymbol{\Theta^a})$) can be solved with 12 independent measurements of the accelerometers, but in this work 24 positions are used based on [21]. This work proposes some different positions from [21] for ease of instrumentation and measurement (Figure 1). Thus, only three measurement files are generated and the rotations are only applied around 3-axes instead of 6-axes to minimize the process time and cost.

In order to solve the over-determined equation system shown in equation (11) the *Levenberg-Marquart* (LM) algorithm is used based on [30]. The LM algorithm is one of the most efficient and popular algorithms due to its better convergence than the other ones for nonlinear minimization according to the combination of the Gradient Descent and the Gauss–Newton algorithms [31]. An initial guess of $\boldsymbol{\Theta}^a$=[1,1,1,0,0,0,0,0,0,0,0,0,0,0,0,0,0,0] is assumed [32]. In order to overcome ill-conditioned problems, the IMU remains static for 5 seconds at 45 degrees rotations approximately [21].

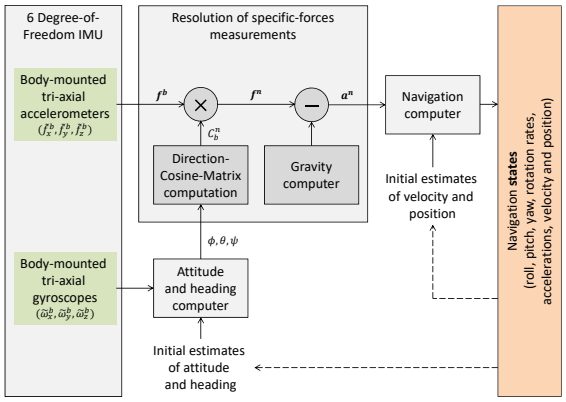

Figure 2: Strapdown inertial navigation system mechanization scheme based on [24].

$$\boldsymbol{F}(\boldsymbol{\Theta^a}) = \sum_{n=1}^{N} (\|h(\tilde{f}_x^b, \tilde{f}_y^b, \tilde{f}_z^b, \boldsymbol{\Theta}^a)^2\| - \|\boldsymbol{g}\|^2)^2 \tag{11}$$

B. MECHANIZATION METHOD

The mechanization is the process where the navigation equations are solved and the navigation states (i.e. attitude, triaxial accelerations, etc.) are obtained. For this purpose the navigation frame is defined where the North coordinate is orientated to the Earth's north, the Down coordinate is oriented to the gravity vector and the East coordinate is the resultant axis.

There are three main techniques to represent the orientation of an IMU: Euler-angles-based, Direction-Cosine-Matrix-based (a.k.a. rotation-matrix-based) and Quaternion-based. In this work Euler-angles-based is proposed because the land-vehicular dynamics avoids gimbal-lock limitation. In addition, the interpretation of the results is geometrical where roll, pitch and yaw angles are directly estimated.

First, the orientation angles (roll -ϕ-, pitch -θ- and yaw -ψ-) between body and navigation frame are calculated based on gyroscopes signals and initial angles estimation. In the simplest implementation, gyroscopes measurements are integrated over time to compute them, solving first order differential equations shown in equations (1)-(3) and rearranged in equation (12). This method assumes gyroscopes measurements are constant during the integration time (it can be considered an accurate enough assumption for 100Hz or higher sampling rates).

$$\begin{bmatrix} \dot{\phi} \\ \dot{\theta} \\ \dot{\psi} \end{bmatrix} = \begin{bmatrix} (\tilde{\omega}_y^b s\phi + \tilde{\omega}_z^b c\phi)t\theta + \tilde{\omega}_x^b \\ \tilde{\omega}_y^b c\phi - \tilde{\omega}_z^b s\phi \\ (\tilde{\omega}_y^b s\phi + \tilde{\omega}_z^b c\phi)/c\theta \end{bmatrix} \tag{12}$$

After that, the rotation matrix (C_b^n) is built based on orientation angles previously computed according to equation (13). The rotation matrix is used to transform accelerometers measurements from body frame (the coordinate system on which the measurements are recorded) to navigation frame (the coordinate system on which the gravity acceleration is completely vertical).

$$C_b^n = \begin{bmatrix} c\theta c\psi & -c\phi s\psi + s\phi s\theta c\psi & s\phi s\psi + c\phi s\theta c\psi \\ c\theta s\psi & c\phi c\psi + s\phi s\theta s\psi & -s\phi c\psi + c\phi s\theta s\psi \\ -s\theta & s\phi c\theta & c\phi c\theta \end{bmatrix} \quad (13)$$

Once on the navigation frame, the gravity acceleration is subtracted and the vehicle tri-axial accelerations (without gravity term) are obtained according to equation (14). The full mechanization process is depicted in Figure 2.

$$\begin{bmatrix} a_x \\ a_y \\ a_z \end{bmatrix} = C_b^n \begin{bmatrix} \tilde{f}_x^b \\ \tilde{f}_x^b \\ \tilde{f}_x^b \end{bmatrix} - \begin{bmatrix} 0 \\ 0 \\ g \end{bmatrix} \quad (14)$$

Note that during the mechanization the errors in raw gyroscopes and accelerometers are propagated with time. This is the reason why IMU stand-alone solutions accumulate error over time and, therefore, additional information sources are needed to mitigate the error growth.

IV. EXPERIMENTAL TESTS DESCRIPTION

The experimental tests aim to record different grade IMUs raw measurements in addition to GNSS and wheel speed sensor data. Then, accelerometers and gyroscopes raw measurements are post-processed in order to estimate the orientation, accelerations, velocity and position of the vehicle. Finally, these variable are statistically compared.

The reference values for raw measurements, attitude and accelerations (named Ground Truth) are built based on the high-end IMU, a wheel speed sensor and a GNSS receiver. The medium-end, low-end and calibrated low-end results will be compared to the solution provided by the fusion of these measurements. The main reason why multi-sensor architecture is proposed for Ground Truth is motivated by the limitations that each sensor presents individually (e.g. drift due to dead-reckoning, GNSS signal loss, etc.) for seamless solution (see Figure 3 to see the challenging scenarios during the test).

The journeys designed for this work cover there and back travels between Beasain and Tolosa, Basque Country, Spain (about 20 km) and were carried out on 20th May, 2019 (Figure 3). The route covers GNSS-outages (e.g. tunnels), GNSS degraded zones (e.g. forests), uphills and downhills, different curve radius turns and constant speed sections. The car was driven on the right side of the road, in a section of 3.5 meters width (note that car's width is rather smaller -around 1.5 m-).

A. TESTING SENSORS

The testing architecture and equipment can be observed in Figure 4. In this work a high-end, a medium-end and a low-end IMUs are used according to the data-sheet parameters and purchase cost. High-end IMU selected is the GEO-FOG 3D Dual model from *KVH* manufacturer. Medium-end IMU is the MTi-300 from *xSens* and low-end IMU is the BMI160 from *Bosch*. All of them are configured to 100Hz sampling rate. Their main characteristics are gathered in Table 1.

According to the Ground Truth generation, the high-end IMU is composed by a MEMS-type accelerometer and fibre-optic gyroscopes. The wheel speed sensor is configured to 0.588 mm/pulse resolution as a trade-off between the minimum and maximum measurable speed (from 0 to 140 km/h). The GNSS receiver is configured in double-antenna, multi-constellation and multi-frequency mode. The GNSS antenna model is OmPlecs-TOP 200 AMR 1500 B L1/L2 H from *Antonics*. Proprietary software from KVH manufacturer (GEO-FOG Manager©) is utilized for data-fusion of high-end IMU, GNSS and wheel speed sensor. All the sensors are connected to a PC and time synchronization is based on the GNSS receiver that sets the timing references.

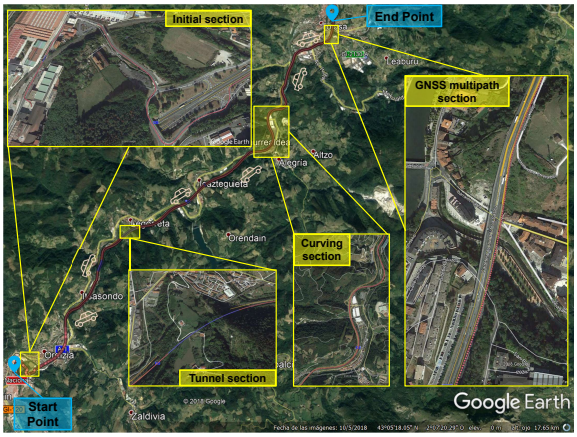

Figure 3: Test track where initial section, tunnels and curved sections are highlighted.

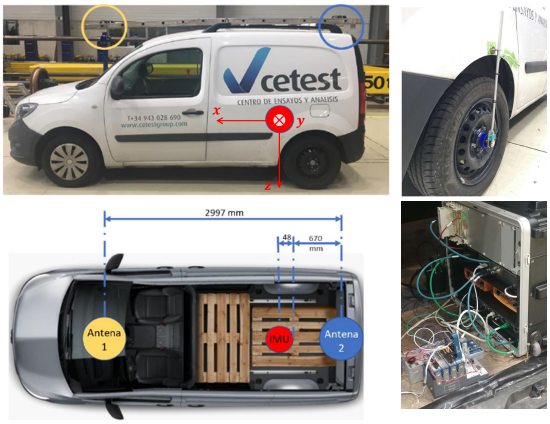

Figure 4: Test equipment (IMUs, GNSS antennas, wheel speed sensor) mounted in the car.

Table 1: IMU's characteristics

		H-end	M-end	L-end
Manufacturer		KVH	xSens	Bosch
Model		GEO FOG	MTi 300	BMI 160
Cost		30.000€	3.000€	3€
Gyroscopes				
Full range	$[deg/s]$	490	450	125
Initial bias	[deg/s]	N/A	0.2	3
In-run bias	[deg/h]	0.05	10	N/A
Noise density	$[(deg/s)/\sqrt{Hz}]$	0.0002	0.01	0.007
g-sensitivity	[(deg/s)/g]	N/A	0.003	0.1
Non-orthogonality	[deg]	N/A	0.05	N/A
Non-linearity	[%]	0.005	0.01	0.1
Accelerometers				
Full range	$[m/s^2]$	98.1	200	19.6
Initial bias	$[m/s^2]$	N/A	0.05	1.47
In-run bias	$[\mu g]$	0.0005	15	N/A
Noise density	$[\mu g/\sqrt{Hz}]$	0.0012	60	300
Non-orthogonality	[deg]	N/A	0.05	N/A
Non-linearity	[%]	0.03	0.1	0.5

Car-mounting of the sensors is represented in Figure 4. The IMUs are mounted in the most stable configuration, i.e. maximizing the contact area between the sensor and the car floor. Consequently, the measuring axes are different for each IMU.

B. EVALUATION METRICS

The statistical analysis presented in this paper is based on the estimation of mean error, standard deviation and the 95% empirical cumulative distribution function (ECDF) of the difference between the Ground Truth and the rest of IMUs.

V. RESULTS AND DISCUSSION

The results discussed in this work evaluate the performance of the different grade IMUs based on three aspects. First, the raw measurements of the gyroscopes and accelerometers are evaluated. Then, the attitude values are estimated (i.e. roll, pitch and yaw) based on the gyroscopes of the IMUs, solving the first order differential equations shown in (1)-(3) with initial values set to zero. Finally, vehicle tri-axial accelerations are calculated using the rotation matrix estimated beforehand by Euler angles and removing the gravity term.

A. RAW MEASUREMENTS

The raw measurements analysis is focused on gyroscopes and accelerometers of the medium-end and low-end IMUs compared to high-end one. In addition, the low-end IMU calibrated and uncalibrated measurements are shown in order to evaluate the performance improvement of the proposed calibration technique.

The gyroscopes measurements (Figure 5a, 5b, 5c) show that the vehicle rotation around the vertical axis (z) is larger than in other two axes (x and y). This fact is completely coherent to the vehicle dynamics where the rotation around yaw angle (due to curve negotiating) is higher than the rolling (related to the cant angle of the road) or pitching (due to the slope of the road) unlike pedestrian or robotics applications. According to the statistical analysis, the mean error reached by medium-end gyroscopes is lower than low-end gyroscopes (59.25% in x-axis, 46.55% in y-axis and 58.16% in z-axis). The similar behaviour can be observed in standard deviation and 95% ECDF metrics: the standard deviation is lower about 63.18% in x-axis, 57.42% in y-axis and 76.91% in z-axis, whereas the 95% ECDF shows even higher differences (70.17% in x-axis, 62.65% in y-axis and 80.20% in z-axis). Once the proposed calibration procedure is applied and the gyroscopes measurements are corrected by the calibration parameters, the low-end gyroscopes results are much closer to medium-end ones: the mean error has been reduced 58.77% in x-axis, 52.94% in y-axis and 73.92% in z-axis, which means that it has been lowered even more than medium-end gyroscopes in y- and z-axes. These improvement has been repeated in standard deviation and 95% ECDF metrics as well.

The accelerometers measurements (Figure 5d, 5e, 5f) merge the vehicle accelerations and the gravity term. In the configuration used for IMUs inside the car, the vertical axis of the car is aligned to the gravity (i.e. the vehicle is levelled when the test begins), so the specific-forces measured by the vertical accelerometers are close to g (9.81 m/s^2). However, little misalignment between the vehicle axes and each IMU axes makes the measurements no to be perfectly cluster around 0 m/s^2 in case of x- and y-axes and around 9.81 m/s^2 in case of z-axis. According to the statistical analysis, the mean errors reached by medium-end accelerometers are 27.19% lower in y-axis and 48.20% lower in z-axis than low-end ones, whereas in x-axis the results are similar. According to the standard deviation and 95% ECDF, several differences between IMU grades can be shown: the medium-end standard deviation is 11.46% lower in x-axis, 32.80% lower in y-axis and 59.80% lower in z-axis than the low-end. In case of 95% ECDF the difference is even larger (23.48% lower in x-axis, 44.24% lower in y-axis and 64.52% lower in z-axis). The calibration plays a key role in the results as shown in Table **??**, where 12 parameters are used to correct the low-end accelerometers measurements. Thus, the mean error (23.71% lower in x-axis, 46.09% lower in y-axis and 62.17% lower in z-axis), the standard deviation (23.58% lower in x-axis, 43.47% lower in y-axis and 62.78% lower in z-axis) and the 95% ECDF (41.33% lower in x-axis, 56.98% lower in y-axis and 71.19% lower in z-axis) are significantly reduced, making the low-end accelerometers more accurate and precise than the medium-end ones.

B. ATTITUDE ESTIMATION

The attitude analysis is based on the comparison of the Euler angles (roll, pitch and yaw) estimated from different grade gyroscopes. The estimation of these angles is carried out by numerical integration of equations (1)-(3) using ODE45 from Matlab R2019a.

An initial section of the journey about 400 seconds has been chosen to show clearly the different grade gyroscopes

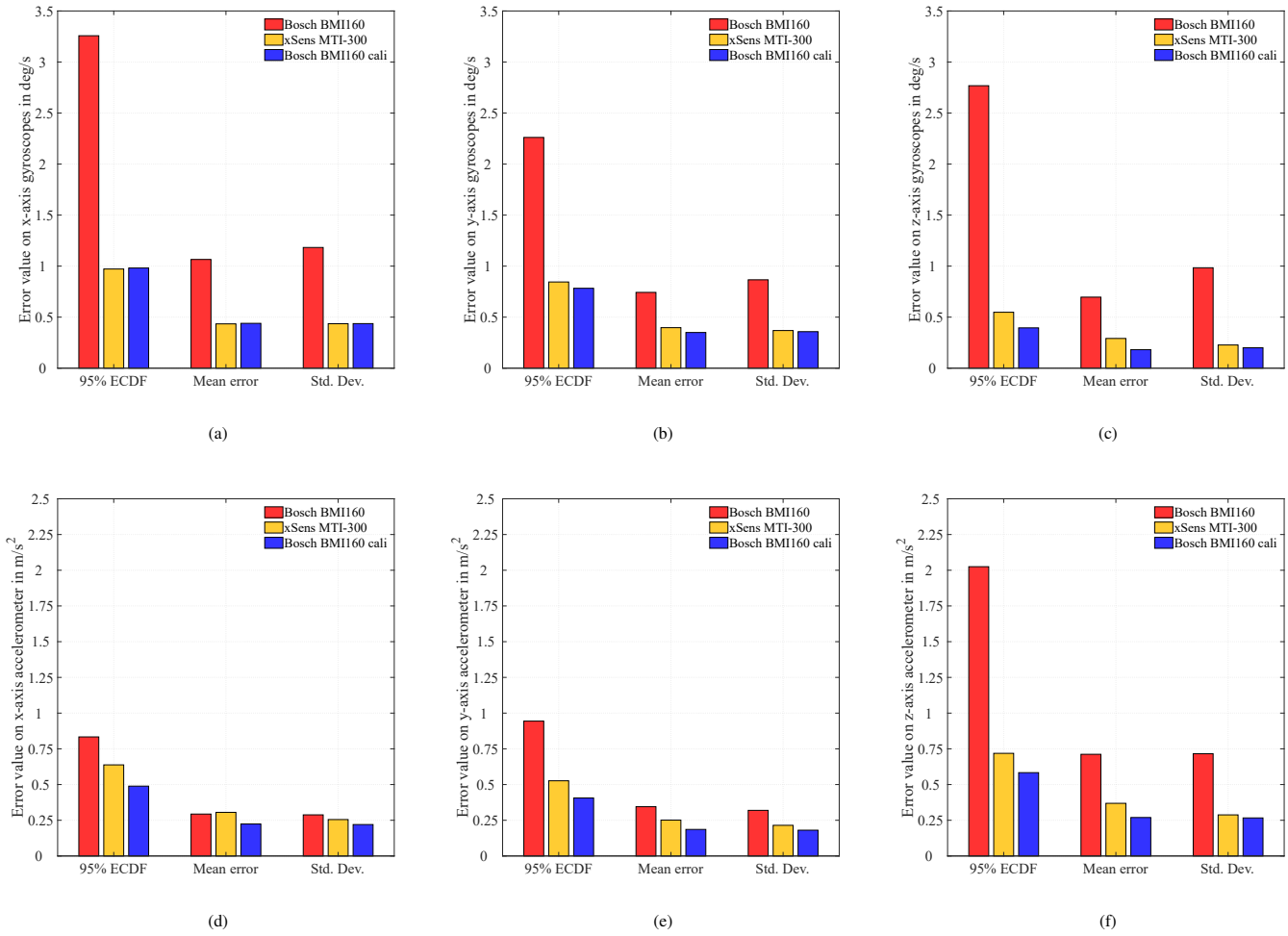

Figure 5: Raw measurements statistical analysis of the gyroscopes (a-c) and accelerometers (d-f) measurements comparing the medium-end (xSens MTi-100), low-end (Bosch BMI160) and low-end calibrated (Bosch BMI160 Calibrated) IMUs to the Ground Truth: (a,d) longitudinal axis -x- measurements; (b,e) lateral axis -y- measurements; (c,f) vertical axis -z- measurements.

and accelerometers measurements (Figure 6). However, the statistical comparison of the medium-end and low-end (calibrated and uncalibrated) measurements to the Ground Truth along whole journey is given in Table 2.

According to Figure 6 the differences between the medium-end and low-end IMU can be noticed: although the two results drift over time (it is most appreciable on yaw-angle estimation due to the larger magnitude it measures), the medium-end IMU solution is closer to the high-end one. Note that the uncalibrated results of the low-end IMU are unusable because the bias integration makes the solution to diverge in the first 50 seconds of the trip. The statistical metrics (Table 2) are in concordance with the plots discussed. The mean error of medium-end IMU is 85.00% lower in roll angle, 90.92% in pitch angle and 93.86% in yaw angle compared to low-end IMU attitude estimation. The same behaviour is shown in standard deviation and 95% ECDF. The calibration necessity is highlighted in the attitude estimation and its contribution in yaw angle calculation is higher than in other two angles (i.e. roll and pitch): the mean error is reduced 91.13%, the standard deviation 92.29% and the 95% ECDF 93.06%. Thus, the yaw angle accuracy and precision is comparable to medium-end IMU. In case of roll and pitch, although the calibration helps to more accurately estimate their values, they do not reach so prominent results.

C. VEHICLE ACCELERATIONS

Once the vehicle's attitude (roll, pitch and yaw) is estimated, the rotation matrix can be built and it can be used to remove the gravity term from accelerometers measurements. This way, the accelerations of the vehicle on the longitudinal, lateral and vertical axes can be estimated. The knowledge of these accelerations can help to detect curved and slope sections of the track and, consequently, it can be used as diagnosis measurements of other sensors (such as wheel speed sensors, that could provide inaccurate measurements

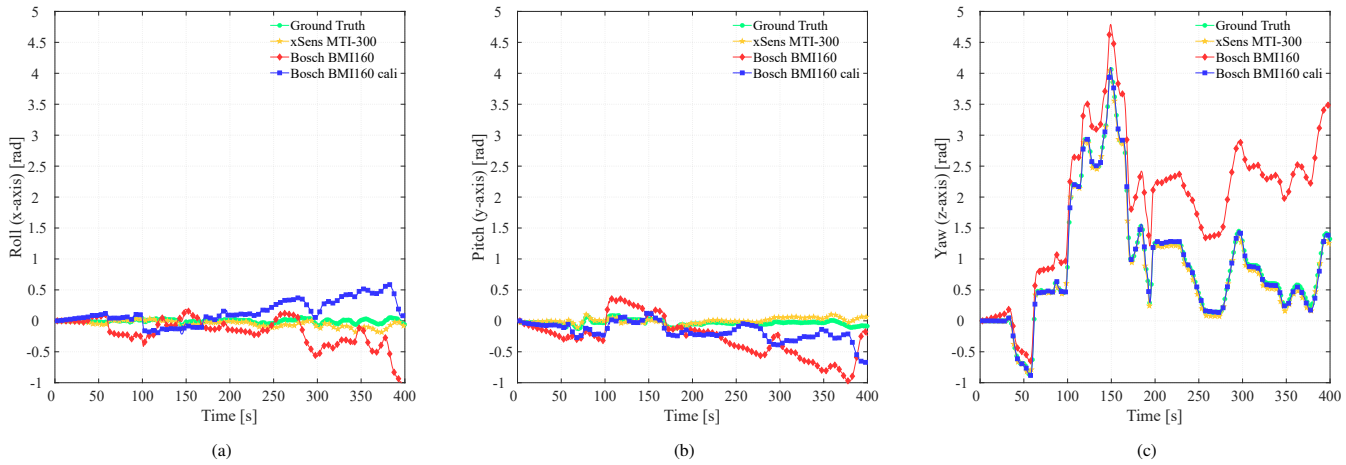

Figure 6: Attitude estimation represented by the Euler angles: (a) Roll or x-axis rotation, (b) Pitch or y-axis rotation and (c) Yaw or z-axis rotation. The plots are limited to the initial 400 seconds of the journey for ease of representation, but the statistical analysis is carried out for all the test.

Table 2: Euler angles statistical analysis comparing M-end, L-end and L-end calibrated to the Ground Truth.

	M-end			**L-end**			**L-end Calibrated**		
	Mean. Error $[rad]$	Std. Dev. $[rad]$	95% ECDF $[rad]$	Mean. Error $[rad]$	Std. Dev. $[rad]$	95% ECDF $[rad]$	Mean. Error $[rad]$	Std. Dev. $[rad]$	95% ECDF $[rad]$
Roll angle	0.0398	0.0332	0.1085	0.2654	0.2917	0.9283	0.1798	0.1485	0.4121
Pitch angle	0.0283	0.0232	0.0800	0.3117	0.2231	0.6884	0.1887	0.1728	0.5239
Yaw angle	0.0758	0.0522	0.1660	1.2346	0.7234	2.3075	0.1095	0.0558	0.1601

M-end = Medium-end. L-end = Low-end. ECDF = Empirical Cumulative Distribution Function.

when rolling radius is far away the nominal value).

In analogous way to previous sections, an initial section of the journey has been used to compute and plot the vehicle accelerations in 3-axes (longitudinal -x-, lateral -y- and vertical -z-). The reference values of 3-axes accelerations are plotted initially; this way, the vehicle accelerations estimated are compared to the reference values (Figure 7).

The medium-end IMU performance is highlighted in the results shown in Table 3, where the accuracy reached, specially on longitudinal axis, is clearly higher than the performance given by low-end IMUs, even after the calibration: the mean error of the longitudinal acceleration is reduced 82.03% in medium-end IMU, whereas the calibration only can reduce 34.61%. The very same behaviour is concluded for standard deviation (reduction of 75.18% in medium-end IMU and 20.28% in calibrated low-end IMU) and 95% ECDF (reduction of 75.35% in medium-end IMU and 23.33% in calibrated low-end IMU). These differences are related to the attitude results, specially to the discrepancies on roll and pitch angles shown in Table 2: note that the roll and pitch angles of medium-end IMU are an order of magnitude more accurate than low-end calibrated results in mean error. As the gravity is projected onto the three axes due to cant and slope, any inaccuracy on roll and pitch angles is propagated to longitudinal acceleration. Thus, part of the gravity remains at final accelerations calculation.

VI. CONCLUSIONS

In the present paper, the performance of different grade IMUs has been evaluated using statistical metrics to experimental data in order to analyse the raw measurements (gyroscopes and accelerometers) and navigation states (attitude and vehicle accelerations).

According to the raw measurements of gyroscopes and accelerometers, the calibration of the low-end IMU has been concluded to be recommended in order to get the performance of the measurements closer to a medium-end IMU: calibrated low-cost gyroscopes present rather similar performance to medium-end ones in mean error, standard deviation and 95% ECDF, specially on x-axis measurements (0.49%, 0.11% and 0.30% difference respectively between the medium-end and low-end calibrated). In case of accelerometers, the calibration contribution is even larger reducing the same metrics along x-axis in 27.77% for mean error, 12.12% for standard deviation and 17.85% for 95% ECDF. It can be explained with the utilization of 12 calibration parameters in accelerometers instead of 3 in gyroscopes.

After the integration of gyroscopes measurements, the Euler angles have been analysed. The attitude estimated by high-end IMU is better than the ones estimated by the rest of

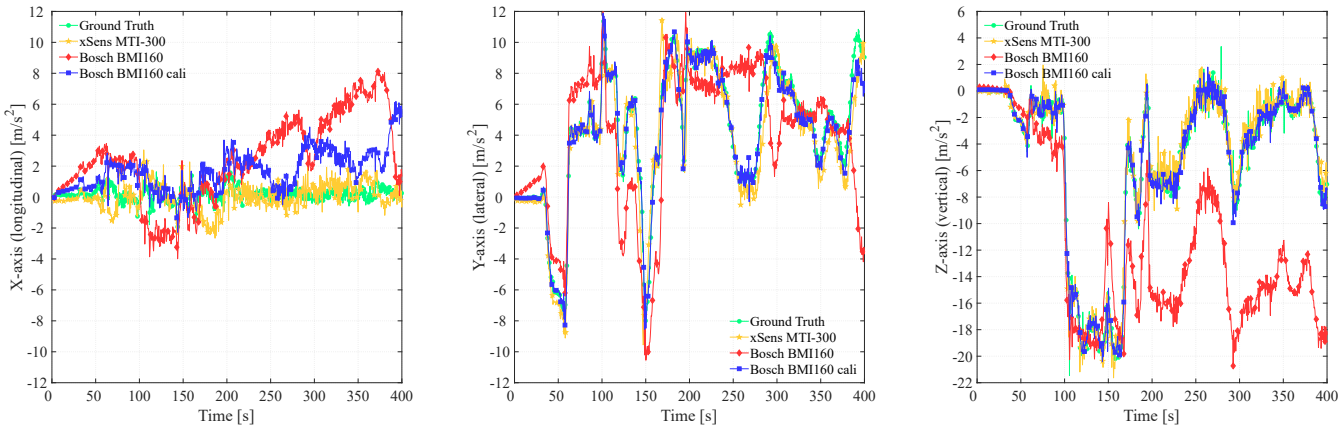

Figure 7: Vehicle tri-axial accelerations once the gravity terms have been removed: (a) Longitudinal acceleration (x-axis), (b) lateral acceleration (y-axis) and (c) vertical acceleration (z-axis). The plots are limited to the initial 400 seconds of the journey for ease of representation, but the statistical analysis is carried out for all the test.

Table 3: Vehicle accelerations statistical analysis comparing M-end, L-end and L-end calibrated to the Ground Truth.

	M-end			**L-end**			**L-end Calibrated**		
	Mean. Error $[m/s^2]$	Std. Dev. $[m/s^2]$	95% ECDF $[m/s^2]$	Mean. Error $[m/s^2]$	Std. Dev. $[m/s^2]$	95% ECDF $[m/s^2]$	Mean. Error $[m/s^2]$	Std. Dev. $[m/s^2]$	95% ECDF $[m/s^2]$
Lon. Acc.	0.5084	0.4882	1.4973	2.8287	1.9671	6.0749	1.8496	1.5682	4.6578
Lat. Acc.	4.6628	2.9534	8.9310	4.7284	2.6892	8.1125	4.7420	2.7341	8.5389
Ver. Acc.	14.314	5.8897	19.683	11.819	6.2160	18.136	5.1016	5.7746	16.908

M-end = Medium-end. L-end = Low-end. ECDF = Empirical Cumulative Distribution Function.
Lon. Acc. = Longitudinal (x-axis) acceleration. Lat. Acc. = Lateral (y-axis) acceleration. Ver. Acc. = Vertical (z-axis) acceleration.

the IMU tested in this work, but the medium-end IMU can be considered to be similar (centesimal order of magnitude mean error and standard deviation have been computed). However, the heading analysis has bring encouraging results for calibrated low-end IMU: after the calibration proposed, the solution mean error reached is only 2.73% higher than the provided by the medium-end IMU. The standard deviation is also in the same order of magnitude (only 0.49% higher in calibrated low-end IMU) as well as the 95% ECDF (only 0.26% higher in calibrated low-end IMU). This way, the yaw estimation by calibrated low-end IMU can be concluded to be comparable to high-end and medium-end IMUs. In future works, map-aided solutions shall be proposed by using yaw angle estimation and track information. This kind of solutions can be propitious for track-constrained positioning solution (e.g. railways) where low-cost IMUs can provide enhanced navigation data (e.g. absolute position, orientation, etc.).

Finally, the vehicle accelerations have been obtained. The errors in roll and pitch angles estimation are propagated to accelerations estimation and significant differences between high-end and the rest of IMUs are computed. Although the calibration improves the low-end IMU solution (mainly the vertical axis accelerations), the mean error and standard deviation are about 2 m/s^2.

Although the results in general show prominent, the lack of noise terms analysis shall make us cautious in long term applications, where calibration parameters can be not constant or subject to temperature, voltage and humidity changes. Further analysis on calibration parameters can be performed in terms of bias instability, temperature dependency, etc so as to guarantee the repeatibility of the results presented in this paper.

ACKNOWLEDGEMENTS

The authors would like to thank CAF Research and Development Department and CETEST for their expertise in inertial sensors experimental tests that directly motivated the writing of this paper.

References

[1] I. P. Prikhodko, B. Bearss, C. Merritt, J. Bergeron, and C. Blackmer, "Towards self-navigating cars using MEMS IMU: Challenges and opportunities," in 2018 IEEE International Symposium on Inertial Sensors and Systems (INERTIAL). Moltrasio: IEEE, Mar. 2018, pp. 1–4. [Online]. Available: https://ieeexplore.ieee.org/document/8358141/

[2] W. Youn and S. A. Gadsden, "Combined Quaternion-Based Error State Kalman Filtering and Smooth Variable Structure Filtering for Robust Attitude Estimation," IEEE Access, vol. 7, pp. 148 989–149 004, 2019. [Online]. Available: https://ieeexplore.ieee.org/document/8865091/

[3] J. Otegui, A. Bahillo, I. Lopetegi, and L. E. Diaz, "A Survey of Train Positioning Solutions," IEEE Sensors Journal,

vol. 17, no. 20, pp. 6788–6797, Aug. 2017. [Online]. Available: http://ieeexplore.ieee.org/document/8022861/

[4] R. Harle, "A Survey of Indoor Inertial Positioning Systems for Pedestrians," IEEE Communications Surveys & Tutorials, vol. 15, no. 3, pp. 1281–1293, 2013. [Online]. Available: http://ieeexplore.ieee.org/document/6407455/

[5] R. Miyazaki, R. Jiang, H. Paul, Y. Huang, and K. Shimonomura, "Long-Reach Aerial Manipulation Employing Wire-Suspended Hand With Swing-Suppression Device," IEEE Robotics and Automation Letters, vol. 4, no. 3, pp. 3045–3052, Jul. 2019. [Online]. Available: https://ieeexplore.ieee.org/document/8743463/

[6] H. Ahmed and M. Tahir, "Accurate Attitude Estimation of a Moving Land Vehicle Using Low-Cost MEMS IMU Sensors," IEEE Transactions on Intelligent Transportation Systems, vol. 18, no. 7, pp. 1723–1739, Jul. 2017. [Online]. Available: http://ieeexplore.ieee.org/document/7775094/

[7] W. J. Park, J. W. Song, C. H. Kang, J. H. Lee, M. H. Seo, S. Y. Park, J. Y. Yeo, and C. G. Park, "MEMS 3d DR/GPS Integrated System for Land Vehicle Application Robust to GPS Outages," IEEE Access, vol. 7, pp. 73 336–73 348, 2019. [Online]. Available: https://ieeexplore.ieee.org/document/8726394/

[8] G. Falco, M. Pini, and G. Marucco, "Loose and Tight GNSS/INS Integrations: Comparison of Performance Assessed in Real Urban Scenarios," Sensors, vol. 17, no. 2, p. 255, Jan. 2017. [Online]. Available: http://www.mdpi.com/1424-8220/17/2/255

[9] X. Meng, H. Wang, and B. Liu, "A Robust Vehicle Localization Approach Based on GNSS/IMU/DMI/LiDAR Sensor Fusion for Autonomous Vehicles," Sensors, vol. 17, no. 9, p. 2140, Sep. 2017. [Online]. Available: http://www.mdpi.com/1424-8220/17/9/2140

[10] O. Heirich, "Bayesian Train Localization with Particle Filter, Loosely Coupled GNSS, IMU, and a Track Map," Journal of Sensors, vol. 2016, pp. 1–15, 2016. [Online]. Available: http://www.hindawi.com/journals/js/2016/2672640/

[11] H. Peng, X. Zhi, R. Wang, J.-y. Liu, and C. Zhang, "A new dynamic calibration method for IMU deterministic errors of the INS on the Hypersonic Cruise Vehicles," Aerospace Science and Technology, vol. 32, no. 1, pp. 121–130, Jan. 2014. [Online]. Available: https://linkinghub.elsevier.com/retrieve/pii/S1270963813002034

[12] J. Guo and M. Zhong, "Calibration and Compensation of the Scale Factor Errors in DTG POS," IEEE Transactions on Instrumentation and Measurement, vol. 62, no. 10, pp. 2784–2794, Oct. 2013. [Online]. Available: http://ieeexplore.ieee.org/document/6564423/

[13] M. Narasimhappa, A. D. Mahindrakar, V. C. Guizilini, M. H. Terra, and S. L. Sabat, "MEMS Based IMU Drift Minimization: Sage Husa Adaptive Robust Kalman Filtering," IEEE Sensors Journal, pp. 1–1, 2019. [Online]. Available: https://ieeexplore.ieee.org/document/8836664/

[14] S. Niespodziany, "Inertial Navigation Static Calibration," Polish Academy of Sciences Committee of Electronics and Telecommunications, May 2018. [Online]. Available: http://journals.pan.pl/dlibra/publication/119518

[15] L. Taylor, E. Miller, and K. R. Kaufman, "Static and dynamic validation of inertial measurement units," Gait & Posture, vol. 57, pp. 80–84, Sep. 2017. [Online]. Available: https://linkinghub.elsevier.com/retrieve/pii/S0966636217302084

[16] Rui Zhang, F. Hoflinger, and L. M. Reind, "Calibration of an IMU Using 3-D Rotation Platform," IEEE Sensors Journal, vol. 14, no. 6, pp. 1778–1787, Jun. 2014. [Online]. Available: http://ieeexplore.ieee.org/document/6728637/

[17] U. Qureshi and F. Golnaraghi, "An Algorithm for the In-Field Calibration of a MEMS IMU," IEEE Sensors Journal, vol. 17, no. 22, pp. 7479–7486, Nov. 2017.

[18] C. Ren, Q. Liu, and T. Fu, "A Novel Self-Calibration Method for MIMU," IEEE Sensors Journal, vol. 15, no. 10, pp. 5416–5422, Oct. 2015. [Online]. Available: http://ieeexplore.ieee.org/document/7115893/

[19] X. Niu, Y. Li, H. Zhang, Q. Wang, and Y. Ban, "Fast Thermal Calibration of Low-Grade Inertial Sensors and Inertial Measurement Units," Sensors, vol. 13, no. 9, pp. 12 192–12 217, Sep. 2013. [Online]. Available: http://www.mdpi.com/1424-8220/13/9/12192

[20] B. Altinoz and D. Unsal, "Determining efficient temperature test points for IMU calibration," in 2018 IEEE/ION Position, Location and Navigation Symposium (PLANS). Monterey, CA: IEEE, Apr. 2018, pp. 552–556. [Online]. Available: https://ieeexplore.ieee.org/document/8373426/

[21] O. Sarkka, T. Nieminen, S. Suuriniemi, and L. Kettunen, "A Multi-Position Calibration Method for Consumer-Grade Accelerometers, Gyroscopes, and Magnetometers to Field Conditions," IEEE Sensors Journal, vol. 17, no. 11, pp. 3470–3481, Jun. 2017. [Online]. Available: http://ieeexplore.ieee.org/document/7902095/

[22] R. Gonzalez and P. Dabove, "Performance Assessment of an Ultra Low-Cost Inertial Measurement Unit for Ground Vehicle Navigation," Sensors, vol. 19, no. 18, p. 3865, Sep. 2019. [Online]. Available: https://www.mdpi.com/1424-8220/19/18/3865

[23] X. Shen, D. Yuan, R. Chang, and W. Jin, "A Nonlinear Observer for Attitude Estimation of Vehicle-Mounted Satcom-on-the-Move," IEEE Sensors Journal, vol. 19, no. 18, pp. 8057–8066, Sep. 2019. [Online]. Available: https://ieeexplore.ieee.org/document/8720200/

[24] D. Titterton and J. Weston, Strapdown Inertial Navigation Technology. The Institution of Engineering and Technology, Michael Faraday House, Six Hills Way, Stevenage SG1 2AY, UK: IET, Jan. 2004. [Online]. Available: http://link.aip.org/link/doi/10.1049/PBRA017E

[25] K. Jerath, S. Brennan, and C. Lagoa, "Bridging the gap between sensor noise modeling and sensor characterization," Measurement, vol. 116, pp. 350–366, Feb. 2018. [Online]. Available: https://linkinghub.elsevier.com/retrieve/pii/S026322411730578X

[26] D. Unsal and K. Demirbas, "Estimation of deterministic and stochastic IMU error parameters," in Proceedings of the 2012 IEEE/ION Position, Location and Navigation Symposium. Myrtle Beach, SC, USA: IEEE, Apr. 2012, pp. 862–868. [Online]. Available: http://ieeexplore.ieee.org/document/6236828/

[27] M. Jafari, T. A. Najafabadi, B. Moshiri, S. S. Tabatabaei, and M. Sahebjameyan, "PEM Stochastic Modeling for MEMS Inertial Sensors in Conventional and Redundant IMUs," IEEE Sensors Journal, vol. 14, no. 6, pp. 2019–2027, Jun. 2014. [Online]. Available: http://ieeexplore.ieee.org/document/6744635/

[28] E. M. Hemerly, "MEMS IMU stochastic error modelling," Systems Science & Control Engineering, vol. 5, no. 1, pp. 1–8, Jan. 2017. [Online]. Available: https://www.tandfonline.com/doi/full/10.1080/21642583.2016.1262801

[29] R. J. Vaccaro and A. S. Zaki, "Statistical Modeling of Rate Gyros," IEEE Transactions on Instrumentation and Measurement, vol. 61, no. 3, pp. 673–684, Mar. 2012. [Online]. Available: http://ieeexplore.ieee.org/document/6068252/

[30] D. Tedaldi, A. Pretto, and E. Menegatti, "A robust and easy to implement method for IMU calibration without external equipments," in 2014 IEEE International Conference on Robotics and Automation (ICRA). Hong Kong, China: IEEE, May 2014, pp. 3042–3049. [Online]. Available: http://ieeexplore.ieee.org/document/6907297/

[31] M. Sipos, P. Paces, J. Rohac, and P. Novacek, "Analyses of Triaxial Accelerometer Calibration Algorithms," IEEE Sensors Journal, vol. 12, no. 5, pp. 1157–1165, May 2012. [Online]. Available: http://ieeexplore.ieee.org/document/6015525/

[32] I. Skog and P. Händel, "Calibration of a MEMS inertial measurement unit," in XVII IMEKO World Congress, 2006, pp. 1–6. [Online]. Available: http://www.academia.edu/download/44800125/PWC-2006-TC3-017u.pdf

JON OTEGUI received a B.Sc. degree in Industrial Technologies Engineering and a M.Sc. degree in Industrial Engineering from the University of Navarra-Tecnun, Donostia, Spain, in 2014 and 2016, respectively. His Master's thesis was focused on the experimental validation process of GNSS positioning technology in railway environment. He is currently pursuing a Ph.D. degree with the Mobility Research Group, DeustoTech, Bilbao, Spain, under the supervision of Dr. Bahillo. His current research interests include the development of data fusion algorithms for train positioning and navigation, IMU and GNSS characterization in railway context and the integration in trains for safety critical applications.

ALFONSO BAHILLO received Telecommunications Engineering and Ph.D. degrees from the University of Valladolid, Valladolid, Spain, in 2006 and 2010, respectively. He received the PMP certification at the PMI in 2014. From 2006 to 2010, he was a Research Engineer with CEDETEL. From 2006 to 2011, he was an Assistant Professor with the University of Valladolid. From 2010 to 2012, he was a Product Owner with LUCE Innovative Technologies, Valladolid. From 2013 and 2017, he was a Post-Doctoral Researcher with the University of Deusto, Bilbao, Spain, and the Project Manager with DeustoTech, Bilbao, where he trains Ph.D. students and collaborates in several national and international research projects. He is currently the Director of DeustoTech. He has worked (leading some of them) in more than 25 regional, national, and international research projects and contracts. He has coauthored over 20 research manuscripts published in international journals and over 40 communications in international conferences, and holds three national patents. His current research interests include local and global positioning techniques and ITS.

IBAN LOPETEGI received a M.Sc. degree in Telecommunication Engineering from the University of Mondragon, Mondragón, Spain, in 2007, and a Ph.D. degree in Electronics and Communications from Newcastle University, Newcastle Upon Tyne, U.K., in 2011. Since 2011, he has been company representative for NGTC of WP7 and for STARS with the CAF Research and Development Department, Beasain, Spain. His current research interests include fail-safe train navigation, global positioning systems and digital maps in railways.

LUIS ENRIQUE DÍEZ received a B.Sc. degree in Telecommunications Engineering from the University of Deusto, Bilbao, Spain, in 2005, the M.Sc. degree in Communication Technologies and Systems from the Polytechnic University of Madrid, Madrid, Spain, in 2012 and a Ph.D. degree from University of Deusto, Bilbao, Spain, in 2019. From 2005 to 2011, he was a Senior IT Consultant with Everis, Madrid. From 2013 to 2014, he was a Research Support Technician with the SOFTLAB Research Group, Carlos III University of Madrid, Getafe, Spain. Since 2014, he has worked within the Mobility Research Group, DeustoTech, Bilbao, Spain. His current research interests include positioning systems, data fusion techniques and context-aware applications.

Each problem that I solved became a rule, which served afterwards to solve other problems.

Rene Descartes

CHAPTER

6

Conclusions and Future Work

Throughout this dissertation the main goal has been pursued: to improve the current train positioning system in terms of functionality, interoperability and cost-efficiency. To do so, an exhaustive evaluation of the state-of-the-art solutions has been presented, an exhaustive experimental tests has been carried out, a flexible simulation framework has been developed and finally, different grade IMUs are compared each other. This chapter summarizes the main conclusions that have been drawn. Then, an outlook is presented for potential innovations and future research.

6.1 Conclusions

As described through this dissertation, positioning accurately and safely a train is nowadays a great challenge. The limitations of the current system and the development of candidate systems such as GNSS and INS has propitiated the research effort in this field, especially over last five years. This work is focused on the integration of an IMU as a complementary source to wheel speed sensors in order to

achieve the functionality, interoperability and cost-efficiency requirements of fail-safe train positioning system.

The first chapter introduces the train positioning and states its relevance on ITS. Then, the current train positioning system is explained and the main limitations are highlighted according to functionality, interoperability, safety, energy and cost criteria. In order to overcome these limitations, GNSS and INS potentialities as candidate systems are shown.

Chapter 2 presents and evaluates the main train positioning solutions published up-to-date. The research gaps found in this work are summed up as follows: First, the lack of details on the experimental tests performed to evaluate candidate systems solution against current solution. Second, the lack of flexible simulation frameworks to test train navigation solution. Third, the ambiguity on the economic cost of the proposed solutions. These research gaps have motivated the rest of the papers.

Chapter 3 focuses on a experimental test to evaluate GNSS and INS-based solution and its performance is compared to current train navigation solution. This work provides a detailed description of the instrumentation and measurement equipment utilized during the test. In addition, it concludes an absolute error in velocity lower than 2 km/h in more than 90% of the test duration can be achievable with high-end GNSS receiver and medium-end IMU. Finally, the estimation of track features (cant, height and curve radius) based on INS solution is provided.

Chapter 4 presents a flexible and one-stop simulation framework to design and test different train navigation algorithms, mechanization methods, etc. in multiples scenarios (changing the features of trains, tracks, sensors and so on). This work overcomes up-to-date simulation frameworks limitations allowing test scenarios with different train and sensors characteristics, speed and track profiles, synthetic and experimental signals, mechanization methods, data fusion algorithms, etc.

Chapter 5 focuses on the cost optimization of the INS, evaluating different grade IMUs (from 3 to 30.000 €) for land-vehicular positioning purpose. This work compares the performance of ultra low-cost INS against medium-end and high-end solutions. In addition, a calibration technique is proposed, making the solution of ultra low-cost INS similar to medium-end INS.

Through all of these contributions, it is my hope that this dissertation helps to overcome the limitations of current train positioning system and to fulfill the research objectives of the thesis.

6.2 Future work

The research interest on train positioning topic will be maintained in future years according to EU research programs. There can be outlined several future steps related to the topic.

The integration of GNSS into the train positioning system will be related to the virtual balise (VB) concept. In order to reduce the maintenance cost of the balises, they can be evolved to virtual nodes on which the accuracy of the on-board system is enhanced by resetting cumulative errors of the odometry. However, the integrity evaluation and monitoring techniques must be adapted to railway context requirements, mainly those related to ERTMS.

The utilization of digital maps as external source for positioning is also a trending topic. The development of map-matching techniques on railways, where the footprints of the sensors can be considered particular, arise as prominent research field. However, the availability and the robustness of the digital maps must be incremented in order to use them as confidence data.

The development of fail-safe positioning systems plays a key role in autonomous driving because the localization of the vehicle is a fundamental data for future developments. The use of artificial intelligence will be necessary to reach the highest automation levels of vehicles where highly dynamic and complex traffic situations, sensors measurements interpretation in real time, behaviour of other users prediction and so on shall be considered.

Bibliography

[1] B. W. Kolosz and S. M. Grant-Muller, "Appraisal and Evaluation of Inter-urban ITS: A European Survey," *IEEE Transactions on Intelligent Transportation Systems*, vol. 16, pp. 1070–1087, June 2015. 1

[2] F. Peyret, P.-Y. Gilliéron, L. Ruotsalainen, and J. Engdahl, *COST TU1302-SaPPART White Paper-Better use of Global Navigation Satellite Systems for safer and greener transport*. No. EPFL-BOOK-212763, Ifsttar, 2015. 1

[3] J. Marais, J. Beugin, and M. Berbineau, "A Survey of GNSS-Based Research and Developments for the European Railway Signaling," *IEEE Transactions on Intelligent Transportation Systems*, vol. 18, pp. 2602–2618, Oct. 2017. 1, 4

[4] J. Otegui, A. Bahillo, I. Lopetegi, and L. E. Diaz, "A Survey of Train Positioning Solutions," *IEEE Sensors Journal*, vol. 17, pp. 6788–6797, Aug. 2017. 2, 4

[5] I. Durazo-Cardenas, A. Starr, A. Tsourdos, M. Bevilacqua, and J. Morineau, "Precise Vehicle Location as a Fundamental Parameter for Intelligent Self-aware Rail-track Maintenance Systems," *Procedia CIRP*, vol. 22, pp. 219–224, 2014. 2

[6] A. Mirabadi, N. Mort, and F. Schmid, "Application of sensor fusion to railway systems," in *IEEE/SICE/RSJ International Conference on Multisensor Fusion and Integration for Intelligent Systems*, pp. 185–192, 1996. 2

[7] Alstom, Ansaldo STS, Bombardier, Invensys, SIEMENS, and Thales, "Performance Requirements for Interoperability (Subset-041)," 2012. 3

[8] A. Neri, P. Salvatori, C. Stallo, and A. Coluccia, "A Multi-sensor Autonomous Integrity Monitoring Approach for Railway and Driver-less Cars," (Miami, Florida), pp. 1605–1621, Oct. 2018. 3

[9] Y. Huang, L. Yang, T. Tang, Z. Gao, F. Cao, and K. Li, "Train speed profile optimization with on-board energy storage devices: A dynamic programming based approach," *Computers & Industrial Engineering*, vol. 126, pp. 149–164, Dec. 2018. 3

[10] X.-H. Zhao, B.-R. Ke, and K.-L. Lian, "Optimization of Train Speed Curve for Energy Saving Using Efficient and Accurate Electric Traction Models on the Mass Rapid Transit System," *IEEE Transactions on Transportation Electrification*, vol. 4, pp. 922–935, Dec. 2018. 3

[11] M. Dominguez, A. Fernandez-Cardador, A. P. Cucala, and R. R. Pecharroman, "Energy Savings in Metropolitan Railway Substations Through Regenerative Energy Recovery and Optimal Design of ATO Speed Profiles," *IEEE Transactions on Automation Science and Engineering*, vol. 9, pp. 496–504, July 2012. 3

[12] W. J. Park, J. W. Song, C. H. Kang, J. H. Lee, M. H. Seo, S. Y. Park, J. Y. Yeo, and C. G. Park, "MEMS 3d DR/GPS Integrated System for Land Vehicle Application Robust to GPS Outages," *IEEE Access*, vol. 7, pp. 73336–73348, 2019. 4

[13] J. Otegui, A. Bahillo, I. Lopetegi, and L. E. Diez, "Evaluation of Experimental GNSS and 10-DOF MEMS IMU Measurements for Train Positioning," *IEEE Transactions on Instrumentation and Measurement*, vol. 68, pp. 269–279, Jan. 2019. 4

[14] "Shift2rail." 4

[15] J. Beugin, C. Legrand, J. Marais, M. Berbineau, and E.-M. El-Koursi, "Safety Appraisal of GNSS-Based Localization Systems Used in Train Spacing Control," *IEEE Access*, vol. 6, pp. 9898–9916, 2018. 4

[16] P. D. Groves, "The Complexity Problem in Future Multisensor Navigation and Positioning Systems: A Modular Solution," *Journal of Navigation*, vol. 67, pp. 311–326, Mar. 2014. 4

[17] F. Böhringer and A. Geistler, "Location in railway traffic: generation of a digital map for secure applications," vol. 1, pp. 459–468, WIT Press, June 2006. 4

[18] O. G. Crespillo, D. Medina, J. Skaloud, and M. Meurer, "Tightly coupled GNSS/INS integration based on robust M-estimators," in *2018 IEEE/ION Position, Location and Navigation Symposium (PLANS)*, (Monterey, CA), pp. 1554–1561, IEEE, Apr. 2018. 4

[19] J. Liu, B.-g. Cai, and J. Wang, "Track-constrained GNSS/odometer-based train localization using a particle filter," in *IEEE Intelligent Vehicles Symposium (IV)*, pp. 877–882, 2016. 4

[20] J. Marais, C. Meurie, D. Attia, Y. Ruichek, and A. Flancquart, "Toward accurate localization in guided transport: Combining GNSS data and imaging information," *Transportation Research Part C: Emerging Technologies*, vol. 43, pp. 188–197, June 2014. 4

[21] I. Skog and P. Handel, "In-Car Positioning and Navigation Technologies—A Survey," *IEEE Transactions on Intelligent Transportation Systems*, vol. 10, pp. 4–21, Mar. 2009. 5

[22] J. Lu, X. Liu, and R. Zhang, "Calibration, Alignment, and Dynamic Tilt Maintenance Method Based on Vehicular Hybrid Measurement Unit," *IEEE Sensors Journal*, vol. 19, pp. 7243–7253, Sept. 2019. 5

[23] O. Sarkka, T. Nieminen, S. Suuriniemi, and L. Kettunen, "A Multi-Position Calibration Method for Consumer-Grade Accelerometers, Gyroscopes, and Magnetometers to Field Conditions," *IEEE Sensors Journal*, vol. 17, pp. 3470–3481, June 2017. 5

[24] F. Müller, C. Reimer, and E. Hinüber, "INS,GNSS,Odometer Data Fusion in Railway Applications," in *Inertial Sensors and Systems*, vol. 2, (Karlsruhe, Germany), 2016. 5

[25] U. Iqbal, A. F. Okou, and A. Noureldin, "An integrated reduced inertial sensor system (RISS) and GPS for land vehicle," in *2008 IEEE/ION Position, Location and Navigation Symposium*, (Monterey, CA, USA), pp. 1014–1021, IEEE, 2008. 5

[26] O. Heirich, P. Robertson, A. C. Garcia, and T. Strang, "Bayesian train localization method extended by 3d geometric railway track observations from inertial sensors," in *15th International Conference on Information Fusion (FUSION)*, pp. 416–423, IEEE, 2012. 5

[27] M. Narasimhappa, A. D. Mahindrakar, V. C. Guizilini, M. H. Terra, and S. L. Sabat, "MEMS Based IMU Drift Minimization: Sage Husa Adaptive Robust Kalman Filtering," *IEEE Sensors Journal*, pp. 1–1, 2019. 5

[28] N. El-Sheimy, H. Hou, and X. Niu, "Analysis and Modeling of Inertial Sensors Using Allan Variance," *IEEE Transactions on Instrumentation and Measurement*, vol. 57, pp. 140–149, Jan. 2008. 5

[29] S. S. Saab, "A map matching approach for train positioning. I. Development and analysis," *IEEE Transactions on vehicular technology*, vol. 49, no. 2, pp. 467–475, 2000. 5

[30] S. S. Saab, "A map matching approach for train positioning. II. Application and experimentation," *IEEE Transactions on vehicular technology*, vol. 49, no. 2, pp. 476–484, 2000. 5

[31] H. Winter, S. Luthardt, V. Willert, and J. Adamy, "Generating Compact Geometric Track-Maps for Train Positioning Applications," *arXiv:1903.05014 [cs]*, Mar. 2019. arXiv: 1903.05014. 5

[32] A. Schindler, G. Maier, and F. Janda, "Generation of high precision digital maps using circular arc splines," in *Intelligent Vehicles Symposium (IV), 2012 IEEE*, pp. 246–251, IEEE, 2012. 5

[33] H. Durrant-Whyte and T. C. Henderson, "Multisensor data fusion," in *Springer Handbook of Robotics*, pp. 867–896, Springer, 2016. 6

[34] B. Khaleghi, A. Khamis, F. O. Karray, and S. N. Razavi, "Multisensor data fusion: A review of the state-of-the-art," *Information Fusion*, vol. 14, pp. 28–44, Jan. 2013. 6

[35] Z. Chen and others, "Bayesian filtering: From Kalman filters to particle filters, and beyond," *Statistics*, vol. 182, no. 1, pp. 1–69, 2003. 6

[36] R. Munguía, "A GPS-aided inertial navigation system in direct configuration," *Journal of applied research and technology*, vol. 12, no. 4, pp. 803–814, 2014. 6

[37] G. Muniandi and E. Deenadayalan, "Train distance and speed estimation using multi sensor data fusion," *IET Radar, Sonar & Navigation*, Nov. 2018. 6

[38] D. Veillard, F. Mailly, and P. Fraisse, "EKF-based state estimation for train localization," in *IEEE SENSORS*, pp. 1–3, 2016. 6

[39] P. Pichlík and J. Zděnek, "Train velocity estimation by extended Kalman filter," in *8th International Conference Electronics, Computers and Artificial Intelligence (ECAI)*, (Ploiesti, Romania), pp. 85–88, 2016. 6

[40] Z. Liu, S.-C. Chan, H.-C. Wu, and J. Wu, "Bayesian unscented Kalman filter for state estimation of nonlinear and non-Gaussian systems," in *Signal Processing Conference (EUSIPCO), 2016 24th European*, pp. 443–447, IEEE, 2016. 6

[41] B. Siebler and S. Sand, "Posterior Cramér-Rao bound and suboptimal filtering for IMU/GNSS based cooperative train localization," in *IEEE/ION Position, Location and Navigation Symposium (PLANS)*, pp. 353–358, 2016. 6

Declaration

I herewith declare that I have produced this work without the prohibited assistance of third parties and without making use of aids other than those specified; notions taken over directly or indirectly from other sources have been identified as such. This work has not previously been presented in identical or similar form to any examination board.

The dissertation work was conducted from 2017 to 2020 under the supervision of Dr. Alfonso Bahillo at the University of Deusto and Dr. Iban Lopetegi at CAF I+D.

Bilbao,

This dissertation was finished writing in Bilbao on Wednesday 5th February, 2020

This page is intentionally left blank